Improved L-Lysine Production in *Corynebacterium glutamicum* by Rational Strain Engineering

Dissertation

zur Erlangung des Grades

des Doktors der Ingenieurwissenschaften

der Naturwissenschaftlich-Technischen Fakultät III

Chemie, Pharmazie, Bio- und Werkstoffwissenschaften

der Universität des Saarlandes

Von

Sarah Schiefelbein

Saarbrücken

2014

Tag des Kolloquiums:	27. Februar 2015
Dekan:	Prof. Dr.-Ing. Dirk Bähre
Berichterstatter:	Prof. Dr. Christoph Wittmann
	Prof. Dr. Gert-Wieland Kohring
Vorsitz:	Prof. Dr. Elmar Heinzle
Akademischer Mitarbeiter:	Dr. Björn Becker

Vorveröffentlichungen der Dissertation

Teilergebnisse aus dieser Arbeit wurden mit Genehmigung der Naturwissenschaftlich-Technischen Fakultät III Chemie, Pharmazie, Bio- und Werkstoffwissenschaften der Universität des Saarlandes, vertreten durch den Mentor der Arbeit, in folgenden Beiträgen vorab veröffentlicht.

Publikationen

Schiefelbein, S., Fröhlich, A., John, G. T., Beutler, F, Wittmann, C. and Becker, J.(2013). "Oxygen supply in disposable shake-flasks: prediction of oxygen transfer rate, oxygen saturation and maximum cell concentration during aerobic growth." Biotechnol Lett. 35(8): 1223-30.

Tagungsbeiträge

Schiefelbein, S., Becker, J., Buschke, N. and Wittmann, C. "L-lysine production by *Corynebacterium glutamicum* utilizing alternative renewable resources." VAAM Annual Conference, March 18-21, 2012, Tübingen, Germany.

Becker, J., Kind, S., Buschke, N., **Schiefelbein, S.** and Wittmann, C. "Systems metabolic engineering of *Corynebacterium glutamicum* for industrial bio-production." VAAM Annual Conference, March 18-21, 2012, Tübingen, Germany.

Schiefelbein, S., Fröhlich, A., John, G. T., Beutler, F, Wittmann, C. and Becker, J. "Oxygen supply in disposable shake-flasks: prediction of oxygen transfer rate, oxygen saturation and maximum cell concentration during aerobic growth." BioMicroWorld, October 2-4, 2013, Madrid, Spain

Mitwirkende

Teile, der in dieser Arbeit veröffentlichten Ergebnisse, wurden von den nachfolgend aufgeführten Studenten unter Anleitung erarbeitet.

Frau Sarah Bromann hat im Rahmen ihrer Masterarbeit „Feintuning von Enzymaktivitäten mittels einer Promotor-Bibliothek in *Corynebacterium glutamicum*“ (2014) am Institut für Bioverfahrenstechnik der TU Braunschweig die Plasmidkonstruktion von pClik_int_*sacB*_$P_{7\text{-}29}$*lysE*, pClik_int_*sacB*_$P_{7\text{-}19}$*lysE* und pClik_int_*sacB*_$P_{6\text{-}43}$*lysE* (Tabelle 4.2) sowie die Stammkonstruktion des Stammes BS542 (Tabelle 4.1) durchgeführt.

Herr Alexander Fröhlich hat im Rahmen seines Forschungspraktikums „Metabolic Engineering von *Corynebacterium glutamicum*“ (2011) am Institut für Bioverfahrenstechnik der TU Braunschweig die Plasmidkonstruktion von pClik_5a_MCS_*gapN* (Tabelle 4.2) sowie die Stammkonstruktion der Stämme BS383 und BS384 (Tabelle 4.1) durchgeführt. Des Weiteren hat er im Rahmen seiner Masterarbeit „Lysinproduktion in *Corynebacterium glutamicum* - Bioprozessintegration und Metabolic Engineering“ (2012) am Institut für Bioverfahrenstechnik der TU Braunschweig die k_La-Bestimmung und Kultivierungen der in Kapitel 4.7 und 5.1 bearbeiteten Fragestellungen durchgeführt.

Frau Friederike Möller hat im Rahmen ihrer Bachelorarbeit „Etablierung eines Screeningverfahrens zur Erstellung einer Promotorbibliothek für *Corynebacterium glutamicum*“ (2012) am Institut für Bioverfahrenstechnik der TU Braunschweig die Plasmidkonstruktion von pClik_5a_MCS_P_{sod}*GFPmut1* (Tabelle 4.2) sowie die Stammkonstruktion des Stammes BS388 (Tabelle 4.1) durchgeführt.

Danksagung

Ganz herzlich bedanke ich mich bei meinem Doktorvater Prof. Dr. Christoph Wittmann für die Bereitstellung des Themas und die Möglichkeit, diese Arbeit unter seiner Betreuung durchzuführen. Deine nützlichen Ratschläge und Ideen waren eine besondere Hilfe und gaben mir häufig eine neue Sicht auf die Dinge.

Insbesondere möchte ich mich auch bei Herrn Prof. Dr. Gert-Wieland Kohring und Herrn Prof. Dr. Elmar Heinzle für die Bereitschaft zur Übernahme des Koreferats bzw. des Prüfungsvorsitz bedanken sowie Herrn Dr. Björn Becker für den Prüfungsbeisitz als akademischer Mitarbeiter.

Herrn Prof. Dr. Rainer Krull vom Institut für Bioverfahrenstechnik in Braunschweig danke ich für die Unterstützung bei den Gesprächen mit unserem Kooperationspartner in Korea.

Bei PAIK KWANG Industrial Co., Ltd. (Korea) bedanke ich mich für die finanzielle Unterstützung meiner Arbeit im Rahmen eines industriellen Kooperationsprojekts zur Verbesserung der Lysinproduktion.

Des Weiteren bedanke ich mich besonders bei Frau Dr. Judith Becker für die enge Zusammenarbeit an diesem Thema. Danke, dass deine Tür jederzeit für mich und meine Fragen offen stand und du immer eine nützliche Idee parat hattest.

Ebenso möchte ich Frau Dr. Rebekka Biedendieck vom Institut für Mikrobiologie der TU Braunschweig danken für die nette Zusammenarbeit und die Hilfe bei der Durchführung und Auswertung der RNA-Analysen.

Ein besonderer Dank geht an meinen „*Coryne*-Partner“ Rudolf Schäfer für die vielen Gespräche und seine unvergleichliche Hilfsbereitschaft in allen Lebenslagen.

Außerdem möchte ich mich bei Frau Friederike Möller sowie „meinen“ Studenten Herrn Alexander Fröhlich, Frau Sarah Bromann, Frau Laura Schild, Herrn Sascha Kießlich und Herrn Konrad Wurm bedanken, die im Rahmen ihrer Abschlussarbeiten zum “Metabolic Engineering von *Corynebacterium glutamicum*“ beigetragen haben. Die Zusammenarbeit mit euch hat mir viel Freude bereitet.

Ein großer Dank gilt meinen vielen netten Kollegen, die mich während meiner Promotion begleitet haben:
Yvonne Göcke und Elena Kempf für die Unterstützung im Laboralltag sowie bei etlichen HPLC-Messungen und RNA-Isolierungen. Meinen Bürokollegen, Annekathrin Bartsch und Thibault Godard, für viele schöne Stunden und fachlichen Diskussionen. Arne, René, Jana, Lisa, Steffi, Franzi, Susanne und Jonathan und all die anderen, die bei gemeinsamen Trainingsstunden, Feierabendbierchen, Kuchenessen, Blödeleien und spontanem Grillen mit dabei waren und die letzten Jahre unvergesslich machten.

Meinen langjährigen Freunden aus Kindheit, Schule und Studium danke ich für die gemeinsame Zeit und die langen Gespräche und dafür, dass ihr immer ein offenes Ohr für mich habt.

Besonders möchte ich Georg danken, dass er jederzeit für mich da war, für seine Geduld beim gemeinsamen Pauken, seinen Halt in schweren Zeiten und seine motivierenden Worte. Danke, für die vielen schönen Momente mit dir!

Meiner lieben Familie danke ich für euren Glauben an mich und eure Unterstützung, für eure Liebe und all das, was keine Worte findet.

Vielen Dank euch allen!

Table of Contents

I Summary

The soil bacterium *Corynebacterium glutamicum* is the major organism for the production of the amino acid L-lysine, an important nutrient in animal feedstock. This study investigated new strategies for bioprocess and genetic engineering of *C. glutamicum* towards production of L-lysine.

In aerobic cultivations, routinely performed in shake-flasks, the dissolved oxygen concentration is a critical often neglected parameter. Here, oxygen mass transfer was determined in disposable shake-flasks under different conditions. Based on the results, a mathematical correlation was developed allowing the prediction of the maximum possible cell concentration achievable without oxygen limitation. The developed tool is valuable for cultivations with costly carbon sources and nutrient additives.

From a metabolic perspective, lysine production depends on a sufficient supply of precursors as well as an accurate regulation of metabolic fluxes. Thus, genetic tools were generated to modify selected genes. The strategies aimed to increase the availability of the essential cofactor NADPH and to manipulate gene expression levels using cofactor-engineering and a promoter library, respectively. In both cases modulation of individual target genes resulted in an increased lysine yield. The developed approaches seem valuable also for other fermentation processes.

II Zusammenfassung

Das Bakterium *Corynebacterium glutamicum* ist der Hauptproduzent für die Aminosäure L-Lysin, einem wichtigen Futtermittelzusatz in der Tiermast. In dieser Studie wurden neue Strategien für die bioprozesstechnische und die genetische Optimierung von *C. glutamicum* für die Produktion von L-Lysin untersucht.

In aeroben Kultivierungen, die üblicherweise in Schüttelkolben durchgeführt werden, ist die Gelöstsauerstoffkonzentration ein kritischer und oft vernachlässigter Parameter. Hier wurde der Sauerstofftransport unter verschiedenen Bedingungen in Einweg-Schüttelkolben bestimmt. Anhand der Ergebnisse wurde ein mathematisches Modell entwickelt, dass die Vorhersage der maximal möglichen Zellkonzentration erlaubt, welche ohne O_2-Limitierung erreicht werden kann. Das entwickelte Modell ist besonders nützlich bei Kultivierungen mit kostspieligen Kohlenstoffquellen und Additiven.

Betrachtet man metabolische Gesichtspunkte, so hängt die Lysin-Produktion von einer ausreichenden Versorgung mit Vorläuferstoffen sowie einer genauen Regulation der Stoffflüsse ab. Daher wurden genetische Tools entwickelt um ausgewählte Gene zu modifizieren. Ziel war es die Verfügbarkeit des Cofaktors NADPH durch Cofaktor-Engineering zu erhöhen sowie Expressionslevel durch eine Promoter-Bibliothek zu manipulieren. In beiden Fällen resultierte die Veränderung einzelner Zielgene in einer Erhöhung der Lysin-Ausbeute. Die entwickelten Verfahren könnten auch für andere Fermentationsprozesse nützlich sein.

1 Introduction

The soil bacterium *Corynebacterium glutamicum* is the major organism for industrial production of amino acids (Becker and Wittmann, 2012b; Ikeda, 2012). Almost 60 years ago, the wild type *C. glutamicum* ATCC 13032 was isolated for the ability to excrete small amounts of L-glutamate (Wittmann and Heinzle, 2002). Alternative designations are *C. glutamicum* DSM 20300, IMET 10482 and NCIB 10025 (Kalinowski, 2005). It is a Gram-positive immobile bacterium with a rod- to club-like morphology and a relatively high GC-content of 53.8 % (Kalinowski et al., 2003).

Shortly after its discovery, first mutant strains of *C. glutamicum* for L-lysine production, an important nutrient in animal feedstock, were patented (Kinoshita et al., 1957; Kinoshita et al., 1961). Back then, strain engineering comprised repeated classical mutagenesis using UV light or chemical mutagens followed by subsequent strain selection (Nakayama et al., 1978). Thus, the integration of random mutations not only resulted in remarkably improved production strains (Leuchtenberger et al., 2005), but also in an accumulation of a number of undesired modifications. As a consequence, traditionally generated production strains tend to nutrient auxotrophies, weak stress tolerance and retarded growth (Kelle et al., 2005; Ohnishi et al., 2002). For example, even though some strains produced lysine with conversion yields of up to 50 % and final lysine titers above 100 g L^{-1} (Ikeda, 2003; Leuchtenberger, 1996), production was typically accompanied by auxotrophies for L-homoserine, L-leucine, thiamin and pantothenic acid, respectively, (Sassi et al., 1998) or extended fermentation times of 5-7 days (Ikeda, 2003).

In the 1970s, new strategies were developed to overcome these limitations. Strains were selected that showed a decreased demand for additional supplements. In these strains, so called leaky strains, the affected pathways were still functional, but on a reduced level. Thus, the required supplement was produced in low intracellular concentrations avoiding feedback-inhibition or repression of key-enzymes (Pfefferle et al., 2003).

In 2003, the complete genome of *C. glutamicum* was sequenced (Ikeda and Nakagawa, 2003; Kalinowski et al., 2003). This and the development of modern techniques to introduce fast and stable genetic modifications facilitated the construction and optimization of more rational designed strains using genetic engineering (Kelle et al., 2005; Kirchner and Tauch, 2003). Due to a better understanding of the regulatory network and the mechanisms involved in lysine production, classical strain construction was gradually rethought. As example “genome-based strain reconstruction” provided first genetically defined lysine production strains (Ohnishi et al., 2002). Extensive analysis of *C. glutamicum* on the level of fluxome (Wittmann et al., 2004), metabolome (Bolten et al., 2007), transcriptome (Wendisch, 2003) and proteome (Schaffer et

al., 2001) then revealed that for an optimal lysine production a sufficient supply of cofactors (e.g. NADPH) and precursors (e.g. oxaloacetate) is essential to optimize production performance (Ikeda and Takeno, 2013; Wittmann and Becker, 2007). More recently, design based systems metabolic engineering enabled strain construction on a global scale providing rationally designed strains. For example, *C. glutamicum* Lys12 bears twelve distinct modifications and achieves a final lysine titer of 120 g L^{-1}, a productivity of 4.0 g L^{-1} h^{-1} and a conversion yield of 0.55 g g^{-1} in fed-batch cultivation (Becker et al., 2011). For this reason, Lys12 was the first strain described that appeared competitive to classically generated strains due to its excellent production properties.

Apart from the genetic background of the strain, process related parameters like pH, temperature and oxygen concentration are important for efficient lysine production. In industry, for example, most fermentations are performed as fed-batch process in stirred-tank bioreactors, whereas in research, batch cultivations in shake-flasks are broadly used. However, the sufficient supply of oxygen during aerobic bacterial growth is often neglected, even though oxygen can easily become limiting due to its low solubility in water (Zimmermann et al., 2006). Thus, a high oxygen transfer rate is essential for microbial growth and product formation in aerobic cultivations (Casas López et al., 2006; Hermann et al., 2001; Tunac, 1989).

Taken together, fermentative production of lysine was improved drastically within the last decades. It is one of the most important biotechnological processes that is expected to reach a world market of 2.5 million tons by 2018 (Byrne, 2014) and a predicted annual growth of up to 8 % (Becker and Wittmann, 2012b) making the identification of new targets for strain engineering an ambitious challenge to remain competitive (Marx et al., 1999). Due to the enormous success of rational strain engineering, further strains were created covering a broad spectrum of different products (Kind et al., 2014; Vogt et al., 2014; Xu et al., 2014b). Today, *C. glutamicum* is an important platform organism for biotechnological fermentation processes of diverse products like diamines (Schneider and Wendisch, 2010), dicarboxylic acids (Okino et al., 2008) and polymers (Liu et al., 2007; Matsumoto et al., 2011) using a broad spectrum of substrates like crude glycerol (Rittmann et al., 2008), hemicellulose (Buschke et al., 2011; Kawaguchi et al., 2006), silage (Neuner and Heinzle, 2011) and many more (Becker and Wittmann, 2012a).

2 Objectives

The aim of the present work was the generation of novel tools to improve lysine production in *C. glutamicum*.

Since oxygen, which has a low solubility in water, is an important substrate in aerobic cultivations a high mass transfer rate is essential. In this regard, a systematic study should be performed to determine the volumetric gas-liquid mass transfer coefficient (k_La), required to evaluate the efficiency of a gas transfer within the liquid phase. Determination should be performed in disposable shake-flasks being important vessels for cultivation in research. Thereby, different parameters like vessel geometry and size as well as filling volume and shaking frequency should be considered. Based on the results a mathematical correlation should be set up to allow a reliable prediction of oxygen transfer rate, oxygen saturation and the maximum cell concentration during aerobic growth.

The second part of this work aimed at genetic engineering of *C. glutamicum*. A first strategy focused on the modulation of the cofactor specificity of NADP(H)-dependent enzymes to NAD(H) on DNA level, using engineering of cofactor specificity. This should be achieved by site-directed mutagenesis of the genes *dapB*, encoding dihydrodipicolinate reductase, and *ddh*, encoding diaminopimelate dehydrogenase, supported by bioinformatics analysis. As a proof of concept, two different *gapDH* genes, encoding glyceraldehyde-3-phosphate dehydrogenase, should be analyzed on their ability to improve lysine production by increasing the availability of NADH and NADPH, respectively. New strains should be further analyzed by cofactor-specific kinetic studies and comparative batch cultivations. A second strategy aimed at controlled regulation of gene expression levels by fine-tuning. Here, a promoter library, based on the strong promoter of superoxide dismutase (P_{sod}), should be constructed by random mutagenesis and used for gene expression studies of the diaminopimelate dehydrogenase, the transketolase operon and the lysine exporter LysE. In detail, characterization of the created mutants should include kinetic and transcriptome analyses as well as comparative cultivations.

3 Theoretical Background

3.1 Discovery of *Corynebacterium glutamicum*

Regarding the historical background of biotechnological fermentation, an important milestone was set by Prof. Kikunae Ikeda in 1908. His original intention was to improve the life expectancy of Japans population that suffered from malnutrition. During his studies, Prof. Ikeda gained different crystals by decomposition of the seaweed *kombu*. One was finally identified as the taste-enhancer monosodium glutamate (Ikeda, 2002). His discovery was a revolution to the Japanese food industry and within short time glutamate became an important additive for the food market. However, its isolation was difficult and harmful to health, since it included decomposition of wheat gluten with HCl.

After World War II the Japanese population suffered from the famine due to food shortages. Consequently, the idea was set to implement an application for the commercial production of food protein by fermentation. It was this innovative idea that eventually led to the industrial production of amino acids and nucleotides and that still marks a breakthrough in biotechnological fermentation (Kinoshita, 1987).

Only a few years later, a large screening program was initiated in the 1950s aiming to discover new organisms that would excrete amino acids, namely glutamate (Kinoshita, 2005). Thus in 1956, a soil bacterium was isolated that accumulated glutamic acid under biotin-limitation (Abe, 1967; Kinoshita et al., 1957). The new organism was initially named *Micrococcus glutamicus* No. 534 (Udaka, 1960). Taxonomical studies revealed *Micrococcus glutamicus* No. 534 as a Gram-positive bacterium with a high GC-content (Abe, 1967). Furthermore, it was found that the bacterium possesses an extraordinary cell wall containing polysaccharides

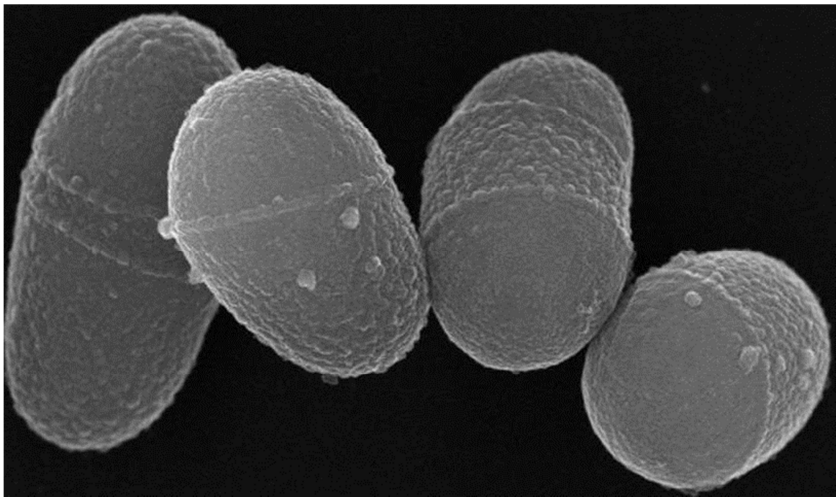

Figure 3-1: Raster electron micrograph of the natural L-glutamate producer *Corynebacterium glutamicum* ATCC13032 cultivated on minimal salt medium with glucose as sole carbon source (Bolten, 2010).

like arabinose and galactose and short-chained mycolic acids of 26-36 carbon atoms. The murrain sacculus consisted of peptidoglycan cross-linked with *meso*-diaminopimelate (Goodfellow et al., 1976; Liebl et al., 1991), while its morphology was rod- to club-like and immobile (Figure 3-1). Due to these facts and its cell wall chemistry regarding mycolic acid as a chemotaxonomic marker, the bacterium was renamed *Corynebacterium glutamicum* and was classified as *Actinobacteria*, order *Actinomycetales*, suborder *Corynebacterineae* and family *Corynebacteriaceae* (Liebl et al., 1991; Stackebrandt et al., 1997). The family of *Corynebacteriaceae* is very diverse and comprises both pathogenic species like *Corynebacterium diphtheriae* as well as saprophytic and non-pathogenic species (Liebl et al., 1991).

From the scientific point of view, *C. glutamicum* offers many advantages. By nature, the organism exhibits a high growth rate, consumes a broad spectrum of different substrates and achieves high cell densities. In addition, its relatively small genome (3,000 kb) is fully sequenced (Haberhauer et al., 2004; Ikeda and Nakagawa, 2003; Kalinowski et al., 2003) and methods to introduce fast and stable genetic modifications have been set up (Kirchner and Tauch, 2003; Sahm et al., 1995). Furthermore, technological developments have enabled analysis of global changes in fluxomics (Wittmann et al., 2004), metabolomics (Bolten et al., 2007) and transcriptomics (Wendisch, 2003) as well as in proteomics (Schaffer et al., 2001). The GRAS (generally recognized as save) status of *C. glutamicum* permits the fermentative production of food additives as well as pharmaceuticals, while the produced biomass can be directly used as animal feedstuff (Wittmann and Becker, 2007).

Regarding economic aspects, the discovery of *C. glutamicum* and the implementation of fermentation processes improved the industrial glutamate production drastically (Ikeda, 2003). Only a few years later, it was found that the bacterium can produce further amino acids (lysine, arginine, ornithine, threonine, etc.) under certain conditions (Kinoshita, 1959). Today, almost all amino acids can be synthesized by fermentation making them the most important biotechnological product with a world market of over four million tons per year. Thereby, the major organisms for industrial production processes are *C. glutamicum* and *Escherichia coli* (Becker and Wittmann, 2012b; Ikeda, 2012).

3.2 Industrial L-Lysine Production

In the last decades, amino acids were utilized in many ways e.g. in the industries for chemicals, pharmaceuticals and cosmetics as well as supplements in dietary and animal feed (Eggeling and Sahm, 1999; Leuchtenberger et al., 2005). Thus, the synthesis of amino acids became a central process in industrial biotechnology (Wittmann and Heinzle, 2002). In contrast to the past, decomposition of a feedstock plays only a subordinate role for the isolation of L-amino acids, today. Instead, fermentative and enzymatic processes are more convenient for large-scale production of pure L-enantiomers (Leuchtenberger et al., 2005).

From the chemical point of view, the basic amino acid lysine consists of six carbon atoms. The secondary amino group has a pK_a-value of 10.8, resulting in a positive charge under physiological conditions (Figure 3-2) (Buddrus and Schmidt, 2011).

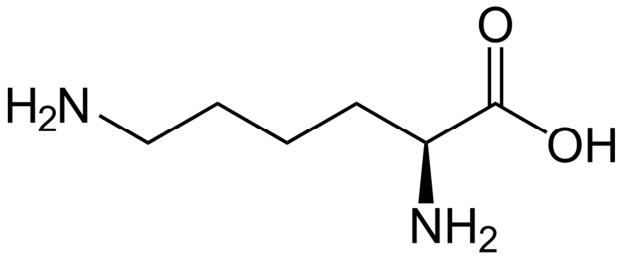

Figure 3-2: Chemical structure of the essential amino acid L-lysine with the formal composition $C_6H_{14}N_2O_2$. Reference: NEUROtiker (WikiCommons).

Since lysine cannot be synthesized by vertebrates, it has to be ingested with food (Xu et al., 2014a). However, the common feed based on wheat, barley and corn is poor in lysine. Thus, supplementation with lysine plays an important role in the fattening of pigs and poultry since 1960 to provide optimal conditions for growth and development (Eggeling and Sahm, 1999). A further advantage of feed additives is the targeted use of the essential compound without the concomitant increase of other amino acids (Pfefferle et al., 2003). In addition, lysine finds applications in human medicine facilitating the absorption of agents or as ingredient of dietary supplement and infusion solutions (Anastassiadis, 2007; Haefner et al., 2007; Oh et al., 1993). More than half a century after the discovery of *C. glutamicum*, the demand for lysine still rises continuously due to the growing meat consumption in developing and emerging countries (Wittmann and Becker, 2007). Associated with the rising demand, the production volume rises steadily resulting in a spiral of increasing competition, reduced prices and even greater demands (Eggeling and Sahm, 1999). To meet the vast needs, bacterial fermentation of carbohydrates became ever more important especially since natural sources for the isolation of lysine like casein-starch and soy are limited (Eggeling and Sahm, 1999). Furthermore, the production efficiency has been drastically improved within the last decades due to systematical strain engineering (Wittmann and Becker, 2007; Becker et al., 2011). Today, *C. glutamicum* is the most popular organism for industrial biosynthesis of lysine (Wittmann and Becker, 2007).
Even though the demand for lysine slumped lately in China as a consequence of diminished animal inventories and a new outbreak of bird flu, the global demand is still growing. According to latest information, the demand for lysine is expected to rise from 1.7 million tons in 2011 to 2.5 million tons by 2018 correlating with an annual growth rate of 5.8 % (Byrne, 2014). In parallel, Becker and Wittmann (2012b) reported that in 2011 the world market for lysine was in fact 1.5 million tons while they even predicted an annual growth of 6-8 %.

In order to meet the high demand for lysine and to guarantee an economical production, nowadays, fermentation is performed in large plants with closely monitored and regulated bioprocesses. Currently, the major suppliers are basically located in Japan (e.g. Ajinomoto), South Korea (e.g. Paik Kwang Industrial and CheilJedang), China (e.g. Global BioChem Technology), India (e.g. Bajaj Healthcare), Germany (e.g. Evonik Degussa Corporation) and the United States (e.g. Archer Daniels Midland) (http://de.panjiva.com/Manufacturers-Of/lysine, 05.08.2014).

Most fermentations are performed as fed-batch process in stirred-tank bioreactors offering optimal yields as well as aeration and production conditions (Kelle et al., 2005). Thereby, the substrate is added in a controlled manner to avoid by-product formation (Kimura, 2005; Leuchtenberger et al., 2005). Within the last decades, fermenter sizes have increased from 50 m^3 to 750 m^3 to benefit from the economy of scale (Ikeda, 2003; Kelle et al., 2005). Consequently, the volume of the inoculum had to be adjusted in parallel to guarantee an optimal initial cell concentration. Thus, successive seed fermentations with increasing culture volumes of up to 50 m^3 are performed (Kelle et al., 2005; Wittmann and Becker, 2007). To assure monoseptic cultivation conditions, it is also of importance that the inoculum preparation is performed under sterile conditions regarding medium preparation, sterilization techniques and plant design as well as operating and maintenance procedures. Already a low level of contaminants might easily outgrow the production strain and the organism with the higher biomass formation yield prevails (Kelle et al., 2005; Marx et al., 2003a). This is also one reason, why continuous fermentation is usually avoided for biosynthesis of lysine. Particularly, the supply of both sterile media and air during the process goes with an increased risk for contamination. In addition, *Corynebacteria* tends to spontaneous mutations under substrate-limited conditions as was reported for a fermentation of L-arginine with *Corynebacterium acetoacidophilum* (Azuma et al., 1988; Azuma and Nakanishi, 1988).

Another important parameter in production of low-cost bulk amino acids like lysine is the choice of the carbon source as this is a major cost factor (Kelle et al., 2005). As depicted in Figure 3-3, fluctuations of the sugar prices have a strong influence on the company's profitability and on global competition resulting in alliances between sugar suppliers and lysine producers (Ikeda, 2003; Wittmann and Becker, 2007). The choice of the advantageous carbon source is also influenced by regional availability of the raw-material. For example, sucrose and dextrose are obtained by hydrolysis of starch from cassava and corn in Asia and the United States, respectively, while sucrose from cane and beet molasses is traditionally used in South America and Europe, respectively (Ikeda, 2003). There is a trend towards utilization of more defined media, avoiding or at least reducing the percentage of complex carbon sources and molasses, which are prone to variation. Thus, better process control and higher purity of the fermentation broth are provided facilitating downstream processing (Kelle et al., 2005).

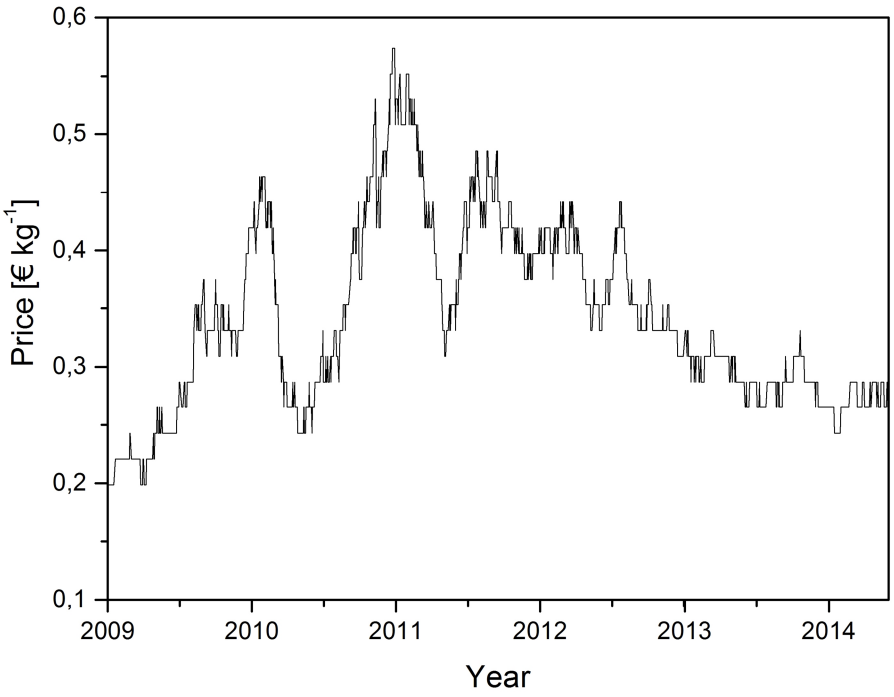

Figure 3-3: Fluctuation of the sugar price in € per kg from January 2009 till June 2014 (http://www.finanzen.net/rohstoffe/zuckerpreis, June 2014).

Apart from carbon, sources for nitrogen, sulphur and phosphate are required as well as optional supplements like amino acids, peptone and corn steep liquor (Ikeda, 2003). To assess the cost efficiency of a production process, it is further essential to regard the conversion yield (Wittmann and Becker, 2007). While during operation parameters like bulk density and a sufficient aeration as well as pH and temperature control are of interest.

Since *C. glutamicum* cannot metabolize lysine and is not inhibited by high extracellular lysine concentrations, fermentation in fed-batch mode is particularly advantageous (Kelle et al., 2005). In addition, efficient purification and formulation of the product is important to reduce the costs of downstream processing (Hermann, 2003). Thereby, downstream processing not only includes cell separation and product isolation, but also the reduction of waste streams. Today, lysine can be purchased in different formulations and purities, depending on the required application. Crystal lysine can be obtained as sulfate salt or as lysine-HCl salt which is less hygroscopic (Kelle et al., 2005). Downstream processing further benefits from the GRAS-status of *C. glutamicum* especially in animal feedstock. Thus, processes have been set up with reduced operating procedures and waste emission like the production of liquid lysine called Biolys® (50 % purity) provided by Evonik Degussa GmbH. In addition, lysine sulfate is available as granulate (40-50 % purity) or as liquid (20-30 % purity) (Kelle et al., 2005). These processes are more economical, provide lower chloride concentrations and offer additional nutrients from the biomass fraction. On the other hand, crystallization processes have fewer restrictions on the quality of the carbon source due to the more extensive purifications steps in downstream processing making them still attractive (Kelle et al., 2005).

To face competition, constant process optimization is required to reduce costs. As a result, repeated fermentation technologies ("semi-continuous") were developed, retaining a certain amount of the fermentation broth as inoculum for the next production cycle (Nakamura et al., 2000). By this, costs and time were saved based on seed and fermenter preparation. Unfortunately, such processes are sensitive to spontaneous mutation by genetically unstable production strains as mentioned before (Hermann, 2003). At present, they are not realized for large scale, yet (Ikeda, 2003). Another problem in present production processes is that traditionally generated production strains are still in use which suffer from auxotrophy and retarded growth, due to undesired mutations (Kelle et al., 2005; Ohnishi et al., 2002). However, it was already shown that modern techniques can overcome these limitations by introduction of only target-oriented mutations (Ohnishi et al., 2002). The generation of sophisticated production strains offers new possibilities for process optimization in future (Becker et al., 2011; Xu et al., 2014b).

3.3 Bioprocess Engineering for improved L-Lysine Production

Besides strain development, the cultivation process itself holds a large potential for optimization. Previous to fermentation, an appropriate cultivation procedure and media composition needs to be chosen, while during fermentation a suitable operational window regarding bulk density, aeration, pH and temperature has to be found. In industry, most fermentations are performed as fed-batch processes in stirred-tank bioreactors offering good performance as well as aeration and production conditions (Kelle et al., 2005), whereas in research batch cultivations in shake-flasks are broadly used. They offer several advantages such as easy handling, high flexibility, parallelization and a high-throughput of experiments (Veglio et al., 1998).
Due to its low solubility in water and, thus, in fermentation media, the mass transfer of oxygen within the liquid phase is a major issue in aerobic cultivations. Especially during screening experiments when rapid bacterial growth requires a high oxygen consumption, a sufficient supply is often neglected (Zimmermann et al., 2006). As a consequence, oxygen can become limiting under unfavorable conditions of mixing and vessel geometry, even though it is crucial for microbial growth and product formation (Casas López et al., 2006; Hermann et al., 2001; Tunac, 1989). Since *C. glutamicum* is a facultative anaerobic to aerobic organism (Collins and Cummins, 1986; Liebl, 2005), oxygen limitation results in the formation of by-products like acetate, lactate and L-alanine derived from pyruvate (Kelle et al., 2005). To avoid this, a high oxygen mass transfer is required, which can be influenced by the shaking frequency and the stirring rate in shake-flasks and stirred-tank bioreactors, respectively. A high power input increases the oxygen transfer rate (OTR) significantly due to a better turbulence and a higher specific area for mass transfer based on smaller gas bubbles. On the other side, the shear rate needs to be considered to avoid mechanical stress by shearing resulting in a decreased productivity (Chmiel and Walitza, 2011). The dissolved oxygen (DO) concentration further

depends on the temperature (Zieminski et al., 1976) and the electrolyte concentration (Schumpe and Deckwer, 1979) as well as the media composition (Rischbieter and Schumpe, 1996) and its viscosity (Akita, 1981).

The driving force of mass transfer is the concentration gradient (Dunn et al., 2003). But since the solubility of oxygen in water is low, this gradient is small as are the driving forces (Chmiel and Walitza, 2011). Figure 3-4 depicts a schematic diagram of the transfer of oxygen from a gas bubble to the reaction site in a biological system (Bailey and Ollis, 1986). The mass transfer is realized by convection and molecular diffusion (Nielsen et al., 2003) and is characterized by different transport resistances:

The first resistant is the transfer through the bulk gas phase to the gas liquid interface (step 1.). From here, the oxygen passes the gas-liquid interface (step 2.) and is transported across the stagnant liquid region (step 3.) and through the well mixed bulk liquid phase (step 4.). For cell pellets and aggregates further barriers need to be considered like the surrounding stagnant liquid region (step 5.), the transport from the liquid to the aggregate (step 6.) and into the pellet (step 7.). Finally, the oxygen needs to pass the bacterial membrane (step 8.) and is transferred to the reaction site (step 9.) which is often neglected due to the small size of most bacterial cells (Nielsen et al., 2003).

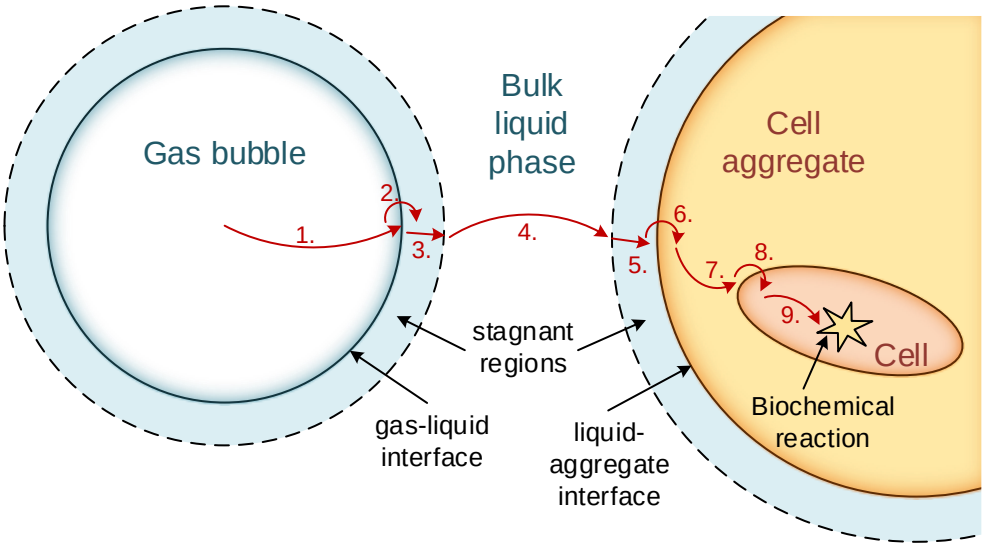

Figure 3-4: Schematic diagram of the resistances that occur during the mass transfer of oxygen from a gas bubble to the reaction site within a bacterial cell. Figure adapted from Bailey and Ollis (1986).

For a sufficient oxygen supply within the medium, the transfer from the bulk gas phase to the bulk liquid phase (step 1.-4.) is of special importance. Since the stagnant region (step 3.) in between is relatively unmixed, oxygen transfer is slow and realized only by diffusion. Thus, it limits the mass transfer rate (Dutta, 2008). Different theories have been developed to describe the oxygen transfer and even though all of them are incomplete, they give an insight into the mechanism of mass transfer at the interface and offer a facilitated model for its calculation.

The first mass transfer theory was the film theory developed by Nernst (1904). Lewis and Whitman (1924) expanded the model, assuming that the stationary interface (step 2.) has a thin laminar film on either side. Here, flow is stagnant and mass transfer only occurs by molecular diffusion. While in the bulk phases turbulent flow guarantees uniform and constant concentrations (c_G and c_L), the interface is in local equilibrium. Thus, the only resistances to mass transfer are the relatively unmixed film layers with the interfacial concentrations c_{Gi} and c_{Li} (Figure 3-5). Based on Fick's law, which describes that the flux of compound A (J_A) is proportional to a constant concentration gradient through the film (Equation 3-1), the mass transfer coefficient k_L depends on the molecular diffusivity of compound A (D_A) and the thickness of the film Z (Equation 3-2).

$$J_A = -D_A \frac{dC}{dZ}$$ **Equation 3-1**

$$k_L = \frac{D_A}{Z}$$ **Equation 3-2**

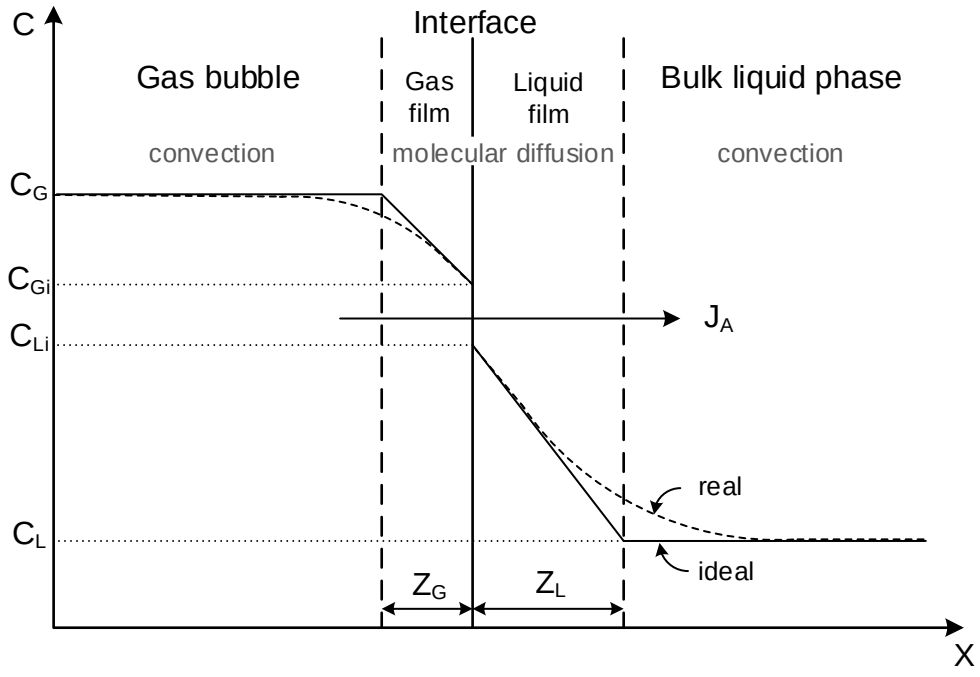

Figure 3-5: Schematic diagram of the concentration gradient of the gaseous compound A during mass transfer into a liquid phase according to the two-film theory. Figure adapted from Christen (2004).

As stated by Fick's law, the mass transfer across the two films is described by Equation 3-3 with Z_G and Z_L representing the thickness of the gas and the liquid films and D_G and D_L for the corresponding effective diffusivities.

$$J_A = D_G \frac{c_G - c_{Gi}}{Z_G} = D_L \frac{c_{Li} - c_L}{Z_L}$$ **Equation 3-3**

Including Equation 3-2, the latter formula can be expressed in terms of the mass transfer coefficients k_G and k_L for both films (Equation 3-4) (Dunn et al., 2003).

$$J_A = k_G(c_G - c_{Gi}) = k_L(c_{Li} - c_L) \quad \textbf{Equation 3-4}$$

At the interface c_{Gi} and c_{Li} are in a local equilibrium. For gases with a low solubility like oxygen and carbon dioxide both concentrations are related to each other by the Henry's law (Nielsen et al., 2003; Taricska et al., 2009):

$$c_{Gi} = H \cdot c_{Li} \quad \textbf{Equation 3-5}$$

The Henry constant is specific for each compound and depends on temperature as well as the chemical composition of the liquid phase (Storhas, 2003). Gases with a low solubility in water further reveal small concentrations gradients in the gaseous phase (c_G - c_{Gi}), as compared to the liquid phase (c_{Li} - c_L) depicted in Figure 3-5. Thus, the main resistance is in the liquid phase (Dunn et al., 2003). In addition, the interfacial concentrations cannot be measured. So, the overall flux in the liquid phase is described by an overall mass transfer coefficient K_L multiplied by the main concentration gradient (Equation 3-6) (Nielsen et al., 2003).

$$J_A = K_L(c_L^* - c_L) \quad \textbf{Equation 3-6}$$

The concentration c_L* is the saturation concentration of the liquid bulk phase which is in equilibrium with the gas bulk phase c_G by the Henry's law.

$$c_L^* = \frac{c_G}{H} \quad \textbf{Equation 3-7}$$

During steady state the mass transfer is constant. Taken together the mass transfer coefficients lead to Equation 3-8 (Chmiel and Walitza, 2011; Nielsen et al., 2003).

$$\frac{1}{K_L} = \frac{1}{k_L} + \frac{1}{H \cdot k_G} \quad \textbf{Equation 3-8}$$

As mentioned before, the main resistance is on the side of the liquid phase. This is also reflected by Equation 3-8. Since k_G is usually considered larger than k_L and the Henry constant for low soluble gases is large, the second term of Equation 3-8 can be neglected (Chmiel and Walitza, 2011; Nielsen et al., 2003).

Finally the reactor volume needs to be included to achieve the volumetric mass transfer rate of compound A (q_A'). As a consequence, the interfacial area (a) is introduced which is defined as the quotient of the bubble's surface (A) to the related liquid volume (V) (Chmiel and Walitza, 2011; Nielsen et al., 2003).

$$q'_A = k_L \frac{A}{V} (c_L^* - c_L) = k_L a (c_L^* - c_L) \quad \textbf{Equation 3-9}$$

Since it is difficult to determine k_L and a separately, their product, termed as volumetric gas-liquid mass transfer coefficient (k_La), is usually calculated together and used to specify the mass transfer (Nielsen et al., 2003). The two-film theory presents a relatively simple relationship between mass transfer coefficient and diffusivity. Since it is just an idealized concept, neither the existence of the films can be proven (Hagen, 2004; Taricska et al., 2009) nor their thicknesses be calculated (Nielsen et al., 2003).

In 1935, Higbie suggested a model where mass transfer is realized by swirling fluid elements, termed as eddies, which travel from the turbulent bulk phase to the laminar film at the interface. It is assumed that each eddy remains at the interface for mass transfer for the same but very short period of time. Thus, the compound is transferred to the surface element (or out) by instationary diffusion during a constant exposure time. Since all elements have the same age when they return to the bulk phase, the film and the interface are replaced frequently. The disadvantage of this model is the assumption that the exposure time for all elements would be identical. Thus, Danckwerts (1951) modified the penetration theory and proposed that the surface elements exist for different periods of time and have different retention times at the interface due to turbulent mixing. As a consequence, the film at the interface is constantly replaced and the time required for mass transfer can be described by a probability function. Unfortunately, the fractional rate of surface renewal cannot be calculated (Dutta, 2008).

DO concentrations and k_La values have been investigated in several studies. It had been shown that related to their material properties, plastic vessels show different wetting properties and consequently differ in their k_La values as compared to common shake-flasks made of glass (Büchs, 2001). Consequently, a sufficient oxygen supply is difficult to predict and, thus, the right choice for an optimal experimental set-up is challenging.

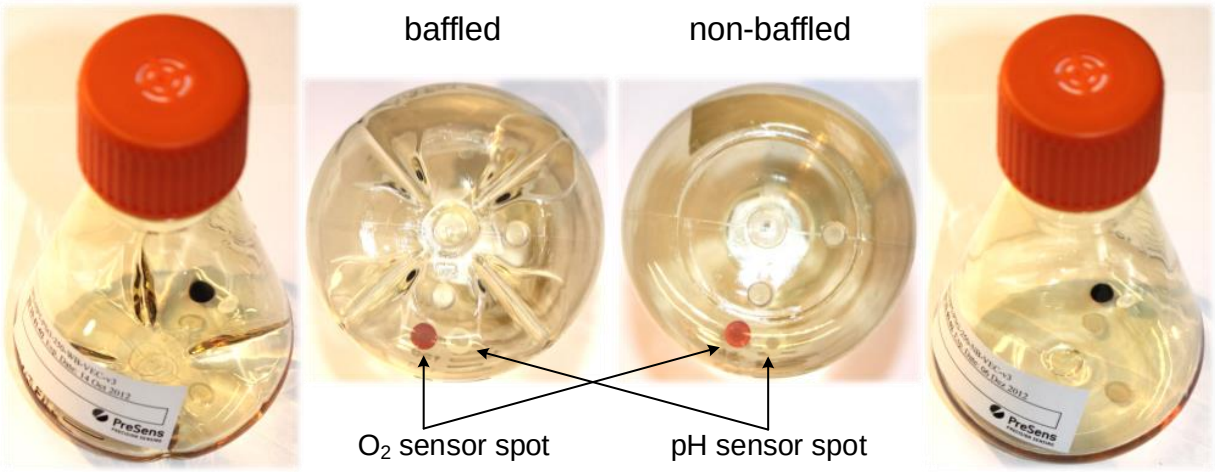

Figure 3-6: Disposable baffled and non-baffled shake-flasks for O_2 and pH determination. The pictures exemplarily show 250 mL flasks. A view of the flasks bottom illustrates the position of baffles and online sensor spots.

Fortunately, conventional vessels equipped with sensor spots for online monitoring of DO are available by now (Ge and Rao, 2012; John et al., 2003; Wittmann et al., 2003). Lately, there is an increasing market for disposable shake-flasks (Figure 3-6) and bioreactors for real-time monitoring of DO as well as pH (Eibl et al., 2010; Schneider et al., 2010). Since the mass transfer can be increased easily by the introduction of baffles within shake-flasks, this finding was transferred to small-scale microbial cultivation systems (Funke et al., 2009). As a result, micro cultivation systems have been developed that possess an extraordinary geometry to guarantee an efficient mass transfer of oxygen even in small reaction volumes (Binder et al., 2012; Huber et al., 2009). Thus, they offer a high-throughput of experiments in parallel required for screening approaches.

3.4 Biosynthesis of L-Lysine by *C. glutamicum* and its Regulation

In microorganisms, the biosynthesis of lysine differs widely. It can be synthesized by two independent routes. One is mostly used by higher fungi, but also by some archaea. It is called the *α*-aminoadipate route using 2-oxoglutarate and acetyl-CoA as precursors for lysine synthesis (Velasco et al., 2002). Bacteria, on the other hand, use the diaminopimelate route based on the precursors aspartate and pyruvate (Wittmann and Becker, 2007). Consequently, the carbon backbone of lysine might have different origins.

The diaminopimelate route can be further distinguished in four different pathways: the acetylase pathway, the aminotransferase pathway, the succinylase pathway and the dehydrogenase pathway (Wittmann and Becker, 2007). The two latter pathways are both active in *C. glutamicum* acting side by side depending on the availability of ammonium ions in the environment. This allows the organism to react flexibly on changing conditions. Since diaminopimelate dehydrogenase (DDH) has a low affinity to ammonium (Sahm et al., 2000), it is only active at high concentrations to catalyze the conversion of tetrahydrodipicolinate to *meso*-diaminopimelate while the succinylase pathway is independent from inorganic ammonium thereby incorporating ammonium from a transaminase reaction. Here, an enzyme cascade is responsible for the formation of *meso*-diaminopimelate. The further decarboxylation of *meso*-diaminopimelate results in the formation of lysine which is excreted by the lysine permease (LysE) (Vrljic et al., 1996). In addition to that, *meso*-diaminopimelate is also an important intermediate for the biosynthesis of the murein sacculus (Wehrmann et al., 1998). In total, one mol of lysine (C_6) is synthesized from aspartate (C_4) and pyruvate (C_3) under the consumption of reducing power provided by four mol of NADPH and the depletion of one mol of CO_2 (Michal and Schomburg, 2012). As a consequence, synthesis of lysine is closely linked to the central carbon metabolism depending on a constant supply of building blocks and energy. For a better understanding of this complex network, the metabolic pathways of *C. glutamicum* are depicted in Figure 3-7.

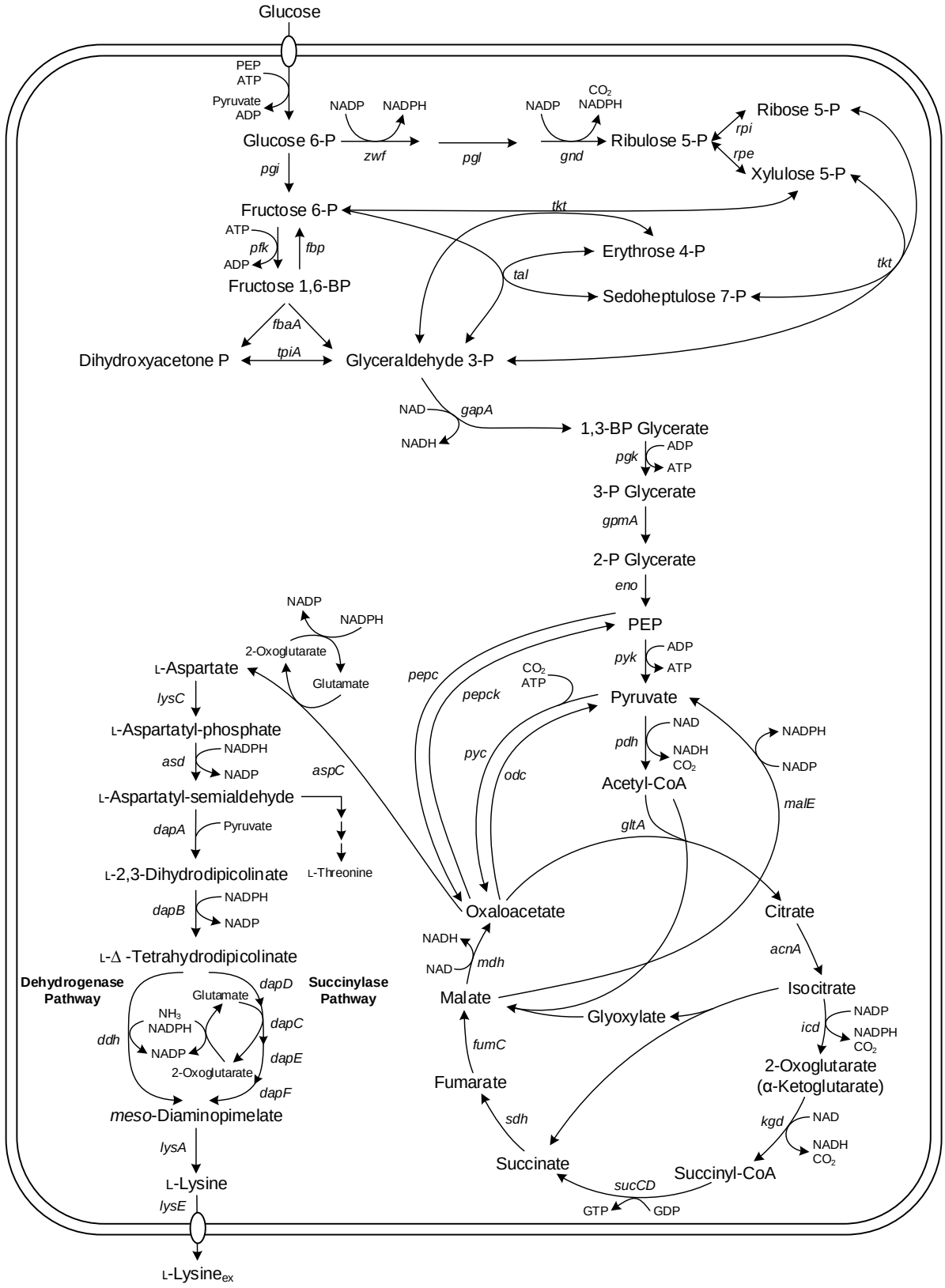

Figure 3-7: Biochemical network for the biosynthesis of lysine and the central carbon metabolism in *C. glutamicum* comprising the glycolysis, the pentose phosphate pathway, the pyruvate node and the tricarboxylic acid cycle. The enzymes involved in the formation of lysine are aspartate kinase (*lysC*), aspartate-semialdehyde dehydrogenase (*asd*), dihydrodipicolinate synthase (*dapA*), dihydrodipicolinate reductase (*dapB*) and subsequent split into (i) the dehydrogenase pathway with diaminopimelate dehydrogenase (*ddh*) and (ii) the succinylase-pathway consisting of tetrahydrodipicolinate succinylase (*dapD*), succinyl-amino-ketoimelate transaminase (*dapC*), succinyl-diaminopimelate desuccinylase (*dapE*), diaminopimelate epimerase (*dapF*). The product *meso*-diaminopimelate is further converted to lysine via the diaminopimelate decarboxylase (*lysA*) and secreted via lysine permease (*lysE*).

As mentioned before, *C. glutamicum* can consume a broad spectrum of different substrates. The major sugars used in industrial fermentation of lysine are glucose, fructose and sucrose derived from starch hydrolysates and molasses. In *C. glutamicum* sugar up-take is realized by a phosphoenolpyruvate (PEP) dependent system, called phosphotransferase system (PTS) (Ikeda, 2012; Moon et al., 2007). During its transport across the bacterial membrane a phosphate residue from PEP is transferred to the sugar molecule catalyzed by special enzyme complexes (Barabote and Saier, 2005; Simoni et al., 1967). Afterwards, the substrate is further metabolized by the central carbon metabolism which comprises the glycolysis, the pentose phosphate pathway (PPP), the pyruvate node and the tricarboxylic acid (TCA) cycle, while the Entner-Doudoroff pathway has not been detected (Eikmanns, 2005; Vallino and Stephanopoulos, 1993; Wittmann et al., 2004; Yokota and Lindley, 2005). Within the PPP 2 mol of NADPH are generated per mol of glucose-6-phosphate via glucose 6-phosphate dehydrogenase (Ihnen and Demain, 1969; Moritz et al., 2000) and 6-phosphogluconate dehydrogenase (Moritz et al., 2000; Ohnishi et al., 2005). Thus, the PPP meets the need of the organism for sufficient supply of anabolic reducing power as well as important metabolites (ribose-5-phosphate and erythrose-4-phosphate), required for the biosynthesis of building blocks (Yokota and Lindley, 2005). Glycolysis involves a series of reactions that finally lead to the formation of pyruvate. It is the most important pathway of fueling reactions providing precursor metabolites required for the formation of anaplerotic building-blocks (Stephanopoulos, 1998; Yokota and Lindley, 2005). Pyruvate is the central metabolite of a complex network, which is responsible for the equilibration of metabolites in the direction of the TCA cycle as well as glycolysis (Sauer and Eikmanns, 2005). The latter is realized by anaplerotic reactions like the conversion of oxaloacetate (C_4) from the TCA cycle to PEP (C_3) catalyzed by PEP-carboxykinase (PEPCK) as well as the reaction of malic enzyme (ME) regenerating NADPH (Wittmann and De Graaf, 2005). The major role of the TCA cycle is the complete oxidation of acetyl-CoA to carbon dioxide providing reducing equivalents (NADH, FADH, GTP) required for the generation of ATP in the respiratory chain. Among the oxidative decarboxylation step of the TCA cycle, NADP is used as a cofactor by the isocitrate dehydrogenase and reduced to NADPH. Another important intermediate is oxaloacetate the precursor of aspartate and, hence, of lysine. Consequently, the TCA cycle serves not only for anabolism, but also for catabolism, offering a high flexibility for metabolic needs by its reversibility (Eikmanns, 2005; Wittmann and Heinzle, 2002).

Natural lysine biosynthesis from aspartate is regulated by feedback-inhibition of aspartate kinase (LysC). LysC is a heterotetramer, consisting of two *α*- and two *β*-units (Yoshida et al., 2007). The genes of both subunits are encoded by the same locus, exhibiting an in-frame overlap (Kalinowski et al., 1991). The catalytic domain of LysC is located at the N-terminal region of the *α*-subunit while the regulatory domain is formed via the C-terminal region of the

α-subunit and the *β*-subunit (Yoshida et al., 2007). Inhibition is initiated by the concerted binding of the end products lysine and threonine to the regulatory domain at high intracellular concentrations (Kalinowski et al., 1991). As a result, the activity of LysC is nearly completely inhibited (Lee, 2005).

3.5 Molecular Strategies for improved L-Lysine Production

Today, the metabolism of *C. glutamicum* can be altered easily via introduction of genetic modifications (Schrumpf et al., 1992). The knowledge of metabolic fluxes and their regulatory mechanisms offers the possibility to improve lysine production rationally by target-oriented genetic engineering. Therefore, the central carbon metabolisms, namely the PPP, the TCA cycle and the lysine biosynthesis pathway are of special interest for strain construction providing a sufficient supply of cofactors and precursors. In general, breeding for high-producing strains focused on an improved precursor supply, namely oxaloacetate, pyruvate and NADPH, combined with a reduction of the by-product formation. In order to realize these strategies, a broad spectrum of target-oriented approaches were developed including identification and isolation of the target genes followed by plasmid construction, transformation and implementation of the modification. As a result, the target gene can be amplified, deleted, deregulated or transferred within a desired production host (Jäger et al., 1992; Kirchner and Tauch, 2003; Tauch et al., 2003; Xie and Tsong, 1990). In the last years, several targets were identified focusing on different strategies to optimize lysine production.

3.5.1 Removal of undesired feedback control

The aspartate kinase, encoded by *lysC*, is the key enzyme of the lysine biosynthesis pathway. Feedback inhibition is mediated by the concerted binding of the end products lysine and threonine derived from aspartate as described before. Today, it is known that deregulation of LysC is essential for the biosynthesis of lysine which can be achieved by different amino acid exchanges offering a large patent coverage (Kelle et al., 2005).

3.5.2 Metabolic engineering of L-lysine biosynthesis and reduction of by-product formation

In addition, overexpression of *lysC*, for example via promoter exchange, turned out to affect lysine production positively due to redirection of the carbon fluxes towards this end product. Being organized in the same operon, the gene *asd*, encoding aspartate semialdehyde dehydrogenase, is overexpressed as well (Cremer et al., 1991). Its product aspartate semialdehyde marks an important branch point in the biosynthesis of amino acids derived from aspartate. The first enzyme of the competitive pathway that leads to the formation of L-threonine is

the homoserine dehydrogenase (Hom). This enzyme also exhibits a stronger specific activity for aspartate semialdehyde, as compared to the dihydrodipicolinate synthase (Miyajima and Shiio, 1970). To assure an efficient lysine production, it is indispensable to reduce the formation of by-products. So, it was found that the addition of 5 mM L-methionine inhibited the gene expression of Hom (Miyajima and Shiio, 1971; Morinaga et al., 1987; Vrljic et al., 1995) while another strategy focused on distinct point mutations to modify the allosteric control of Hom on a molecular basis (Archer et al., 1991; Reinscheid et al., 1991).

The biosynthesis of *meso*-diaminopimelate, an important building-block for the biosynthesis of lysine and peptidoglycan (Wehrmann et al., 1998), is catalyzed by two competitive pathways either the diaminopimelate or the succinylase pathway. Since DDH has a low affinity towards NH_3 by nature (Wehrmann et al., 1998), adaption of the medium by supplementation with ammonium is recommended for lysine production (Wittmann and Becker, 2007).

3.5.3 Improvement of precursor supply and NADPH availability

Besides these strategies, it is important to provide a sufficient supply of precursors and co-factors that are directly involved in lysine production (Ikeda and Takeno, 2013; Wittmann and Becker, 2007). Labeling experiments revealed the supply of oxaloacetate as bottleneck in lysine production. According to the results, carboxylic reactions around the pyruvate node are positively correlated with an optimized oxaloacetate production while decarboxylating enzymes rather support the consumption of oxaloacetate (Wittmann and Heinzle, 2001; Wittmann and Heinzle, 2002). Experiments confirmed that the pyruvate carboxylase is the major bottle neck in lysine production (Peters-Wendisch et al., 2001). The enzyme catalyzes the direct conversion of pyruvate to oxaloacetate by the incorporation of CO_2. Overexpression of pyruvate carboxylase improved lysine production significantly as well as the deletion of PEP carboxykinase (Petersen et al., 2001; Peters-Wendisch et al., 2001; Riedel et al., 2001) and the deregulation of the feedback inhibition of PEP carboxylase, as reported recently (Chen et al., 2014). In addition to oxaloacetate, the availability of NADPH as electron carrier is essential for the biosynthesis of lysine. Flux analysis identified the PPP as major pathway for the regeneration of NADPH and predicted a positive correlation between an increased activity of the PPP and lysine formation. Thus, different strategies were developed to force a redirection of metabolic fluxes through the PPP including disruption of the *pgi* gene (Marx et al., 2003b), overexpression of the *fbp* gene (Becker et al., 2005) and the *tkt*-operon (Becker et al., 2011) as well as modification of the *gnd* gene to release the enzyme from feedback inhibition (Ohnishi et al., 2005). These modifications are even more important for cultivations using fructose as carbon source. Here, only 14.4 % of the carbon flux is directed through the PPP, as compared to 62.3 % on glucose (Kiefer et al., 2004).

3.6 Novel Approaches for optimized L-Lysine Production

Strain breeding is an iterative process characterized by a strong competitive pressure due to its innovative strength always searching for new targets to patent. Especially rational strain designs gained more popularity in the last decade. Lately, new and efficient strategies for metabolic engineering have been developed focusing, for example, on engineering of cofactor use and the construction of promoter libraries to improve the cofactor's availability and the gene expression level, respectively.

3.6.1 Engineering of cofactor use in enzymes of *C. glutamicum*

In general, engineering of cofactor specificity implies the manipulation of a cofactor's concentration in order to improve the production of a desired compound. While traditional attempts focused on a redirection of metabolic fluxes via overexpression (Becker et al., 2011) or deletion (Chemler et al., 2010), new strategies aim to modify the cofactor binding site of a certain enzyme on DNA level (Wang et al., 2013). As a consequence, the type of cofactor and its amount can be manipulated specifically to optimize the metabolic network. Many studies focused on the alteration of the cofactor specificity for NAD(H) and NADP(H), which only differ by their residue at the 2' position of the adenosine ribose (Bommareddy et al., 2014; Hoelsch et al., 2013; Katzberg et al., 2010). While the former cofactor has a hydroxyl group, NADPH is characterized by its phosphomonoester group, making it much less stable than NADH (Wu et al., 1986). Coenzyme specificity is mediated by interaction of these residues with the nucleotide binding fold of the enzyme which, in general, shows a preference for a distinct cofactor (Lunzer et al., 2005). Interestingly, for many NADP(H)-dependent dehydrogenases a higher cofactor specificity was observed than for NAD(H)-dependent suggesting that the hydroxyl group allows fewer specific enzyme-cofactor interactions than does the 2'-phosphate group (Chen and Yang, 2000).

The nucleotide binding fold is typically characterized by two symmetrical sets of Rossmann folds, a secondary sequence motive consisting of α and β helices (Rossmann et al., 1974). The two halves of the α/β-structure can vary in their consistence but are usually connected by an α-helix. A classical Rossmann fold is the $\beta_1\alpha_1\beta_2\alpha_2\beta_3$-motif. Together with the second mononucleotide binding domain ($\beta_4\alpha_4\beta_5\alpha_5\beta_6$), both motifs form a six-stranded topology consisting of parallel β-sheets flanked by α-helices (Figure 3-8) (Bottoms et al., 2002; Rossmann et al., 1974).

Even though Rossmann folds are very common motifs that share certain structural similarities, the primary sequence shows large variations apart from some homologies (Dym and Eisenberg, 2001; Wierenga et al., 1985). Its most prominent characteristics are three conserved glycine (Gly) molecules in a specific spacing preceded by hydrophobic amino acids. This Gly-rich motive is also used as "fingerprint" required for the identification of binding folds

(Wierenga et al., 1986). Thus, for different NAD(P)(H)-dependent dehydrogenases, for example, very similar consensus sequences have been identified which are characterized by a conserved (V/I)(A/G)(V/I)-XGX(X)GXXG motif (Cirilli et al., 2003; Pisabarro et al., 1993).

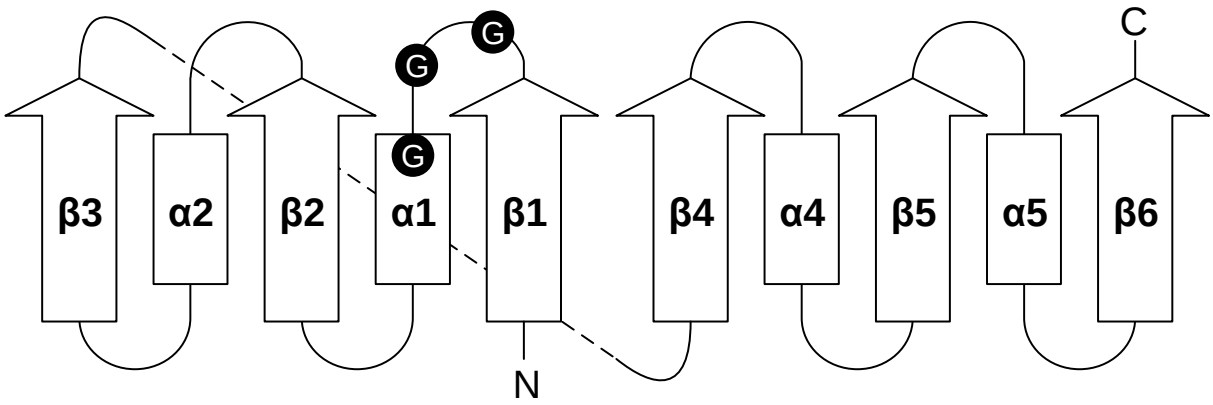

Figure 3-8: Schematic diagram of a classical Rossmann fold. Arrows indicate β-strands while α-helices are depicted by rectangles. Figure adapted from Bottoms et al. (2002).

Usually, the first glycine residue of the motif is located at the C-terminus of the first *β*-strand forming a tight loop of the protein backbone, while the latter glycine residues are located at or near the N-terminus of the adjacent *α*-helix. Being the smallest amino acid, the glycine motif facilitates a close interaction between the cofactor and the enzyme (Geertz-Hansen et al., 2014). Approximately 20-30 amino acids downstream of this Gly-rich region, at the C-terminus of the second *β*-strand, another important residue is located that gives evidence of the enzyme's specificity for a certain cofactor. Here, basic residues, in general, indicate a NADP(H) specificity while acidic residues rather interact with NAD(H) (Wierenga et al., 1985). In detail, the nucleotide binding fold interacts with the 2'- and 3'-hydroxyl group of the adenosyl ribose ring and with the negatively charged 2'-phosphate of NADP(H), respectively, via hydrogen bonds (Cirilli et al., 2003; Reddy et al., 1996). Thereby, acidic residues like aspartate (Asp) and glutamate (Glu) are typically found in NAD(H)-dependent enzymes but have also been identified in those with a dual specificity as well as NADP(H)-dependency, while basic residues, especially arginine (Arg), are supposed to be found in NADP(H)-dependent enzymes (Scrutton et al., 1990).

Usually, rational protein design is accompanied by sequence alignments and computational simulations using three-dimensional structural models (Katzberg et al., 2010; Lunzer et al., 2005). By site-directed mutagenesis, predicted amino acids can be manipulated according to the computational design (Chen et al., 2013; Chen et al., 2014). As a result, Katzberg et al. (2010) successfully modified the cofactor specificity of a NADP(H)-dependent dehydrogenase, designated as Gre2p ("genes de respuesta a estres" (stress-response gene)), from *Saccharomyces cerevisiae* by two different single amino acid exchanges from polar but uncharged (Asn) to charged (Asp or Glu) leading to a close-to-balance dual cofactor specificity.

Introduction of distinct point mutations is advantageous for industrial processes. They offer new possibilities to maximize production and a large patent coverage. In addition, genetic modifications provide a deeper insight in the functionality of enzymes and their architecture. These information are essential for rational protein engineering as they facilitate the future design of tailor made enzymes as well as save experimental time (Katzberg et al., 2010).

3.6.2 Synthetic promoter libraries

Optimal production conditions require an accurate adjustment of metabolic fluxes. Classical attempts focused either on the deletion of a target gene or its overexpression via strong promoters followed by subsequent evaluation of the effects. This, however, does not allow an integrated approach since only discrete extremes were observed. Another strategy to improve production is the modulation of gene expression in a quasi-continuum of discrete expression levels by promoter libraries (Hammer et al., 2006).

Promoters are important regulatory elements containing different sequence motifs that control and influence transcription as well as translation of the subsequent gene (Figure 3-9). It was found that the rate-limiting step in mRNA transcription is its initiation at the transcription start site (TSS) at position +1 rather than the elongation step (Jacques and Dreyfus, 1990; Petern and Pearson, 1975). Recognition of the promoter is facilitated by the -35 element, the -10 element and the spacer in between as well as the extended -10 element. In *E. coli* those elements have the consensus sequences $^{-35}$TTGACA^{-30}, $^{-12}$TATAAT^{-7} and $^{-15}$TG^{-14}, respectively, while the spacer sequence is variable (Hook-Barnard and Hinton, 2007). Pátek et al. (2013) reported that the consensus sequence of the -35 and the extended -10 element of housekeeping promoters in *C. glutamicum* would be $^{-35}$TTGNCA^{-30} and $^{-14}$GNTANANTNG^{-5}, respectively. In *E. coli* the spacer length can vary from 15-19 bp with an optimum of 17 bp (Robison et al., 1998) while in *C. glutamicum* most spacer comprise 17 ± 1 bp (Pátek and Nešvera, 2013).

Previous to transcription initiation, double-stranded DNA (dsDNA) is partly melted due to thermal fluctuations allowing transcription factors, namely σ^{70} factors in both *E. coli* and *C. glutamicum* (Paget and Helmann, 2003; Pátek and Nešvera, 2011), to interact with the single-stranded DNA (ssDNA) at position -11 to -7 of the -10 element (Murakami and Darst, 2003). In addition, further σ^{70} factors bind to dsDNA of the -35 element, the extended -10 element and the -12 base of the -10 element (Murakami and Darst, 2003). This underlines the importance of these regulatory sequence elements for gene expression. Interestingly, bases of the -35 element are less conserved in *C. glutamicum* than those of the -10 element (Pátek, 2005). Furthermore, it was found that the spacer influences the promoter's strength significantly (Jensen and Hammer, 1998b) making it an interesting target for the construction of promoter libraries (Rytter et al., 2014; Tornøe et al., 2002).

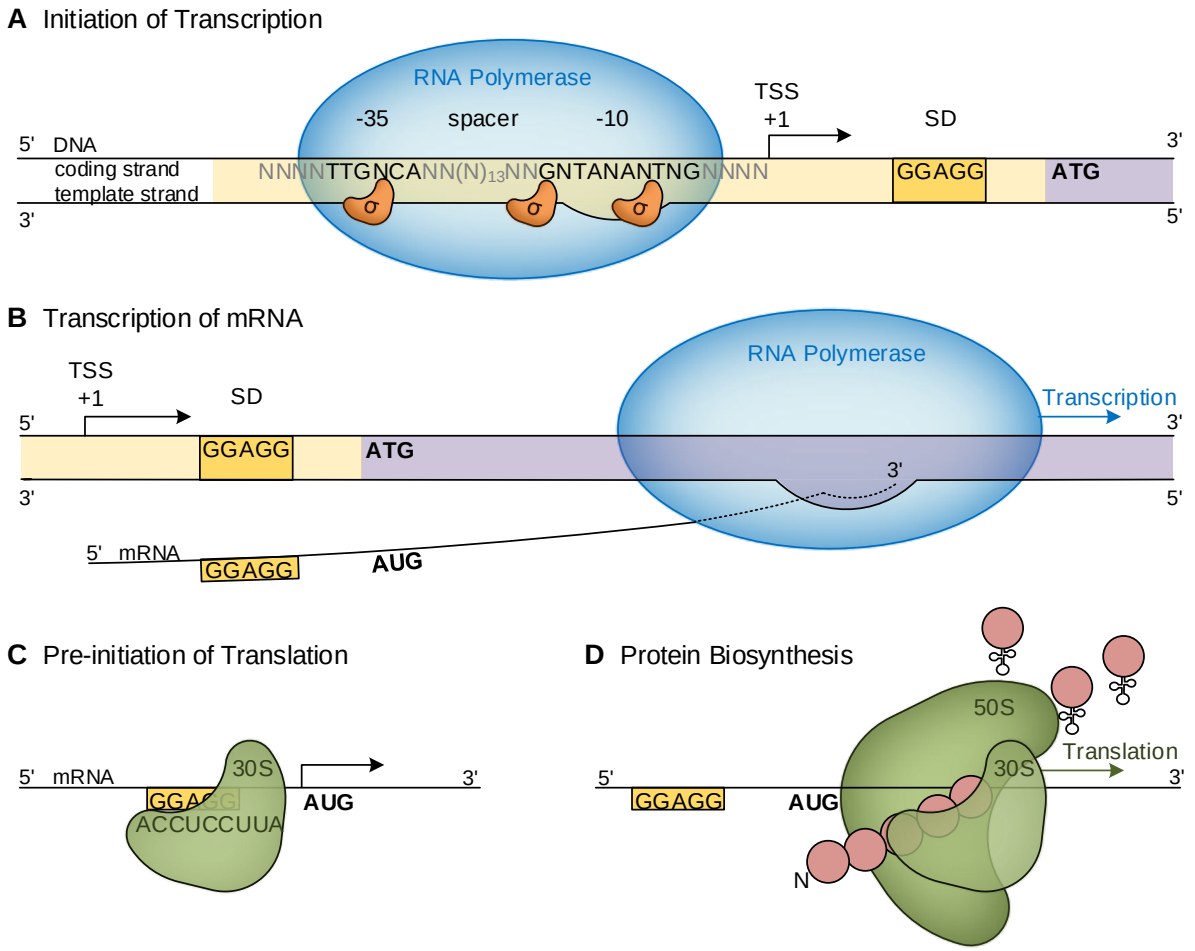

Figure 3-9: Schematic diagram of a classical promoter and its influence on transcription and translation. The promoter (yellow area) includes the -35 and -10 element, the spacer in between and the transcription start site (TSS) at position +1 as well as the Shine-Dalgarno (SD) sequence. Transcription is initiated by the binding of the RNA polymerase (blue) to the sigma factors (orange) (A). The gene (purple area) is transcribed into mRNA from 3'→5' beginning at position +1 (B). For translation, the complementary 16S rRNA anchors the small ribosomal subunit (30S) to the mRNA (C). Protein biosynthesis (red) is initiated at the start codon (here: AUG) after binding of the 50S subunit to form a 70S complex (green) (D). The graphic depicts classical consensus sequences identified for the -35 and -10 element, the SD sequence and the 16S rRNA.

Transcription is initiated by binding of the core RNA polymerase to σ factors, forming a RNA polymerase holoenzyme complex. During elongation, RNA polymerase traverses the template DNA from 3'→5' synthesizing mRNA, required for protein translation. For that reason, the promoter sequence holds a further motive, i.e. the Shine-Dalgarno (SD) sequence, where the ribosome binds previous to translation (Shine and Dalgarno, 1974; Shine and Dalgarno, 1975). It is located within the 5' UTR (untranslated region), also termed as leader sequence, of the mRNA reaching from the TSS to the first base upstream of the start codon which is the start site of translation. This sequence typically contains a short purine-rich sequence (typical core motif GGAGG) which is complementary to the highly conserved 3' end of the 16S rRNA (5'-ACCUCCUUA-3') anchoring the small ribosomal subunit (30S) to the mRNA (Shine and Dalgarno, 1974; Shine and Dalgarno, 1975). Thus, a pre-initiation complex is formed

(Dontsova et al., 1991). Next, the 50S ribosomal subunit is joined mediated by different initiation factors to form a 70S complex initializing translation of the open reading frame (ORF).
Being an important recognition motif, modulation of the SD sequence strongly influences protein synthesis (Band and Henner, 1984; Jacob et al., 1987; Zhou and Petracca, 2000). Interestingly, several genes in *C. glutamicum* have been found without a SD sequence resulting in leaderless transcripts (Pátek, 2005). Here, the 70S complex is directly bound to initiate translation (Moll et al., 2002; Udagawa et al., 2004), but until now their regulatory function is not completely understood (Pátek and Nešvera, 2013).
Since the regulatory elements mentioned influence gene expression, they are favored targets for the construction of promoter libraries. One attempt to create promoters of varied strength is the construction of synthetic promoter libraries (SPL). Here, special primers are used including conserved sequences for the -35 and -10 elements with a randomized spacer sequence in between. These randomized promoters allow the conjunction with a target gene via a homologue overhang using only one PCR step (Jensen and Hammer, 1998a; Solem and Jensen, 2002). By doing so, this strategy permits the construction of inducible promoter libraries by introduction of operator- or activator-binding sites within the sequence of the oligonucleotide (Hammer et al., 2006). Another approach focused on the modulation of native promoters using mutagenic PCR. The randomized promoters are linked to a reporter gene for example *lux*, encoding luciferase, or *gfp*, encoding green fluorescent protein. Afterwards, the library is screened and certain promoters are selected for the linkage with a target gene requiring further PCR steps (Alper et al., 2005). Hammer et al. (2006) reasoned that compared to the SPL technology the mutagenic PCR would be less efficient since less useful promoters were obtained resulting in extensive pre-screenings. On the other hand, the use of reporter genes permits a pre-calculation of the promoter's strength facilitating the selection procedure.
Nevertheless, both strategies function in the same manner and show the same potential to tune gene expression in a broad range but also precisely (Hammer et al., 2006; Mijakovic et al., 2005). Promoter libraries have been tested successfully in many organisms including *E. coli* (Koebmann et al., 2002; Lutz and Bujard, 1997), *Pichia pastoris* (Hartner et al., 2008; Qin et al., 2011) and *C. glutamicum*. Thus, they have the potential to optimize already existing rationally designed production strains for desired traits by re-creating their metabolic networks to achieve a targeted modulation of protein expression.

4 Materials and Methods

4.1 Strains

E. coli DH5α and NM522 were obtained from Invitrogen (Karlsruhe, Germany). Both strains were used as hosts for vector amplification, while NM522 bearing the plasmid pTc additionally allowed a *C. glutamicum* specific DNA-methylation.

The wild-type *C. glutamicum* ATCC 13032 (American Type Strain and Culture Collection, Manassas, VA, USA) was used as background for strain construction by genetic engineering. Sequence information was derived from the KEGG database (www.genome.jp/kegg). Table 4-1 lists all strains, used in the present work.

Table 4-1: Bacterial strains used in the present work for metabolic and genetic engineering

Strain	Description and Application	Reference
E. coli DH5α	Heat shock competent *Escherichia coli* used for amplification of the transformation vector	Invitrogen
E. coli NM522	Heat shock competent *E. coli* used for amplification of the transformation vector, cells further bear the plasmid pTc required for DNA-methylation	Invitrogen
C. glutamicum ATCC 13032	Wild type of *Corynebacterium glutamicum*	ATCC
BS1	*C. glutamicum* ATCC 13032+ lysC^{T311I} Feedback resistant aspartokinase by nucleotide exchange in *lysC* (*cg0306*) resulting in the amino acid exchange T311I	(Becker et al., 2005)
BS27	BS1 + Δ*ddh* Deletion of *ddh* (*cg2900*), encoding diaminopimelate dehydrogenase	BASF SE
BS222	BS1 + 2x*ddh* Overexpression of *ddh* (*cg2900*), encoding diaminopimelate dehydrogenase, by implementation of an additional gene copy	(Becker et al., 2011)
BS242	BS222 + Δ*pck*, P$_{sod}$*dapB, 2xlysA,* P$_{sod}$*lysC, hom*^{V59A}, P$_{sod}$*pyc*^{P458S}, *icd*$^{ATG\rightarrow GTG}$, P$_{eftu}$*fbp* Deletion of *pck* (*cg3169*), encoding PEP-carboxykinase + overexpression of *dapB* (*cg2163*), encoding dihydrodipicolinate reductase, *pyc* (*cg0791*), encoding pyruvate carboxylase, and *lysC* (*cg0306*) by replacement of the native promoter by the *sod* promoter + overexpression of *lysA* (*cg1334*), encoding diaminopimelate decarboxylase, by implementation of an additional gene copy + nucleotide exchanges in *hom* (*cg1337*), encoding homoserine dehydrogenase, and *pyc* (*cg0791*) resulting in the amino acid exchanges V59A and P458S, respectively + replacement of the start codon of *icd* (*cg0766*), encoding isocitrate dehydrogenase, from ATG to GTG + overexpression of *fbp* (*cg1157*), encoding fructose 1,6-bisphosphatase, by replacement of the native promoter by the *eftu* promoter	(Becker et al., 2011)
BS244	BS242 + P$_{sod}$*tkt* Overexpression of the *tkt*-operon comprising the genes *tkt* (*cg1774*), encoding transketolase, *tal* (*cg1776*), encoding transaldolase, *zwf* (*cg1778*), encoding glucose-6-phosphate 1-dehydrogenase, *opcA* (*cg1779*), encoding a putative subunit of glucose 6-phosphate dehydrogenase and *pgl* (*cg1780*), encoding 6-phosphogluconolactonase, by replacement of the native promoter by the *sod* promoter	(Becker et al., 2011)

Strain	Description and Application	Reference
BS290	BS244 + P_{sod}*lysE* Overexpression of *lysE* (*cg1224*), encoding the lysine efflux permease, by replacement of the native promoter by the *sod* promoter	IBVT, Braunschweig
BS343	BS1 + pClik_5a_MCS Episomal expression of pClik_5a_MCS; used as reference	This work
BS344	BS244 + pClik_5a_MCS Episomal expression of pClik_5a_MCS; used as reference	This work
BS371	BS1 + pClik_5a_MCS_*dapB*_R Overexpression of *dapB* (*cg2163*), encoding dihydrodipicolinate reductase, with native cofactor binding site: AEIGVDDD (amino acid (aa) 32-39) by episomal gene expression; used as reference	This work
BS372	BS1 + pClik_5a_MCS_*dapB*_1 Overexpression of *dapB* (*cg2163*) with modified cofactor binding site: AELDAGDP (aa 32-39) by episomal gene expression	This work
BS373	BS1 + pClik_5a_MCS_*dapB*_2 Overexpression of *dapB* (*cg2163*) with modified cofactor binding site: AELDAGDD (aa 32-39) by episomal gene expression	This work
BS374	BS1 + pClik_5a_MCS_*dapB*_3 Overexpression of *dapB* (*cg2163*) with modified cofactor binding site: AEIDADDD (aa 32-39) by episomal gene expression	This work
BS375	BS1 + pClik_5a_MCS_*dapB*_4 Overexpression of *dapB* (*cg2163*) with modified cofactor binding site: AELEAGDD (aa 32-39) by episomal gene expression	This work
BS376	BS1 + pClik_5a_MCS_*dapB*_5 Overexpression of *dapB* (*cg2163*) with modified cofactor binding site: AALEAGDD (aa 32-39) by episomal gene expression	This work
BS383	BS1 + pClik_5a_MCS_*gapN* Overexpression of *gapN* (SMU_676), encoding NADP-dependent glyceraldehyde-3-phosphate dehydrogenase, by episomal gene expression	This work
BS384	BS244 + pClik_5a_MCS_*gapN* Overexpression of *gapN* (SMU_676) by episomal gene expression	This work
BS388	BS181 + P_{sod}*GFPmut1* Overexpression of the reporter gene *GFPmut1* (Cormack et al., 1996), encoding green fluorescent protein of the jellyfish *Aequorea victoria*	Previous work
BS453	BS244 + pClik_5a_MCS_P_{eftu}*ddh*_R Overexpression of *ddh* (*cg2900*), encoding diaminopimelate dehydrogenase, with native cofactor binding site: IFSRR (aa 33-37) by episomal gene expression and replacement of the native promoter by the *eftu* promoter; used as reference	This work
BS454	BS244 + pClik_5a_MCS_P_{eftu}*ddh*_1 Overexpression of *ddh* (*cg2900*) with modified cofactor binding site: IFERR (aa 33-37) by episomal gene expression and replacement of the native promoter by the *eftu* promoter	This work
BS474	BS27 + pClik_5a_MCS_P_{eftu}*ddh*_R Overexpression of native *ddh* (*cg2900*), encoding diaminopimelate dehydrogenase, native cofactor binding site: IFSRR (aa 33-37) by episomal gene expression and replacement of the native promoter by the *eftu* promoter; used as reference	This work
BS475	BS27 + pClik_5a_MCS_P_{eftu}*ddh*_1 Overexpression of *ddh* (*cg2900*) with modified cofactor binding site: IFERR (aa 33-37) by episomal gene expression and replacement of the native promoter by the *eftu* promoter	This work

Strain	Description and Application	Reference
BS476	BS27 + pClik_5a_MCS_P*eftu*_*ddh*_2 Overexpression of *ddh* (*cg2900*) with modified cofactor binding site: IFQRR (aa 33-37) by episomal gene expression and replacement of the native promoter by the *eftu* promoter	This work
BS477	BS27 + pClik_5a_MCS_P*eftu*_*ddh*_3 Overexpression of *ddh* (*cg2900*) with modified cofactor binding site: IFSRL (aa 33-37) by episomal gene expression and replacement of the native promoter by the *eftu* promoter	This work
BS478	BS27 + pClik_5a_MCS_P*eftu*_*ddh*_4 Overexpression of *ddh* (*cg2900*) with modified cofactor binding site: IFSRE (aa 33-37) by episomal gene expression and replacement of the native promoter by the *eftu* promoter	This work
BS479	BS27 + pClik_5a_MCS_P*eftu*_*ddh*_5 Overexpression of *ddh* (*cg2900*) with modified cofactor binding site: IFSDD (aa 33-37) by episomal gene expression and replacement of the native promoter by the *eftu* promoter	This work
BS487	BS27 + pClik_5a_MCS_P*eftu*_*ddh*_6 Overexpression of *ddh* (*cg2900*) with modified cofactor binding site: IFERL (aa 33-37) by episomal gene expression and replacement of the native promoter by the *eftu* promoter	This work
BS488	BS27 + pClik_5a_MCS_P*eftu*_*ddh*_7 Overexpression of *ddh* (*cg2900*) with modified cofactor binding site: IFERE (aa 33-37) by episomal gene expression and replacement of the native promoter by the *eftu* promoter	This work
BS489	BS27 + pClik_5a_MCS_P*eftu*_*ddh*_8 Overexpression of *ddh* (*cg2900*) with modified cofactor binding site: IFEDD (aa 33-37) by episomal gene expression and replacement of the native promoter by the *eftu* promoter	This work
BS490	BS27 + pClik_5a_MCS_P*eftu*_*ddh*_9 Overexpression of *ddh* (*cg2900*) with modified cofactor binding site: IIDVQ (aa 33-37) by episomal gene expression and replacement of the native promoter by the *eftu* promoter	This work
BS506	BS242 + $P_{5\text{-}19}$*tkt* Overexpression of the *tkt*-operon by replacement of the native promoter by the modified *sod* promoter $P_{5\text{-}19}$	This work
BS507	BS242 + $P_{1\text{-}08}$*tkt* Overexpression of the *tkt*-operon by replacement of the native promoter by the modified *sod* promoter $P_{1\text{-}08}$	This work
BS508	BS242 + $P_{6\text{-}43}$*tkt* Overexpression of the *tkt*-operon by replacement of the native promoter by the modified *sod* promoter $P_{6\text{-}43}$	This work
BS509	BS242 + $P_{7\text{-}29}$*tkt* Overexpression of the *tkt*-operon by replacement of the native promoter by the modified *sod* promoter $P_{7\text{-}29}$	This work
BS526	BS242 + $P_{9\text{-}42}$*tkt* Overexpression of the *tkt*-operon by replacement of the native promoter by the modified *sod* promoter $P_{9\text{-}42}$	This work
BS527	BS242 + $P_{10\text{-}18}$*tkt* Overexpression of the *tkt*-operon by replacement of the native promoter by the modified *sod* promoter $P_{10\text{-}18}$	This work
BS529	BS1 + P*sod*_*ddh* Overexpression of *ddh* (*cg2900*), encoding diaminopimelate dehydrogenase, by replacement of the native promoter by the *sod* promoter	This work

Strain	Description and Application	Reference
BS530	BS1 + $P_{7\text{-}19}$*ddh* Overexpression of *ddh* (*cg2900*) by replacement of the native promoter by the modified *sod* promoter $P_{7\text{-}19}$	This work
BS531	BS1 + $P_{6\text{-}43}$*ddh* Overexpression of *ddh* (*cg2900*) by replacement of the native promoter by the modified *sod* promoter $P_{6\text{-}43}$	This work
BS532	BS1 + $P_{7\text{-}29}$*ddh* Overexpression of *ddh* (*cg2900*) by replacement of the native promoter by the modified *sod* promoter $P_{7\text{-}29}$	This work
BS533	BS1 + $P_{5\text{-}19}$*ddh* Overexpression of *ddh* (*cg2900*) by replacement of the native promoter by the modified *sod* promoter $P_{5\text{-}19}$	This work
BS534	BS1 + $P_{1\text{-}08}$*ddh* Overexpression of *ddh* (*cg2900*) by replacement of the native promoter by the modified *sod* promoter $P_{1\text{-}08}$	This work
BS535	BS1 + $P_{5\text{-}02}$*ddh* Overexpression of *ddh* (*cg2900*) by replacement of the native promoter by the modified *sod* promoter $P_{5\text{-}02}$	This work
BS536	BS1 + $P_{9\text{-}42}$*ddh* Overexpression of *ddh* (*cg2900*) by replacement of the native promoter by the modified *sod* promoter $P_{9\text{-}42}$	This work
BS542	BS244 + $P_{7\text{-}29}$*lysE* Overexpression of *lysE* (*cg1224*) by replacement of the native promoter by the modified *sod* promoter $P_{7\text{-}29}$	This work
BS550	BS244 + $P_{7\text{-}19}$*lysE* Overexpression of *lysE* (*cg1224*) by replacement of the native promoter by the modified *sod* promoter $P_{7\text{-}19}$	This work
BS551	BS244 + $P_{6\text{-}43}$*lysE* Overexpression of *lysE* (*cg1224*) by replacement of the native promoter by the modified *sod* promoter $P_{6\text{-}43}$	This work
BS553	BS1 + pClik_5a_MCS_*gapA* Overexpression of *gapA* (cg1791), encoding NAD-dependent glyceraldehyde-3-phosphate dehydrogenase, by episomal gene expression	This work
BS554	BS244 + pClik_5a_MCS_*gapA* Overexpression of *gapA* (cg1791) by episomal gene expression	This work
BS566	BS222 + Δ*lysR* Deletion of 431 bp within *lysR* (*cg2899*), encoding a transcriptional regulator of the LysR family	This work
BS567	BS529 + Δ*lysR* Deletion of 431 bp within *lysR* (*cg2899*)	This work

4.2 Plasmids and Primers

Genome-based transformation of *C. glutamicum* was conducted via the integrative plasmid pClik_int_*sacB* leading to stable genetic modifications (Figure 4-1). The basic vector has a size of 4.3 kb and possesses a multiple cloning site (MCS), an origin of replication (ORI) for *E. coli* as well as an ORF for kanamycin resistance (Kan^R) and *sacB*, encoding levansucrase of *Bacillus subtilis*. Kan^R and *sacB* serve as positive selection markers for the two recombination events during genetic recombination (Jäger et al., 1992; Jäger et al., 1995).

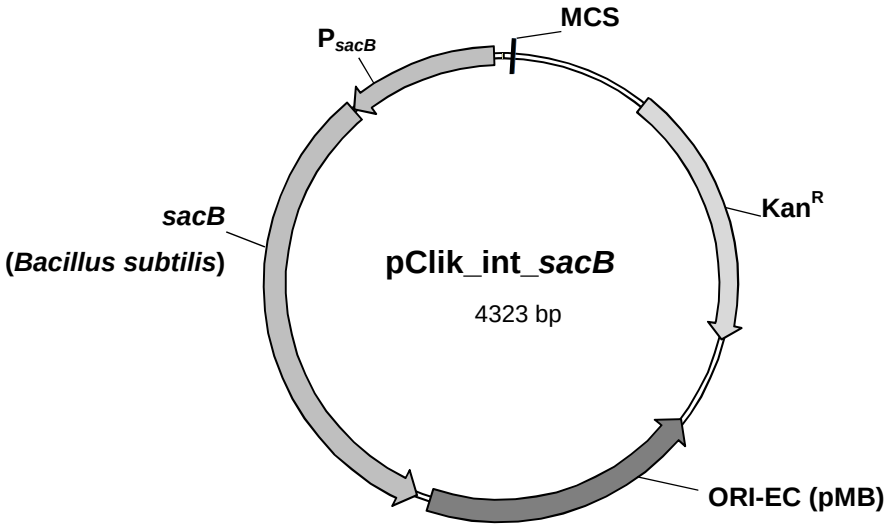

Figure 4-1: Basic transformation vector pClik_int_*sacB* used for stable genetic recombination of *C. glutamicum*. The vector possesses a MCS, an ORI for *E. coli* and positive selection markers (Kan^R and *sacB*).

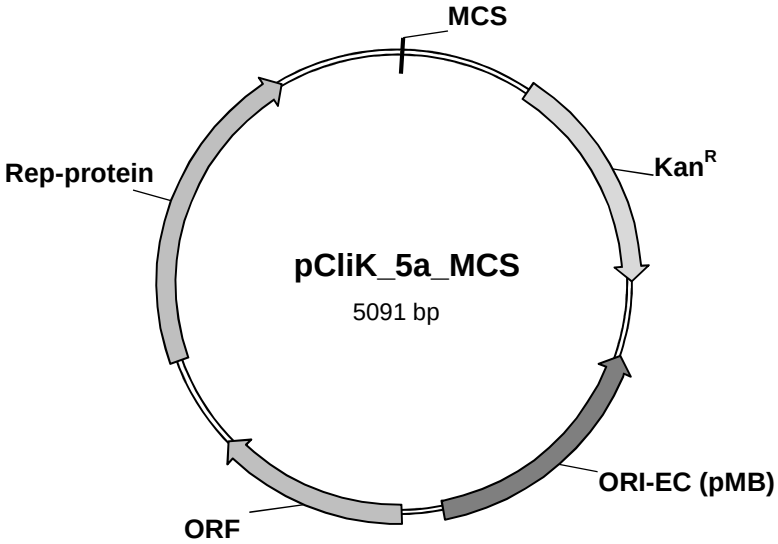

Figure 4-2: Basic transformation vector pClik_5a_MCS used for plasmid-based gene expression in *C. glutamicum*. The vector possesses a MCS, an ORI for *E. coli* and *C. glutamicum* as well as ORFs for the Rep-protein required for replication and Kan^R used as a positive selection marker.

Plasmid-based gene expression was realized via the episomal replicating vector pClik_5a_MCS (Figure 4-2). The basic vector has a size of 5.1 kb and possesses a MCS, an ORI for *E. coli* as well as an ORF for Kan^R. In contrast to pClik_int_*sacB*, the vector has an additional ORF for the Rep-protein that triggers replication of the vector.

For plasmid construction, target DNA was amplified and fused by PCR using site specific primers. End primers additionally contained artificial restriction sites required for site-directed ligation within the MCS of the basic transformation vector. Plasmid and primer designs were performed using the software Vector NTI 9.0.0 (Invitrogen GmbH, Karlsruhe, Germany). All plasmids and primers used for strain construction are listed in Table 4-2 and in the appendix (Table 7-1), respectively.

Table 4-2: Plasmids used in the present work for metabolic and genetic engineering of *C. glutamicum*

Plasmid	Description and Application	Reference
pTC	Vector system used for the episomal expression of the DNA-methyltransferase of *C. glutamicum* bearing an ORF for Tet^R as well as an ORI for *E. coli*	BASF SE
pClik_int_*sacB*	Vector system used for integrative transformation of *C. glutamicum* bearing a MCS, an ORF for Kan^R and *sacB* and an ORI for *E. coli*	BASF SE
pClik_5a_MCS	Vector system used for episomal transformation of *C. glutamicum* bearing a MCS, an ORF for Kan^R as well as an ORI for *E. coli* and *C. glutamicum*	BASF SE
pClik_5a_MCS_*dapB*_R	Episomal vector system for the expression of *dapB* (*cg2163*) with native cofactor binding site: AEIGVDDD (aa 32-39); used as reference	This work
pClik_5a_MCS_*dapB*_1	Episomal vector system for the expression of *dapB* (*cg2163*) with modified cofactor binding site: AELDAGDP (aa 32-39)	This work
pClik_5a_MCS_*dapB*_2	Episomal vector system for the expression of *dapB* (*cg2163*) with modified cofactor binding site: AELDAGDD (aa 32-39)	This work
pClik_5a_MCS_*dapB*_3	Episomal vector system for the expression of *dapB* (*cg2163*) with modified cofactor binding site: AEIDADDD (aa 32-39)	This work
pClik_5a_MCS_*dapB*_4	Episomal vector system for the expression of *dapB* (*cg2163*) with modified cofactor binding site: AELEAGDD (aa 32-39)	This work
pClik_5a_MCS_*dapB*_5	Episomal vector system for the expression of *dapB* (*cg2163*) with modified cofactor binding site: AALEAGDD (aa 32-39)	This work
pClik_5a_MCS_*ddh*_R	Episomal vector system for the expression of *ddh* (*cg2900*) with native cofactor binding site: IFSRR (aa 33-37); used as reference	This work
pClik_5a_MCS_*ddh*_1	Episomal vector system for the expression of *ddh* (*cg2900*) with modified cofactor binding site: IFERR (aa 33-37)	This work
pClik_5a_MCS_*ddh*_2	Episomal vector system for the expression of *ddh* (*cg2900*) with modified cofactor binding site: IFQRR (aa 33-37)	This work
pClik_5a_MCS_*ddh*_3	Episomal vector system for the expression of *ddh* (*cg2900*) with modified cofactor binding site: IFSRL (aa 33-37)	This work
pClik_5a_MCS_*ddh*_4	Episomal vector system for the expression of *ddh* (*cg2900*) with modified cofactor binding site: IFSRE (aa 33-37)	This work
pClik_5a_MCS_*ddh*_5	Episomal vector system for the expression of *ddh* (*cg2900*) with modified cofactor binding site: IFSDD (aa 33-37)	This work
pClik_5a_MCS_*ddh*_6	Episomal vector system for the expression of *ddh* (*cg2900*) with modified cofactor binding site: IFERL (aa 33-37)	This work

Plasmid	Description and Application	Reference
pClik_5a_MCS_*ddh*_7	Episomal vector system for the expression of *ddh* (*cg2900*) with modified cofactor binding site: IFERE (aa 33-37)	This work
pClik_5a_MCS_*ddh*_8	Episomal vector system for the expression of *ddh* (*cg2900*) with modified cofactor binding site: IFEDD (aa 33-37)	This work
pClik_5a_MCS_*ddh*_9	Episomal vector system for the expression of *ddh* (*cg2900*) with modified cofactor binding site: IIDVQ (aa 33-37)	This work
pClik_5a_MCS_ P_{sod}*GFPmut1*	Episomal vector system for the expression of the reporter gene *GFPmut1* used for analysis of the P_{sod} promoter library	This work
pClik_int_*sacB*_P_{sod}*ddh*	Integrative vector system for the replacement of the native promoter of *ddh* (*cg2900*) by the native *sod* promoter	This work
pClik_int_*sacB*_$P_{7\text{-}19}$*ddh*	Integrative vector system for the replacement of the native promoter of *ddh* (*cg2900*) by the modified *sod* promoter $P_{7\text{-}19}$	This work
pClik_int_*sacB*_$P_{6\text{-}43}$*ddh*	Integrative vector system for the replacement of the native promoter of *ddh* (*cg2900*) by the modified *sod* promoter $P_{6\text{-}43}$	This work
pClik_int_*sacB*_$P_{7\text{-}29}$*ddh*	Integrative vector system for the replacement of the native promoter of *ddh* (*cg2900*) by the modified *sod* promoter $P_{7\text{-}29}$	This work
pClik_int_*sacB*_$P_{5\text{-}19}$*ddh*	Integrative vector system for the replacement of the native promoter of *ddh* (*cg2900*) by the modified *sod* promoter $P_{5\text{-}19}$	This work
pClik_int_*sacB*_$P_{1\text{-}08}$*ddh*	Integrative vector system for the replacement of the native promoter of *ddh* (*cg2900*) by the modified *sod* promoter $P_{1\text{-}08}$	This work
pClik_int_*sacB*_$P_{5\text{-}02}$*ddh*	Integrative vector system for the replacement of the native promoter of *ddh* (*cg2900*) by the modified *sod* promoter $P_{5\text{-}02}$	This work
pClik_int_*sacB*_$P_{9\text{-}42}$*ddh*	Integrative vector system for the replacement of the native promoter of *ddh* (*cg2900*) by the modified *sod* promoter $P_{9\text{-}42}$	This work
pClik_int_*sacB*_Δ*lysR*	Integrative vector system for deletion of 431 bp within *lysR* (*cg2899*)	This work
pClik_int_*sacB*_$P_{5\text{-}19}$*tkt*	Integrative vector system for the replacement of the native promoter of the *tkt*-operon by the modified *sod* promoter $P_{5\text{-}19}$	This work
pClik_int_*sacB*_$P_{1\text{-}08}$*tkt*	Integrative vector system for the replacement of the native promoter of the *tkt*-operon by the modified *sod* promoter $P_{1\text{-}08}$	This work
pClik_int_*sacB*_$P_{6\text{-}43}$*tkt*	Integrative vector system for the replacement of the native promoter of the *tkt*-operon by the modified *sod* promoter $P_{6\text{-}43}$	This work
pClik_int_*sacB*_$P_{7\text{-}29}$*tkt*	Integrative vector system for the replacement of the native promoter of the *tkt*-operon by the modified *sod* promoter $P_{7\text{-}29}$	This work
pClik_int_*sacB*_$P_{9\text{-}42}$*tkt*	Integrative vector system for the replacement of the native promoter of the *tkt*-operon by the modified *sod* promoter $P_{9\text{-}42}$	This work
pClik_int_*sacB*_$P_{10\text{-}18}$*tkt*	Integrative vector system for the replacement of the native promoter of the *tkt*-operon by the modified *sod* promoter $P_{10\text{-}18}$	This work
pClik_int_*sacB*_$P_{7\text{-}29}$*lysE*	Integrative vector system for the replacement of the native promoter of *lysE* (*cg1224*) by the modified *sod* promoter $P_{7\text{-}29}$	This work
pClik_int_*sacB*_$P_{7\text{-}19}$*lysE*	Integrative vector system for the replacement of the native promoter of *lysE* (*cg1224*) by the modified *sod* promoter $P_{7\text{-}19}$	This work
pClik_int_*sacB*_$P_{6\text{-}43}$*lysE*	Integrative vector system for the replacement of the native promoter of *lysE* (*cg1224*) by the modified *sod* promoter $P_{6\text{-}43}$	This work
pClik_5a_MCS_*gapN**	Episomal vector system for overexpression of *gapN* (*SMU_676*)	This work
pClik_5a_MCS_*gapA*	Episomal vector system for the overexpression of *gapA* (*cg1791*)	This work

* *gapN* (*SMU_676*) was amplified from genomic DNA of *Streptococcus mutans* UA159 provided by the Helmholtz Centre for Infection Research (Braunschweig, Germany)

4.3 Chemicals

Tryptone, brain heart infusion (BHI) medium, agar, peptone, yeast extract and beef extract were purchased from Difco Laboratories (Detroit, Michigan, USA). All other chemicals were either of technical or HPLC grade for cultivations and analyses, respectively, and were obtained from Sigma-Aldrich (Steinheim am Albuch, Germany), Merck (Darmstadt, Germany), Fluka (Buchs, Switzerland) or Becton and Dickinsons (Franklin Lakes, New Jersey, USA).

4.4 Medium Composition

All media and solutions were prepared in ultrapure water (Millipore water purification system, Merck KGaA, Darmstadt Germany). Sterilization was performed at 121 °C for 20 min or by filtration. Agar plates were prepared by adding 18 g L^{-1} agar. For selection and cultivation during strain construction, kanamycin (Kan), tetracycline (Tet) and sucrose were added to the media. While sucrose (100 g L^{-1}) was added before autoclaving, kanamycin (50 µg mL^{-1}) and tetracycline (12.5 µg mL^{-1}) were added to the sterilized and cooled solution (50-60 °C). Media that contained antibiotics were stored at 4 °C.

4.4.1 Complex media

For cultivation of *E.coli* a lysogeny broth (LB) complex medium was applied as listed in Table 4-3.

Table 4-3: Composition of LB complex medium for cultivation of *E. coli*

Yeast extract	5 g
Tryptone	10 g
NaCl	5 g
add up to 1 L with ultrapure water and sterilize at 121 °C for 20 min	

After heat shock transformation of *E. coli*, cells were cultivated with SOC (super optimal broth (SOB) with catabolite repression) medium for regeneration of the cells according to the given composition (Table 4-4).

Table 4-4: Composition of SOC complex medium for cultivation of *E. coli*

Yeast extract	5 g
Tryptone	20 g
NaCl	0.5 g
250 mM KCl	10 mL
add up to 975 mL with ultrapure water and sterilize at 121 °C for 20 min	
+ 1 M Glucose, sterilized by filtration	20 mL
+ 2 M $MgCl_2$, sterilized by filtration	5 mL

Complex medium for cultivation of *C. glutamicum* consisted of BHI medium (Table 4-5). If cells were treated by electroporation, the BHI medium additionally contained 500 mM sorbitol (BHIS medium). For this purpose, a 2 M stock solution of sorbitol was autoclaved separately and added to the sterilized BHI medium in an appropriate amount. After regeneration, the cells were plated on BHIS agar plates containing kanamycin.

Table 4-5: Composition of BHI complex medium used for cultivation of *C. glutamicum*

BHI	37 g
add up to 1 L with ultrapure water and sterilize at 121 °C for 20 min	

For stable genetic modification, the second recombination event was controlled using a complex medium (CM), supplemented with sucrose or kanamycin. Resistant *C. glutamicum* cells were selected on sucrose, added to the medium before sterilization, while kanamycin was added afterwards for selection of kanamycin deficient cells. Finally, separately autoclaved solutions of glucose and urea were added to the sterilized medium as listed in Table 4-6.

Table 4-6: Composition of CM complex medium for cultivation of *C. glutamicum*

Peptone	10 g
Beef extract	5 g
Yeast extract	5 g
NaCl	2.5 g
add up to 925 mL with ultrapure water and sterilize at 121 °C for 20 min	
+ Glucose (400 g L^{-1}), sterilized at 121 °C for 20 min	25 mL
+ Urea (40 g L^{-1}), sterilized at 121 °C for 20 min	50 mL

4.4.2 Minimal salt medium

For cultivation of *C. glutamicum* in minimal salt medium, stock solutions were prepared and sterilized separately according to the given compositions (Table 4-7). The minimal salt medium included either glucose or fructose as sole carbon source with a final concentration of 10 g L^{-1}.

Table 4-7: Composition of the stock solutions of the minimal medium for cultivation of *C. glutamicum*

Solution A	
NaCl	1 g
$CaCl_2$	55 mg
$MgSO_4 \cdot 7\ H_2O$	200 mg
add up to 500 mL with ultrapure water and sterilize at 121 °C for 20 min	
Solution B	
$(NH_4)_2SO_4$	15 g
NaOH	pH 7.0
add up to 100 mL with ultrapure water and sterilize at 121 °C for 20 min	

Solution C	
K_2HPO_4	31.6 g
KH_2PO_4	7.7 g
	pH 7.8
add up to 100 mL with ultrapure water and sterilize at 121 °C for 20 min	

Solution D	
$FeSO_4 \cdot 7\ H_2O$	20 mg
HCl	pH 1.0
add up to 10 mL with ultrapure water and sterilize by filtration	
store at 4 °C	

Substrate solution - Glucose	
Glucose	10 g
add up to 100 mL with ultrapure water and sterilize at 121 °C for 20 min	

Substrate solution - Fructose	
Fructose	10 g
add up to 100 mL with ultrapure water and sterilize at 121 °C for 20 min	

Vitamin solution	
Biotin	2.5 mg
Thiamine · HCl	5.0 mg
Pantothenic acid calcium salt	5.0 mg
add up to 20 mL with ultrapure water and sterilize by filtration	
store at 4 °C	

Trace element solution	
$FeCl_3 \cdot 6\ H_2O$	200 mg
$MnSO_4 \cdot H_2O$	200 mg
$ZnSO_4 \cdot 7\ H_2O$	50 mg
$CuCl_2 \cdot 2\ H_2O$	20 mg
$Na_2B_4O_7 \cdot 10\ H_2O$	20 mg
$(NH_4)_6Mo_7O_{24} \cdot 4\ H_2O$	10 mg
HCl	pH 1.0
add up to 1 L with ultrapure water and sterilize by filtration	
store at 4 °C	

DHB solution	
3,4-Dihydroxybenzoic acid	300 mg
6 M NaOH	500 µL
add up to 10 mL with ultrapure water and sterilize by filtration	
store at 4 °C	

Based on the stock solutions, the final medium was freshly prepared as listed in Table 4-8.

Table 4-8: Final composition of the minimal salt medium for cultivation of *C. glutamicum*

Solution A	500 mL
Solution B	100 mL
Solution C	100 mL
Solution D	10 mL
Substrate solution	100 mL
Vitamin solution	20 mL
Trace element solution	10 mL
DHB solution	1 mL
add up to 1 L with ultrapure water and sterilized at 121 °C for 20 min	

4.5 Strain Conservation as Stock Cultures

Bacterial cultures of *E. coli* NM522 or *C. glutamicum* were cultivated in liquid complex media (LB for *E. coli* or BHI for *C. glutamicum*). During exponential growth, samples were taken and mixed with the same volume of 60 % (v/v) glycerol. Stock cultures were frozen in liquid nitrogen and stored at -80 °C.

4.6 Strain Construction

4.6.1 Isolation of chromosomal DNA from *C. glutamicum*

For isolation of chromosomal DNA from *C. glutamicum*, phenolic extraction was performed. Shortly, a stock culture of *C. glutamicum* was plated on a BHI agar plate and incubated for 48 h at 30 °C. Harvested cell material was transferred in a 2 mL Eppendorf tube and dissolved in 550 µL ultrapure water and one spatula tip of glass beads (0.15-0.25 mm Worf Glaskugeln GmbH, Mainz, Germany). After addition of 700 µL of a mixture of phenol-chlorophorm-isoamylalcohol (Roth, Karlsruhe, Germany), cell disruption was conducted in a ribolyzer (MM301, Retsch, Haan, Germany) for 45 sec with a frequency of 30 sec^{-1}. Cell debris was removed by centrifugation for 5 min at 16,000 × *g* at 4 °C and the supernatant was transferred to another 2 mL Eppendorf tube. Precipitation of DNA was achieved by addition of 65 µL 3 M sodium acetate (pH 5.5) and 1.3 mL 100 % (v/v) ethanol. After another centrifugation step, the DNA pellet was dried at room temperature for 10 min prior to resuspension in 100 µL ultrapure water and storage at -20 °C.

4.6.2 Preparation of DNA from cell extracts

For strain verification, cell extracts were prepared by cell disruption. Cell material from an agar plate was diluted in 550 µL ultrapure water with one spatula tip of glass beads (0.15-0.25 mm, Worf Glaskugeln GmbH, Mainz, Germany) and disrupted in a ribolyzer (MM301, Retsch, Haan, Germany) for 30 sec at a frequency of 30 sec^{-1}. Cell debris was removed by centrifugation for 5 min at 16,000 × *g* at 4 °C (Eppendorf centrifuge 5415R, Hamburg, Germany) to gain a cell extract used as template for amplification by PCR.

4.6.3 Polymerase chain reaction

Amplification of target DNA fragments and strain verification were performed by PCR using the mastercycler EP gradient (Eppendorf, Hamburg, Germany). Target DNA fragments used for strain construction or sequencing were amplified with the PWO mastermix (Roche Applied Science, Mannheim, Germany) containing a polymerase with proof-reading-function, while the PCR mastermix (Roche Applied Science, Mannheim, Germany) was used for amplification during strain verification. Introduction of point mutations and construction of target DNA fragments used as inserts were performed by fusion PCR. For this purpose, self-complementary fusion primers were designed including a sequence overlap to connect different DNA fragments by PCR. In addition, end primers included artificial recognition sites for restriction enzymes required for site-directed ligation events. All primers were purchased from Life Technologies (Glasgow, Paisley, United Kingdom) and are listed in the appendix (Table 7-1). The annealing temperature T_a was calculated by the amount of the nucleobases guanine (G) and cytosine (C) divided by the length of the primer (N) as depicted in Equation 4-1.

$$T_a = 64.9\,°C + \frac{41\,°C \cdot (G + C - 16.4)}{N} - 3\,°C \qquad \textbf{Equation 4-1}$$

The elongation time t_e of the PWO and PCR master was 1.0 kb and 1.5 kb per min, respectively. DNA amplification included 30 PCR cycles using a temperature profile which was individually determined depending on annealing temperature T_a and elongation time t_e (Table 4-9).

Table 4-9: Temperature profile used for amplification of DNA

Step	Temperature [°C]	Time [min]	Number of Cycles
Denaturation	95	2	1x
Denaturation	95	0.5	
Annealing of Primers	T_a	0.5	30 x
Elongation	72	t_e	
Final Elongation	72	5	1x
Hold	15	∞	

Purified genomic DNA of *C. glutamicum* was used as template for amplification during strain construction (section 4.6.1), while DNA from cell extracts was used for strain verification (section 4.6.13). Furthermore, 10 % (v/v) dimethyl sulfoxide (DMSO) was added to the reaction mixture to facilitate amplification (Table 4-10).

Table 4-10: Composition of the reaction mixtures using PWO or PCR master

	PWO master		PCR master	
Components	**Volume [µL]**	**Final Concentration**	**Volume [µL]**	**Final Concentration**
Template DNA	x	5-500 ng	x	5-500 ng
forward Primer	1	0.2 µM	0.5	0.2 µM
reverse Primer	1	0.2 µM	0.5	0.2 µM
DMSO	5	10 % (v/v)	2.5	10 % (v/v)
Master mix	25	1x	12.5	1x
	add up to 50 µL with ultrapure water		add up to 25 µL with ultrapure water	

PCR products were purified directly using the GeneJet™ PCR Purification Kit (Thermo Scientific, Waltham, USA) or from an agarose gel after gel electrophoresis (section 4.6.6) using the GeneJet™ Gel Extraction Kit (Thermo Scientific, Waltham, USA), according to the manufacture's protocol. The concentration of DNA was analyzed by a spectrophotometer (NanoDrop ND-1000, Thermo Scientific, Waltham, USA).

4.6.4 Engineering of cofactor specificity

The native cofactor binding sites of DapB (EC: 1.3.1.26) and DDH (EC: 1.4.1.16) were modified by fusion PCR using primers that lead to distinct point mutations according to the bioinformatics analysis performed by BASF SE (working group of Dr. Wolfgang Höffken). Consequently, amino acid exchanges were introduced to achieve a change of specificity of the cofactor binding site from NADP(H) to NAD(H).

In order to change the cofactor specificity of DDH, its structure was taken from the protein database (PDB code 3DAP) and displayed with the program Quanta 98 (Molecular Simulations Inc., San Diego, USA, 1998). By visual inspection Ser35 was chosen for mutation. Ser35 forms a hydrogen bond to the phosphate of NADP. The mutations were selected to introduce a steric clash and an unfavorable electrostatic interaction with the phosphate of NADP.

For *C. glutamicum* DapB no x-ray structure was deposited at the PDB. The closest homolog in the data base was dihyrodipicolinate reductase from *M. tuberculosis* (PDB code 1P9L) with a sequence identity of 65 %. Since this protein is NAD dependent the sequence at the NAD binding site was used as a guide for designing new mutants for DapB.

As a result, the native sequences of the cofactor binding sites were annotated as AEIGVDDD (amino acid 32-39) and IFSRR (amino acid 33-37) for DapB and DDH, respectively. Primer

design was performed according to the bioinformatics analysis using the software Vector NTI 9.0.0 (Invitrogen GmbH, Karlsruhe, Germany). All primers used for plasmid construction are listed in the appendix (Table 7-1).

The gene variants were introduced into pClik_5a_MCS to achieve a plasmid-based gene expression. Transcription of *dapB* and *ddh* were initiated by the native promoter of *dapB* and the strong promoter P_{eftu} (elongation factor thermo unstable), respectively. Plasmid construction and introduction of distinct modifications were validated by sequencing using the LIGHTrun™ sequencing service from GATC Biotech AG (Konstanz, Germany) according to the user's guide.

4.6.5 Random mutagenesis of the *sod*-promoter

For mutagenesis of the *sod* promoter, the JBS dNTP-Mutagenesis Kit (Jena Bioscience, Jena, Germany) was used in order to introduce random point mutations based on mutagenic dNTP analogs by a two-step PCR process. *GFPmut1* (Cormack et al., 1996) was used as reporter during plasmid-based expression.

During the first PCR step, dNTP analogs incorporated into the amplified DNA which, subsequently, resulted in point mutations. Thereby, the number of PCR-cycles controls the rate of mutagenesis. Here, 25 cycles were performed which correlated with a rate of mutagenesis of 15 % according to the manufacture's protocol. For the second PCR step 30 cycles were performed. The temperature profile for DNA amplification is listed in Table 4-11.

Table 4-11: Temperature profile used for mutagenesis and amplification of P_{sod}

Step	Temperature [°C]	Time [min]	Number of Cycles
Denaturation	92	2	1x
Denaturation	92	1	25 x (1st PCR)
Annealing of Primers	55	1	30 x (2nd PCR)
Elongation	72	2	
Final Elongation	72	0.5	1x
Hold	15	∞	

Purified genomic DNA of *C. glutamicum* served as template for amplification of P_{sod} during the first PCR step. The first PCR mixture, additionally, included the dNTP analogs 8-oxo-dGTP and dPTP. For the second PCR procedure the dNTP analogs were replaced by usual dNTPs leading to random point mutations. The primers P254 and P258 were used for the amplification of *GFPmut1* while P_{sod} was amplified using the primers P257 and P259. The latter product consisted of a mixture of modified *sod* promoters which were directly connected to *GFPmut1* by fusion PCR. All primers used for plasmid construction are listed in the appendix (Table 7-1) while the composition of the mutagenic PCR mixture is depicted in Table 4-12.

Table 4-12: Composition of the reaction mixtures using the JBS dNTP-Mutagenesis Kit

	1. PCR		2. PCR	
Components	**Volume [µL]**	**Final Concentration**	**Volume [µL]**	**Final Concentration**
Template DNA	x	5-500 ng	1	5-500 ng
forward Primer	1	0.2 µM	1	0.2 µM
reverse Primer	1	0.2 µM	1	0.2 µM
Mutagenesis Buffer	5	1x	5	1x
dNTP-Mix	2.5	0.5 µM	2.5	0.5 µM
dPTP-Mix	2.5	0.5 µM	-	-
8-oxo-dGTP	2.5	0.5 µM	-	-
Taq-Polymerase	1	0.1 U	1	0.1 U
	add up to 50 µL with ultrapure water		add up to 50 µL with ultrapure water	

The insert mixture was introduced into the episomal replicating plasmid pClik_5a_MCS by ligation and the ligation product was transferred into *E. coli* by heat shock transformation. Sequencing and sequence alignment of selected promoter sequences were performed by GATC Biotech AG (Konstanz, Germany) and the software Geneious® V. 6.1.6 (Biomatters Ltd., Auckland, New Zealand). In addition, the software BPROM (http:// www.softberry.com/berry.phtml) was used for the prediction of the TSS.

4.6.6 Gel electrophoresis

PCR products and linearized plasmid DNA were validated by gel electrophoresis. For that reason, an agarose gel (1 % (w/v) agarose in 1x TAE buffer) was prepared. 1x TAE buffer was diluted from a 50x TAE stock solution. The composition of the TAE stock solution is given in Table 4-13.

Table 4-13: Composition of 50x TAE stock solution used for gel electrophoresis

Tris	242 g
0.5 M EDTA, pH 8.0	100 mL
Acetic acid	52 mL
add up to 1 L with ultrapure water	

Before loading, DNA samples were mixed with 10 % (v/v) OrangeG loading dye. The composition of 10x OrangeG is displayed in Table 4-14.

Table 4-14: Composition of 10x OrangeG loading dye

50 % (v/v) Glycerol solution	50 mL
1 M EDTA, pH 8.0	100 mL
OrangeG	75 mg

The agarose gel was loaded with at least 500 ng of DNA per slot. A DNA size standard (GeneRuler™ 1 kb DNA Ladder, Thermo Scientific, Waltham, USA) was loaded in parallel according to the manufacture's protocol. Gel electrophoresis was performed at 110 V and 300 mA for 65 min (B1A easy cast mini gel or D2 wide gel system, Owl Separation Systems, Inc., Portsmouth, New Hampshire, USA with Power Pack P25T, Biometra, Göttingen, Germany) in 1x TAE buffer. Afterwards, gels were stained in a 0.5 mg L^{-1} solution of ethidium bromid and analyzed under UV light by the Gel iX Imager (Intas Imaging Instruments GmbH, Göttingen, Germany).

4.6.7 Enzymatic digestion and ligation

Enzymatic digestion was utilized during the construction of transformation vectors and for plasmid validation. It was performed at 37 °C for 20 min using two distinct FastDigest restriction enzymes (Thermo Scientific, Waltham, USA). The composition of the reaction mixture is listed in Table 4-15.

Table 4-15: Composition of the reaction mixture used for enzymatic digestion

	purified PCR products		plasmid DNA	
Components	**Volume [µL]**	**Final Concentration**	**Volume [µL]**	**Final Concentration**
Template DNA	x	1000 ng	x	500 ng
FastDigest Buffer	3	1x	2	1x
Enzyme I	1	1 U	0.8	0.8 U
Enzyme II	1	1 U	0.8	0.8 U
	add up to 30 µL with ultrapure water		add up to 20 µL with ultrapure water	

For ligation, target DNA fragments were introduced into the MCS of the transformation vectors pClik_int_*sacB* or pClik_5a_MSC by site-directed ligation with the Rapid DNA Dephos and Ligation Kit (Roche Applied Science, Mannheim, Germany). Therefore, the insert and the transformation vector were treated separately with restriction enzymes. Afterwards, the insert was purified as described in section 4.6.3 and its concentration was determined. The linearized vector was then treated with alkaline phosphatase from the kit, according to the manufacture's protocol, to remove the phosphate residues. For ligation 50 ng of the transformation vector were used at a vector:insert ratio of 1:3 according to Equation 4-2.

$$\text{Amount of Insert [µL]} = \frac{50\ \text{ng} \cdot \text{Size of Insert [bp]}}{\text{Size of Vector [bp]}} \cdot 3 \qquad \textbf{Equation 4-2}$$

The composition of the ligation mixture is displayed in Table 4-16. Ligation was performed at 24 °C for 20 min. Subsequently, the mixture was used to transform *E. coli* DH5α by heat shock transformation.

Table 4-16: Composition of the ligation mixture using T4 DNA Ligase and 50 ng vector DNA

Components	Volume [µL]	Final Concentration
Vector DNA, dephosphorylated	x	50 ng
Insert DNA	x	x
DNA Dilution Buffer	2	1x
	add up to 10 µL with ultrapure water	
+ T4 DNA Ligation Buffer	10	1x
+ T4 DNA Ligase	1	5 U

4.6.8 Generation of heat shock competent *E. coli* cells

For preparation of heat shock competent *E. coli* (DH5*α* and NM522), cells were cultivated in LB medium, enriched with 20 mM $MgSO_4$ on a rotary shaker (shaking diameter 5 cm, Multitron II, Infors AG, Bottmingen, Switzerland). For cultivation of *E. coli* NM522, carrying the pTC plasmid, the medium additionally contained 12.5 µg L^{-1} tetracycline.

A starter culture (5 mL in a 50 mL baffled shake-flask) was inoculated and incubated overnight at 37 °C and 230 rpm. Subsequently, 2 mL of starter culture were used to inoculate the main culture (250 mL in 2 L baffled shake-flask), which was incubated at 23 °C and 250 rpm until an optical density OD_{600} of 0.4-0.6 was reached. Subsequently, cells were harvested by centrifugation in 50 mL falcon tubes at 4 °C and 1,200 × *g* for 10 min (Biofuge Stratos, Heraeus/Kendro, Osterode, Germany) and washed once with 80 mL TB buffer (Table 4-17). Previous to each centrifugation step, cells were incubated on ice for 10 min.

Table 4-17: Composition of TB buffer

0.5 M Pipes-NaOH, pH 6.7	2 mL
0.5 M $CaCl_2$ solution	3 mL
2 M KCl solution	12.5 mL
1 M $MnCl_2$ solution	5.5 mL
add up to 100 mL with ultrapure water	

The washed cells were resuspended in 20 mL TB buffer and 1.5 mL DMSO and incubated on ice for 10 min. Finally, aliquots of 220 µL were transferred into pre-cold and sterile 1.5 mL Eppendorf tubes, frozen in liquid nitrogen and stored at -80 °C.

4.6.9 Transformation of *E. coli* by heat shock

Heat shock competent *E. coli* cells (DH5α and NM522) were used for transformation of vector DNA.

After being thawed on ice, 50 µL of competent cells were transferred to a sterile 1.5 mL Eppendorf tube and mixed with 5 µL of vector DNA. Subsequently, cells were incubated at 4 °C

for 30 min. The heat shock was then carried out in a thermo block (Thermomixer comfort, Eppendorf, Hamburg, Germany) at 45 °C for 45 sec followed by addition of 900 µL SOC medium and incubation at 37 °C for 1 h. Finally, cells were harvested by centrifugation 16,000 × *g* for 1 min (Eppendorf centrifuge 5415R, Hamburg, Germany), the supernatant was decanted and the cells resuspended in about 100 µL of residual medium. For selection, cells of *E. coli* DH5α and NM522 were plated on LB^{Kan} and $LB^{Kan+Tet}$ agar plates, respectively, and incubated at 37 °C for 24 h.

4.6.10 Purification of plasmid DNA

Plasmid DNA was isolated using the GeneJet™ Plasmid miniprep Kit (Thermo Scientific, Waltham, USA) according to the manufacture's protocol. All cultivations were carried out on a rotary shaker (shaking diameter 5 cm, Multitron II, Infors AG, Bottmingen, Switzerland) at 37 °C and 230 rpm.

Single colonies of DH5α and NM522 were used to inoculate 5 mL of LB^{Kan} and 50 mL of $LB^{Kan+Tet}$, respectively, and grown overnight. Since the plasmid DNA, obtained from *E. coli* DH5α was only required for strain verification, single mini preparations were performed with 4 mL of main culture. In contrast, *E. coli* NM522 was used to obtain plasmid DNA for transformation of *C. glutamicum,* which requires high final concentrations. Consequently, 10 identical mini preparations were pooled after elution and concentrated by evaporation with a speedvac (Concentrator 5301, Eppendorf AG, Hamburg, Germany).

Final concentrations of isolated plasmid DNA were determined by a spectrophotometer (NanoDrop ND-1000, Thermo Scientific, Waltham, USA).

4.6.11 Generation of electro competent *C. glutamicum* cells

All cultivations were carried out on a rotary shaker (shaking diameter 5 cm, Multitron II, Infors AG, Bottmingen, Switzerland) at 30 °C and 230 rpm using BHI medium. A stock culture of *C. glutamicum* was plated on a BHI agar plate and incubated at 30 °C for 48 h. A 10 mL starter culture was inoculated with a single cell from the same plate and incubated overnight. Subsequently, the starter culture was harvested by centrifugation at 5,000 × *g* (Biofuge Stratos, Heraeus/Kendro, Osterode, Germany) for 10 min and resuspended in a 0.9 % (w/v) solution of NaCl. The cells were used to inoculate a 50 mL main culture to an optical density OD_{660} of 0.4. When an OD_{660} of 1.5-2.0 was reached, the main culture was harvested by centrifugation at 5,000 × *g* for 10 min (Biofuge Stratos, Heraeus/Kendro, Osterode, Germany). The cell pellet was washed twice with a 10 % (v/v) solution of glycerol and resuspended in 8 mL of the same solution per gram cell wet weight. The electro competent cells were then stored on ice until electroporation.

4.6.12 Transformation of *C. glutamicum* by electroporation

For electroporation, 200 µL of competent *C. glutamicum* cells were transferred to an electroporation cuvette (BTX Cuvette Plus™ with 2 mm gap, Harvard Apparatus, Massachusetts, USA) and mixed with 2-5 ng and 0.2-0.5 ng of vector DNA based on pClik_int_*sacB* and pClik_MCS-5a, respectively. Subsequently, the preparation was incubated on ice for 5 min. Transformation of *C. glutamicum* was performed by electroporation using a GenePulser XCell (Bio-Rad, Hercules, California, USA) at 2.5 kV, 25 µF and 400 Ω. If the electroporation time was lower than 8 ms, competent cells were further diluted with 10 % (v/v) solution of glycerol.
Immediately after electroporation, 900 µL BHIS medium was added to the cells and the mixture was incubated at 30 °C for 1.5 h. Finally, cells were harvested by centrifugation (9,300 × *g* for 1 min, Eppendorf centrifuge 5415R, Hamburg, Germany), the supernatant was decanted and the cells were resuspended in about 100 µL of residual medium. For selection, *C. glutamicum* cells were plated on $BHIS^{Kan}$ agar plates and incubated at 30 °C for 48 h.

4.6.13 Selection and verification of transformed mutants

Cells that had been transformed with vector DNA based on pClik_int_*sacB* had to pass through a second recombination event. For this purpose, 5 mL of BHI medium were inoculated with single colonies and incubated overnight on a rotary shaker (shaking diameter 5 cm, Multitron II, Infors AG, Bottmingen, Switzerland) at 30 °C and 230 rpm. The bacterial culture was then diluted with a 0.9 % (w/v) solution of NaCl, plated on CM^{Sac} agar plates and incubated at 30 °C for 48 h to gain single colonies. Colonies were picked and streaked on raster plates of Cm^{Sac} and CM^{Kan}. Both were incubated at 30 °C for 24 h. Colonies that were grown on CM^{Sac}, but not on CM^{Kan}, were further evaluated for a positive transformation event by PCR using cell extracts.
For analysis of a transformation event, based on pClik_MCS_5a, single colonies were streaked on BHI^{Kan} agar plates and incubated at 30 °C for 24 h. Cell material was used directly to prepare a cell extract required for verification by PCR as described before.

4.7 Determination of the volumetric Gas-Liquid Mass Transfer Coefficient (k_La)

The volumetric gas-liquid mass transfer coefficient (k_La) was quantified in baffled and non-baffled disposable shake-flasks (Figure 3-6) of different vessel sizes (125 mL, 250 mL and 500 mL, PreSens Precision Sensing GmbH, Regensburg, Germany) with variation of the working volume (10-40 % of the total volume) and the shaking frequency (50 rpm, 150 rpm and 250 rpm). Measurement was performed in 100 mM phosphate buffer (pH 7.0) at 30 °C and 37 °C. Dissolved oxygen (DO) was monitored online with the PreSens shake-flask reader SFR (PreSens Precision Sensing GmbH, Regensburg, Germany). The sensor device was installed in an orbital shaker (shaking diameter 5 cm, Multitron II, Infors AG, Bottmingen, Switzerland) as described by Schneider et al. (2010).

For k_La determination, shake-flasks were equilibrated with buffer and 0.1 mM cobalt nitrate. Calibration of the sensors was carried out as described in the SFR user manual. Complete oxygen depletion was achieved by addition of a 200 g L^{-1} sodium sulfite stock solution (Hermann et al., 2001). Since comparative studies with 500 mL baffled shake-flasks with lowest filling volume and highest shaking frequency (e.g. highest expected k_La) had shown that the use of the standard flask cap had no influence on k_La determination (k_La = 281 ± 37 h^{-1} (without cap) and k_La = 292 ± 15 h^{-1} (with cap)) all experiments were performed in triplicate without the standard cap of the shake-flasks for better handling.

$$\frac{dC}{dt} = OTR - OUR = k_La \cdot (c^* - c) - q_{O2} \cdot X \qquad \textbf{Equation 4-3}$$

The volumetric gas-liquid mass transfer coefficient k_La was determined between 20 % and 90 % oxygen saturation using Berkeley MADONNA (Version 8.0.1) for data fitting by a regression curve (Figure 4-3) according to Equation 4-3 (Garcia-Ochoa et al., 2010). If required, a baseline correction for 0 % oxygen saturation was performed. For k_La estimation, a stoichiometric correlation between flask size (V_{max}), shaking frequency (n) and k_La was compiled on basis of the experimental data. Mathematical fitting was performed using either a Gaussian (Equation 4-4) or a parabolic function (Equation 4-5) for baffled and non-baffled shake-flasks, respectively.

$$k_La = a \cdot e^{-0.5 \cdot \left(\left(\frac{n - x_0}{b}\right)^2 + \left(\frac{V_{max} - y_0}{c}\right)^2\right)} \qquad \textbf{Equation 4-4}$$

$$k_La = y_0 + a \cdot n + b \cdot V_{max} + c \cdot n^2 + d \cdot V_{max}^2 \qquad \textbf{Equation 4-5}$$

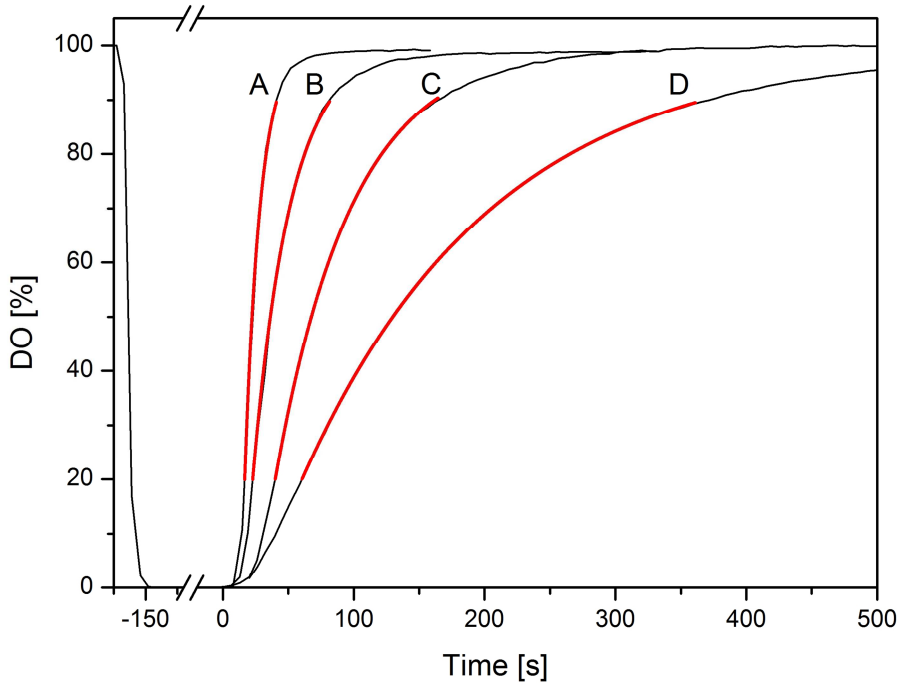

Figure 4-3: Time profile of dissolved oxygen concentration used for determination of k_La. Complete oxygen depletion was achieved by addition of sodium sulfite. The red line indicates a fitting curve calculated on basis of Equation 4-3. Data represent k_La determination for 250 mL baffled shake-flask, 30 °C, 250 rpm and 30 % filling (A), 500 mL baffled shake-flask, 37 °C, 150 rpm, 10 % filling (B), 500 mL baffled shake-flask, 30 °C, 150 rpm, 30 % (C) and 500 mL non-baffled shake-flask, 37 °C, 150 rpm, 40 % (D). 100 % DO corresponds to 0.232 mmol O_2 L^{-1} at 30 °C and 0.212 mmol O_2 L^{-1} at 37 °C, respectively.

4.8 Cultivation of *Corynebacterium glutamicum*

4.8.1 Cultivation of *C. glutamicum* in shake-flasks

For routine batch cultivation experiments, cells were incubated in baffled shake flasks with a filling volume of 10 % at 30 °C and 230 rpm on a rotary incubator (shaking diameter 5 cm, Multitron II, Infors AG, Bottmingen, Switzerland).

First, a stock culture of *C. glutamicum* was plated on a BHI agar plate and incubated at 30 °C for 48 h. For the first starter culture, 10 mL BHI complex medium was inoculated with a single colony and incubated for about 10 h. Bacterial cells were harvested during exponential growth by centrifugation (5,000 × *g* at 4 °C, Biofuge Stratos, Heraeus/Kendro, Osterode, Germany), resuspended in a sterile 0.9 % (w/v) solution of NaCl and used to inoculate a second starter culture of 25 mL minimal salt medium. After about 10 h of cultivation, the second starter culture was harvested as described before and used as inoculum for the main culture. Main cultures were performed in 25 mL minimal saltmedium in triplicate with a constant pH at 7.0 ± 0.3 (766 Calimatic, Knick GmbH and Co. KG, Berlin, Germany).

For the verification of predicted cultivation processes, main cultures were grown in 250 mL baffled shake-flasks (PreSens, Regensburg, Germany) at 30 °C and 150 rpm using a filling volume of 10 % and 30 %, respectively. The latter was used for determination of the specific growth rate μ [h^{-1}] and the specific oxygen uptake rate q_{O2} [mmol g^{-1} h^{-1}] by Equation 4-6.

$$q_{O_2} = \frac{k_L a \cdot (c^* - c) - \frac{dC}{dt}}{X}$$ **Equation 4-6**

Subsequently, experimentally determined rates for growth and oxygen uptake were used to predict a time-dependent increase of biomass formation and decrease of DO concentration for aerobic growth under the given conditions with 10 % filling volume.

4.8.2 Cultivation of *C. glutamicum* in a micro bioreactor system

For small-scale fermentations, starter cultures of *C. glutamicum* were cultivated in deep well plates (riplate BV 10 mL, HJ-Bioanalytik GmbH, Mönchengladbach, Germany) at 30 °C and 1,000 rpm on a plate shaker (Inkubator 1000, Heidolph Instruments GmbH and Co. KG, Schwabach, Germany). Main cultures were performed in MTP-48-FlowerPlates® (m2p-labs GmbH, Baesweiler, Germany) with DO optodes using a micro fermentation system BioLector® (shaking diameter 3 mm, m2p-labs GmbH, Baesweiler, Germany) at 30 °C with a cycle time of 10 min, a shaking frequency of 700 rpm and a relative humidity of 95 %.

During cultivation, plates were sealed with a gas permeable membrane (HJ Bioanalytik GmbH, Mönchengladbach, Germany) to avoid contamination and evaporation. Bacterial growth was analyzed by backscatter measurement at 620 nm with a gain of 5 while the emission intensity of GFP was measured at 520 nm with excitation at 488 nm and a gain of 100. The collected data were analyzed with the software BioLection version 2.3.1.3 (m2p-labs GmbH, Baesweiler, Germany).

For expression studies of modified *sod* promoters derived from random mutagenesis, a MTP-48-FlowerPlate® (m2p-labs GmbH, Baesweiler, Germany) containing 1 mL BHI medium (50 µg mL^{-1} kanamycin) per well was directly inoculated with single colonies of P_{sod} mutants of *C. glutamicum*. The changes of the backscatter signals for bacterial growth and *gfp* expression were recorded by the micro cultivation system BioLector®. The biomass-specific GFP expression was taken as value for the relative promoter activity.

For gene expression studies of *C. glutamicum*, both starter cultures were cultivated in 3 mL BHI and minimal salt medium, respectively, for about 10 h. The main cultures were performed in six identical biological replicates with 1 mL minimal salt medium per well and inoculated with 60 µL of the second starter culture. Exclusively, expression studies of P_{sod}*tkt* were performed in 1.5 mL minimal salt medium. While the changes of the backscatter signals for biomass formation and oxygen consumption were recorded online by the BioLector®, samples from three biological replicates were taken regularly during exponential growth for analysis of product formation and glucose consumption. The remaining three replicates were harvested and pooled during exponential growth for the isolation of RNA required for quantification of gene expression. In some cases finale yields were determined after about 12 h of stationary growth.

4.9 Analytical Methods for Strain Characterization

4.9.1 Determination of cell concentration

Determination of the cell concentration was either performed manually by an optical measurement using the spectrophotometer (Libra S11, Biochrome, Cambridge, UK) at 660 nm in 1.5 mL polystyrene cuvettes (Plastibrand, Wertheim, Germany or Sarstedt AG and Co., Nümbrecht, Germany) or automatically during cultivation in a micro fermenter.

For the manual procedure, 500 µL of cell suspension was taken under sterile conditions and transferred to a 1.5 mL reaction tube. Since water was used as a reference, samples were diluted with water to an OD_{660} of 0.05-0.3 on an analytical balance (CP225D, Sartorius, Göttingen, Germany). All dilutions and measurements were performed in duplicate. Independent from the genetic background, the measured OD_{660} values correlate with the cell dry weight (CDW) of *C. glutamicum* by Equation 4-7 (Becker et al., 2009).

$$\mathrm{CDW}\ [\mathrm{g\ L^{-1}}] = 0.255\ \cdot \mathrm{OD}_{660} \qquad \textbf{Equation 4-7}$$

During cultivation in the micro fermenter, bacterial growth was monitored online with a backscatter measurement at 620 nm with a gain of 5 ($BS_{G:5}$). For determination of the correlation factor between OD_{660} and $BS_{G:5}$, seven different strains based on BS1 and BS244 were cultivated in MTP-48-FlowerPlates as described before. In parallel, samples were taken during exponential growth and the optical density was determined photometrically at 660 nm. Again, a correlation factor was determined that was independent from the genetic background as depicted in Figure 4-4 and by Equation 4-3.

$$\mathrm{OD}_{660} = 0.4298\ \cdot \mathrm{BS}_{\mathrm{G:5}} - 1.2983 \qquad \textbf{Equation 4-8}$$

As a result, Equation 4-9 was formulated to calculate the CDW from data gained by backscatter measurement.

$$\mathrm{CDW}\ [\mathrm{g\ L^{-1}}] = 0.1096 \cdot \mathrm{BS}_{\mathrm{G:5}} - 0.3311 \qquad \textbf{Equation 4-9}$$

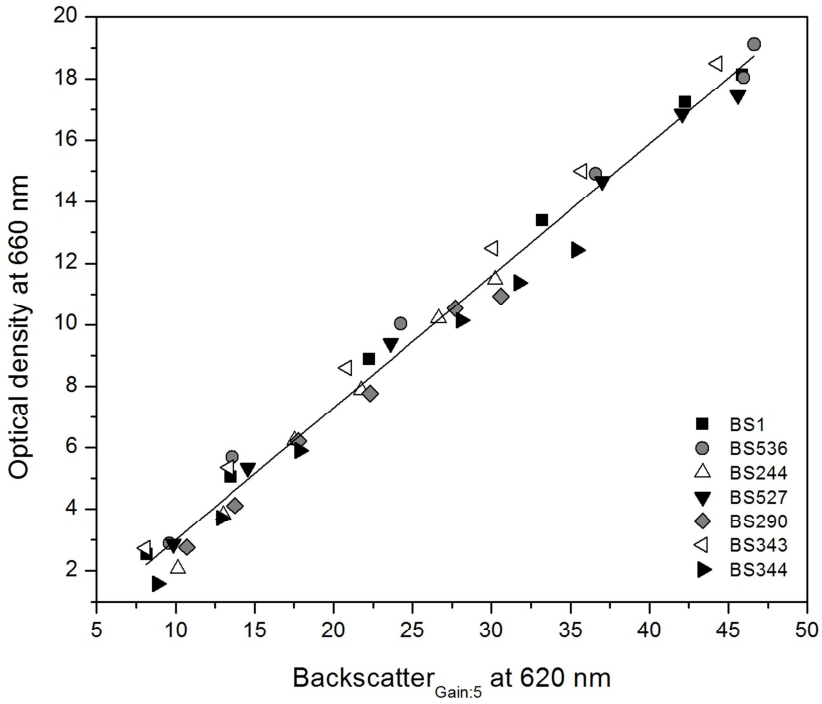

Figure 4-4: Correlation between optical density OD_{660} and $BS_{G:5}$ at 620 nm for *C. glutamicum* BS1, BS536, BS244, BS527, BS290, BS343 and BS344.

4.9.2 Quantification of amino acids

Amino acid concentrations were determined in 1:10-diluted (w/w) culture supernatants obtained by centrifugation at 16,000 × *g* for 1 min (Eppendorf centrifuge 5415R, Hamburg, Germany). Dilution was performed on an analytical balance (CP225D, Sartorius, Göttingen, Germany) with a 235 µM solution of *α*-amino butyric acid (ABU) as internal standard. Quantification was performed by HPLC (Agilent 1200 Series, Agilent Technology, Waldbronn, Germany) as described by Krömer et al. (2005).

Samples were automatically derivatized with *ortho*-phthaldialdehyde (OPA) and injected to the system. Separation was achieved on a RP column (Gemini 5µ C18 110A, 150 x 4.6 mm, Phenomenex, Aschaffenburg, Germany) equipped with a pre-column (Gemini C18, MAX-RP, 4 x 3 mm, Phenomenex, Aschaffenburg, Germany) as stationary phase and by the mixing ratio of eluent A (40 mM NaH_2PO_4, pH 7.8) and B (45 % (v/v) acetonitrile, 45 % (v/v) methanol, 10 % (v/v) ultrapure water) used as mobile phase. Elution was performed by a gradient of 100-20 % and 0-80 % of eluent A and eluent B, respectively, within 26 min. The flow rate was adjusted to 1 mL min^{-1} at 40 °C. The gradient used for lysine determination is depicted in Table 4-18.

Table 4-18: Gradient of eluent A and B used as mobile phase with a flow rate of 1 mL min^{-1} at 40 °C

Time [min]	Eluent A [%]	Eluent B [%]
0.0	100	0
26.0	20	80

4.9.3 Quantification of glucose

Glucose concentrations were determined in dilutions of supernatants which were obtained as described before (section 4.9.2). Quantification was performed by a biochemical analyzer (2700 STAT Plus™, Yellow Springs Instrument, Ohio, USA) with an upper detection limit of 2.5 g L^{-1}.

4.10 Biochemical Methods

4.10.1 Preparation of crude cell extract

To gain crude cell extracts, cells were cultivated in deep well plates filled with 5 mL BHI medium per well. For each preparation, 4 mL of exponential growing cells were harvested in the same 2 mL Eppendorf tube by repeated centrifugation (5 min, 5,000 × *g*, 4 °C, Biofuge Stratos, Heraeus/Kendro, Osterode, Germany), washed twice with an enzyme specific disruption buffer and then resuspended in 500 µL of the same buffer together with one spatula tip of glass beads (0.125-0.106 mm, Worf Glaskugeln GmbH, Mainz, Germany). Cell disruption was performed twice in a FastPrep®-24 (M.P. Biomedicals, California, USA) at 6 m s^{-1} for 30 sec with a break for 5 min during which the tubes were incubated on ice. Finally, cellular debris was removed by centrifugation (2 x 5 min, 16,000 × *g*, 4 °C, Eppendorf centrifuge 5415R, Hamburg, Germany) and the crude cell extracts were transferred to a clean 1.5 mL Eppendorf tube.

4.10.2 Quantification of total protein amount

Total protein concentrations were determined with the Pierce® BCA Protein Assay Kit (Thermo Scientific, Rockford, USA) according to the manufacture's protocol. A dilution series in a range of 50-700 mg L^{-1} was prepared from the provided solution of 2,000 mg L^{-1} bovine serum albumin (BSA) used as protein standard. Dilutions of BSA and crude cell extracts were prepared on an analytical balance (CP225D, Sartorius, Göttingen, Germany). Determination of the protein concentration was performed manually by an optical measurement using the spectrophotometer (Libra S11, Biochrome, Cambridge, UK) at 562 nm in 1.5 mL polystyrene cuvettes (Plastibrand, Wertheim, Germany or Sarstedt AG and Co., Nümbrecht, Germany).

4.10.3 Determination of enzyme activity

Crude cell extracts were used to determine the enzyme activities in triplicate in a total volume of 200 µL in 96-well-plates with flat-bottom (MTP-Plate, Kisker Biotech GmbH and Co. KG, Steinfurt, Germany) using a Tecan microplate reader system (Sunrise-basic, Tecan Austria GmbH, Grödig, Austria). Online monitoring was performed by the data analysis software Magellan™ V.6.4 (Tecan Austria GmbH, Grödig, Austria). Negative controls were carried out either

without substrate or cell extract, respectively. All reactions were initiated by addition of the pre-warmed reaction mixture at 30 °C. Enzyme activities were calculated from the change in absorbance [A min^{-1}] at 340 nm and the extinction coefficient of NAD(P)H (ε_{340} = 6.22L $mmol^{-1}$ cm^{-1}). Afterwards, enzyme activities were correlated with the appropriate protein concentrations to obtained specific enzyme activities [U mg^{-1}] with 1 U = 1 µmol min^{-1} at 30 °C.

Diaminopimelate Dehydrogenase (DDH, EC: 1.4.1.16) (Cremer et al., 1988)

The disruption buffer used for DDH analyses contained 10 mM $MgCl_2$ and 100 mM Tris-HCl buffer (pH 7.5) while the reaction mixture consisted of 10 mM $MgCl_2$, 2 mM NADP or NAD and 200 mM glycine/NaOH (pH 10.5). Enzyme activity was measured in reverse-direction with 10 µL cell extract and 8 mM *meso*-diaminopimelate as substrate.

Transketolase (TKT, EC: 2.2.1.1) (Becker et al., 2011)

Preparation of crude cell extract was performed using 100 mM Tris-HCl (pH 7.8) as disruption buffer, while the reaction mixture consisted of master mix A and B as further described. Determination of TKT activity was achieved by coupled chemical reactions. In the first step ribulose 5-phosphate and xylulose 5-phosphate, which were required as substrate by TKT, were synthesized from ribose 5-phosphate (R5P) by the coupling enzymes ribose 5-phosphate isomerase (RPI) and ribulose 5-phosphate epimerase (RPE). The TKT reaction led to the formation of glyceraldehyde 3-phosphate which was further converted by an enzyme mixture of triosephosphate isomerase (TPI) and glycerophosphate dehydrogenase (GDH) using NADH as cofactor. Master mix A contained disruption buffer, RPI, RPE, TPI-GDH and NADH while master mix B contained disruption buffer, thiaminpyrophosphate (TPP) and $MgCl_2$. Cofactors and coupling enzymes were added to the pre-warmed master mixtures and incubated at 30 °C for 5 min. Afterwards, both mixtures were combined and added to the 96-well plate in which crude cell extracts and R5P as substrate were provided. All reaction mixtures were started at once to avoid a loss of catalytic enzyme activity. The reaction mixture contained 50 mM disruption buffer, 1 U RPI, 1 U RPE, 1 U TPI-GDH, 0.5 mM NADH, 0.2 mM TPP, 10 mM $MgCl_2$, 20 mM R5P and 10 µL of crude cell extract.

Glyceraldehyde-3-Phosphate Dehydrogenase (GapDH, EC: 1.2.1.9 and 1.2.1.12) (Crow and Wittenberger, 1979)

Cell disruption was performed in 10 mM $MgCl_2$ and 100 mM Tris-HCl buffer (pH 8.3). The same buffer was used as reaction buffer. The NAD-dependent GapDH activity of GapA (EC: 1.2.1.12) and the NADP-dependent GapDH activity of GapN (EC: 1.2.1.9) were analyzed with 10 µL cell extract at pH 9.3 with 1 mM NAD, using 4 mM D/L-glyceraldehyde 3-phosphate as substrate and at pH 8.3 with 1 mM NADP and 2 mM D/L-glyceraldehyde 3-phosphate, respectively.

4.11 Gene Expression Analysis

4.11.1 Isolation of RNA

Previous to the extraction procedure, cell suspensions from cultivation experiments were mixed with a RNA stabilizing solution (RNALater®, Applied Biosystems, Austin, USA) at the ratio of 8:1. The solutions were mixed by inversion and split up into 2 mL aliquots. Cells were harvested by centrifugation for 20 sec at full speed (Eppendorf centrifuge 5415R, Hamburg, Germany). Subsequently, the supernatant was discarded and the cell material was shock frozen in liquid nitrogen. Previous to extraction, the cell material had to be lyophilized for 24 h (Alpha 1-4 LD plus, Christ, Osterode, Germany). Meanwhile and afterwards, samples were stored at -80 °C.

For RNA extraction, the RNeasy Plus Mini Kit (Qiagen, Hilden, Germany) was used. Therefore, samples and all materials were transported, pre-cooled and stored in liquid nitrogen. At the beginning, the lyophilized cell material was transferred to a kryo-tube (Nalgene Cryoware, Nalgene Nunc, Rochester, New York, USA), a dismembrator ball with a diameter of 9 mm (Sartorius Stedim Biotech, Göttingen, Germany) was added and tubes were placed in a dismembrator box. Cell disruption was performed in a homogenizator (Mikro-Dismembrator S, Sartorius, Göttingen, Germany) at 2,000 min^{-1} for 10 sec. Subsequently, 600 µL lysis buffer (RTL plus with 1 % (v/v) β-mercaptoethanol) were added and mixed by shaking. The suspension was transferred to a new 1.5 mL Eppendorf tube and incubated in a thermo block (Thermomixer comfort, Eppendorf, Hamburg, Germany) at 56 °C for 2 min. Afterwards, the mixture was transferred to a QiaShredder column and centrifuged for 3 min at 16,000 × *g* (Eppendorf centrifuge 5415R, Hamburg, Germany). The flow trough was further transferred to a gDNA eliminator column followed by centrifugation for 30 sec at 3,300 × *g* (Eppendorf centrifuge 5415R, Hamburg, Germany). The flow through was mixed by pipetting with 600 µL 70 % (v/v) ethanol and transferred in portions of 600 µL to an RNeasy mini column. After centrifugation for 15 sec at 3,300 × *g* and discarding of the flow through, the column was washed with 350 µL of RW1 buffer using the same conditions. Subsequently, the tube was transferred to a clean 1.5 mL Eppendorf tube and 80 µL of a DNase mastermix (10 µL DNase I stock solution + 70 µL RDD buffer) were added to the membrane and incubated for 30 min at 28 °C and 600 min^{-1}. Afterwards, the column was washed one more time with RW1 buffer as described before and transferred to a new receiver tube to perform two further washing procedures under the same conditions using 500 µL of RPE buffer, each. Finally, the column was transferred to a clean 1.5 mL Eppendorf tube, air-dried for 10 min at room temperature and eluted stepwise (2 x 20 µL and 2 x 10 µL) with RNase-free water. The purified RNA samples were stored at -80 °C until further processing.

4.11.2 Verification of RNA quality

For determination of RNA concentrations, a spectrophotometer (NanoDrop ND-1000, Thermo Scientific, Waltham, USA) was used. Verification of RNA quality was performed using the Bioanalyzer 2100 (Agilent Technology, Waldbronn, Germany) and the RNA 6000 Nano LabChip® Kit (Agilent Technology, Waldbronn, Germany), according to the manufacture's protocol.

4.11.3 Quantitative-real-time PCR

Previous to quantitative-real-time PCR (qRT-PCR), mRNA was transcribed into cDNA (complementary DNA) due to higher stability and conformation without secondary structures.

First, purified RNA samples were diluted with RNase-free water to concentrations of about 50 ng μL^{-1}. For cDNA synthesis, reverse transcriptase Superscript III (Invitrogen, Carlsbad, California, USA) was used according to the manufacturer's protocol. The reaction mixture had a total volume of 20 µL, including 550 ng of RNA used as template and 200 ng of random primers, respectively. After incubation of the RNA at 65 °C for 5 min in a thermo block (Thermomixer comfort, Eppendorf, Hamburg, Germany), annealing of the primers was facilitated by incubation on ice for 55 sec. Finally, the remaining compounds were added and cDNA synthesis was performed at 50 °C for 50 min.

For qRT-PCR, cDNA samples were diluted at a ratio of 1:10 with ultra-pure water. The composition of the reaction mixture, including a Hot *Taq* polymerase (Peqlab Biotechnologie, Erlangen, Germany) for DNA amplification, and the temperature profile used for qRT-PCR are depicted in Table 4-19 and Table 4-20, respectively.

Amplification was performed in the Light Cycler® 480 II (Roche, Basel, Switzerland) with six biological replicates each, using water as negative control. All primers used for qRT-PCR are listed in Table 4-21.

Table 4-19: Composition of the reaction mix used for amplification of DNA by qRT-PCR

	qRT-PCR	
Components	**Volume [µL]**	**Final Concentration**
Template cDNA or water	2	x
forward Primer	1.25	0.5 µM
reverse Primer	1.25	0.5 µM
dNTPs	0.5	0.2 mM
PCR buffer	2.5	1 x
$MgCl_2$	2.5	2.5 mM
Hot *Taq* polymerase	0.1	0.02 U
SYBR® Green I	2.5	0.4 x
	add up to 25 µL with ultrapure water	

Table 4-20: Temperature profile used for amplification of DNA by qRT-PCR

Step	Temperature [°C]	Time [sec]	Number of Cycles
Denaturation	95	300	1x
Denaturation	95	20	45 x
Annealing of Primers	T_a	20	
Elongation	72	30	
Fluorescence detection	84	10	
Final Elongation	72	120	1x
Hold	15	∞	

Table 4-21: Sequence and annealing temperature T_a of the site-specific primers used in the present work for the quantification of relative gene expression by qRT-PCR

Primer	Sequence (5' → 3')	T_a [°C]	Construction
119_*ddh*_fw	CTGAGCAGGCACCAAAGTTC	51	*ddh*
120_*ddh*_rv	GTCGCAAAGCATCGGAGTG	50	*ddh*
122_*tkt*_fw	TCCTCAACGGCATTTCCCTC	51	*tkt*
123_*tkt*_rv	GCAGCCAAGGTTTCAACAGG	51	*tkt*
137_*lysE*_fw	AACCAACCGTGCCCGATGAC	53	*lysE*
138_ *lysE*_rv	AACCAGATCAGGCTTGCCGC	53	*lysE*
140_ *lysR*_fw	GAGGGAAGCGGTAAGTTTGC	51	*lysR*
141_ *lysR*_rv	ACACAGACCCCGCAAACTCC	53	*lysR*

For determination of relative gene expression levels, quantification was performed by analyses of the melting curve. Since the fluorophore SYBER® green exclusively intercalates with double-stranded DNA, the fluorescence signal drops, when the temperatures increase during qRT-PCR causing single-stranded DNA. Thereby, the strength of the signal depends on the generation rate of the amplified qRT-PCR product, indicating the amount of the template and, thus, the gene expression level.

The software of the Light Cycler® 480 II (Version 1.5, Roche, Basel, Switzerland) was used to get four-parametric sigmoid functions of each amplification curve. The second derivative maximum (SDM) of each melting curve was calculated to determine the crossing point (CP). Relative concentrations of the samples were calculated according to the CP values of a dilution series of known relative concentrations. Afterwards, the results were normalized to the native P_{sod} construct (100 %).

5 Results and Discussion

5.1 Process Engineering – Oxygen Supply in disposable Shake-Flasks

For define cultivation of *Corynebacterium glutamicum* a robust and straightforward method for quantification and prediction of oxygen saturation was developed, since sufficient oxygen supply is crucial for microbial growth and product formation (Casas López et al., 2006; Hermann et al., 2001; Tunac, 1989). For this reason, systematic investigations of oxygen in disposable shake-flasks were performed considering vessel size, filling volume and the agitation speed.

The volumetric gas-liquid mass transfer coefficient (k_La) of oxygen was quantified in buffer-filled baffled and non-baffled disposable shake-flasks of different size (125, 250 and 500 mL), filling volume (10-40 % of the total volume) and shaking frequency (50, 150 and 250 rpm) as well as at different temperatures (30 °C and 37 °C), respectively. As illustrated in Figure 4-3, dissolved oxygen (DO) was completely removed from the liquid bulk by the addition of sodium sulfite. As soon as the redox-reaction catalyzed by cobalt ions was completed, the DO level increased due to mass transfer from the gas phase till the sensor signal converged to 100 % saturation. The experimental data were used to determine the k_La value for the given conditions (Equation 4-3) applying fitting by a regression curve. The good fit of the experimental data (solid red line in Figure 4-3) and the small standard deviations between replicates indicate high precision. The observed effects of filling volume, shaking frequency and temperature on the k_La value are summarized for different flask sizes in Figure 5-1.

Overall, remarkably high k_La values of up to 350 h^{-1} resulted. These significantly exceed that of glass vessels under similar conditions (Wittmann et al., 2003). For non-baffled shake-flasks the k_La was, generally, lower as compared to baffled flasks and reached maximal values of 100 h^{-1}. Among the investigated parameters, the shaking frequency had the most significant impact on the oxygen transfer (Figure 5-1and Figure 5-2). The filling volume, however, hardly influenced oxygen transfer and became only relevant for filling ratios higher than 30 %. Interestingly, the vessel size had no relevant influence on the mass transfer coefficient of non-baffled flasks (Figure 5-1and Figure 5-2, D, E), whereas it showed some slight effect on k_La in baffled flasks (Figure 5-1and Figure 5-2, A-C). This is probably linked to the chosen vessel geometry (Büchs, 2001). Whereas non-baffled flasks exhibit a plane inner surface, the baffles introduce a structure within the vessel. The resulting changes depend on baffle height and depth as well as vessel height and diameter and, thus, obviously influence the oxygen transport. Despite its impact on O_2 solubility (Ries et al., 2010), the temperature increase from 30 °C to 37 °C had no impact on the k_La (Figure 5-1and Figure 5-2).

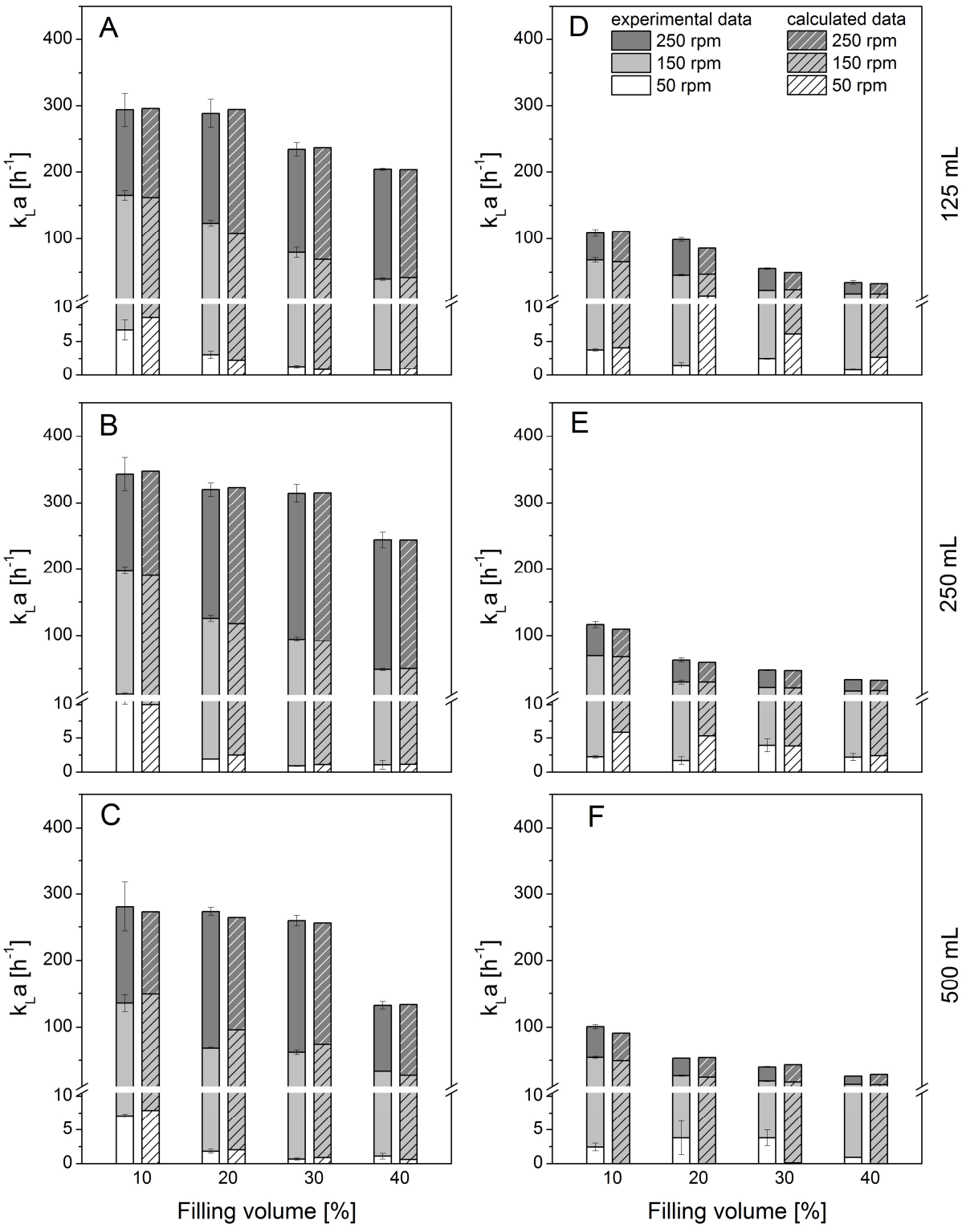

Figure 5-1: Comparison of experimental (plain-colored) and predicted (dashed) k_La values of baffled (A-C) and non-baffled (D-F) shake-flasks at 30 °C. For different flask sizes (125, 250 and 500 mL) the effects of filling volume (10-40 % of the total volume) and shaking frequency (50, 150 and 250 rpm) are shown.

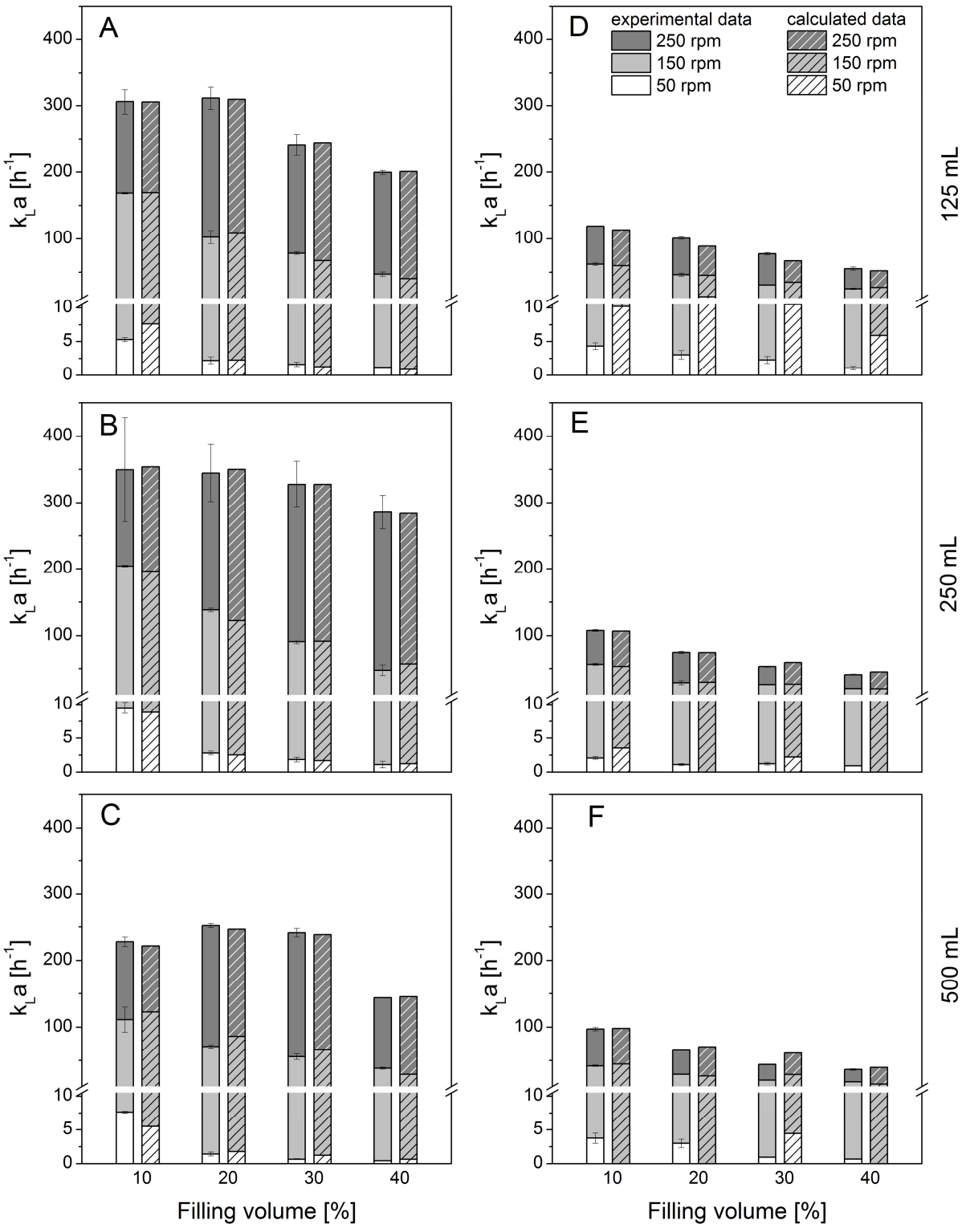

Figure 5-2: Comparison of experimental (plain-colored) and predicted (dashed) k_La values of baffled (A-C) and non-baffled (D-F) shake-flasks at 37 °C. For different flask sizes (125, 250 and 500 mL) the effects of filling volume (10-40 % of the total volume) and shaking frequency (50, 150 and 250 rpm) are shown.

Based on the experimental data, mathematical correlations for the determination of the volumetric gas-liquid mass transfer coefficients were established (Table 5-1).

Table 5-1: Empirically determined parameters for k_La estimation in baffled and in non-baffled disposable shake-flasks using a Gaussian fitting (Equation 4-4) and a parabolic fitting (Equation 4-5), respectively.

	Filling volume			
Parameter	**10 %**	**20 %**	**30 %**	**40 %**
30 °C				
x_0	225.96	235.32	238.56	271.60
y_0	294.78	276.87	324.56	257.66
a	376.10	333.95	336.85	256.42
b	65.47	59.23	55.96	67.41
c	289.68	347.81	245.81	221.02
	R^2 = 0.99	**R^2 = 0.99**	**R^2 = 0.99**	**R^2 = 0.99**
37 °C				
x_0	223.56	237.20	247.80	272.48
y_0	259.62	264.77	309.06	282.91
a	386.72	358.91	338.99	304.90
b	63.13	59.50	60.95	67.17
c	247.92	280.30	227.68	185.67
	R^2 = 0.99	**R^2 = 0.99**	**R^2 = 0.99**	**R^2 = 0.99**

	Filling volume			
Parameter	**10 %**	**20 %**	**30 %**	**40 %**
30 °C				
y_0	-39.53	28.27	2.85	-5.43
a	0.78	0.27	$9.67 \cdot 10^{-2}$	0.15
b	$7.97 \cdot 10^{-2}$	-0.26	$-2.16 \cdot 10^{-2}$	$1.04 \cdot 10^{-2}$
c	$-8.00 \cdot 10^{-4}$	$3.00 \cdot 10^{-4}$	$4.00 \cdot 10^{-4}$	$1.85 \cdot 10^{-5}$
d	$-2.00 \cdot 10^{-4}$	$3.00 \cdot 10^{-4}$	$8.95 \cdot 10^{-6}$	$-3.34 \cdot 10^{-5}$
	R^2 = 0.99	**R^2 = 0.93**	**R^2 = 0.98**	**R^2 = 0.99**
37 °C				
y_0	-4.80	26.65	15.81	7.26
a	0.46	0.20	0.16	0.17
b	-0.07	-0.24	-0,14	-0.10
c	$2 \cdot 10^{-4}$	$6 \cdot 10^{-4}$	$4 \cdot 10^{-4}$	$2 \cdot 10^{-4}$
d	$5.52 \cdot 10^{-5}$	$3 \cdot 10^{-4}$	$2 \cdot 10^{-4}$	$1 \cdot 10^{-4}$
	R^2 = 0.99	**R^2 = 0.97**	**R^2 = 0.94**	**R^2 = 0.97**

The values were obtained by correlating flask size [mL], shaking frequency [rpm] and k_La [h^{-1}] for different filling volumes and temperatures. Baffled flasks were best described by a Gaussian fitting (Equation 4-4), while for non-baffled flasks a parabolic fitting (Equation 4-5) of the data gave satisfying fitting. The fitted parameters refer to the corresponding equations.

For each filling volume analyzed, an individual correlation was established for 30 °C and for 37 °C, respectively. This is illustrated in Figure 5-3 for baffled shake-flasks, investigated at 30 °C with 10 % filling (R^2 = 0.99). Optimal parameter estimation was hereby obtained for Gaussian fitting (Equation 4-4) of k_La values from baffled flasks and for parabolic fitting (Equation 4-5) of k_La values from non-baffled flasks. The parameter estimates are given in Table 5-1. Obviously, a robust and precise prediction of the k_La value was achieved, which is reflected by the excellent agreement between experimental and calculated data (Figure 5-1and Figure 5-2). At low experimental k_La values (<5 h^{-1}), corresponding calculations yielded slight negative values, which were then set to zero. Beyond previously established empirical correlations for standard non-baffled glass vessels (Seletzky et al., 2007), the novel correlations now enable k_La estimation for a broader experimental set-up.

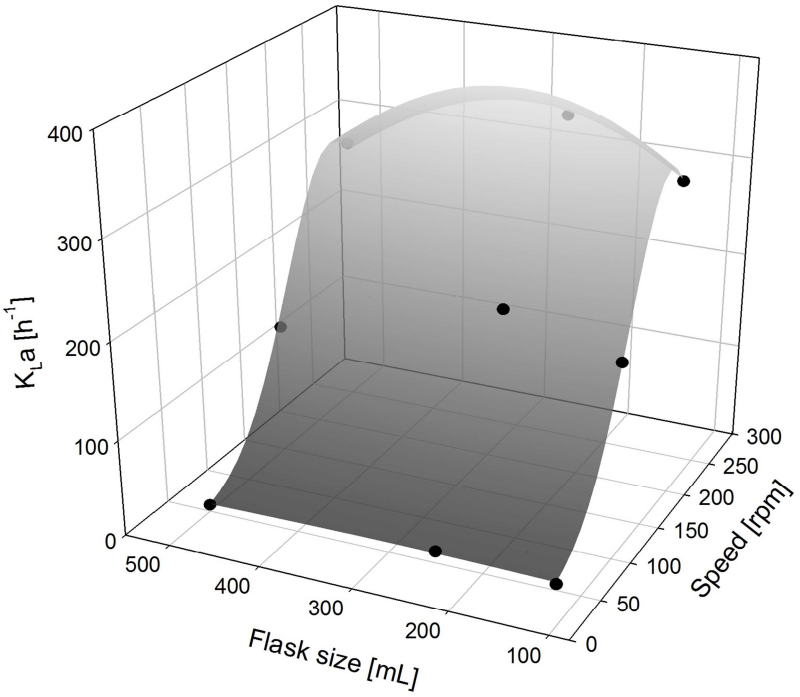

Figure 5-3: Correlation of k_La [h^{-1}], flask size [mL] and shaking frequency [rpm] for baffled shake-flasks with 10 % filling volume at 30 °C. Parameters for Gaussian fitting (Equation 4-4) were estimated with an excellent regression coefficient of R^2 = 0.99 (Table 5-1).

In a next step, the deduced mathematical correlations for prediction of the volumetric gas-liquid mass transfer coefficient were validated by predicting the non-oxygen limited growth of *C. glutamicum* ATCC 13032.

First, specific rates of growth (μ) and oxygen consumption (q_{O2}) of *C. glutamicum* were determined from cultivations in minimal salt medium with glucose as sole carbon source. Cultivation experiments were performed in 250 mL baffled shake-flasks at 30 % filling and 150 rpm. As depicted in Figure 5-4, the dissolved oxygen dropped immediately after inoculation and be-

came limiting (<20 %) after 4 h of cultivation and a cell concentration of only 1 g L^{-1}. As a consequence, growth of *C. glutamicum* was disturbed and switched from non-limited exponential growth to a rather linear growth behavior until a final cell concentration of 4.5 g L^{-1} was reached. Oxygen thereby constantly remained at 0 % saturation. From the first hours of non-limited growth, the specific rates for growth (μ) and oxygen uptake (q_{O2}) were determined to 0.38 h^{-1} and 14.2 mmol g^{-1} h^{-1}, respectively. These values were considered as basic physiological properties of the strain in the given medium at sufficient oxygen supply. They served as basis to predict the time course of cell growth and DO level for a *C. glutamicum* cultivation at other experimental conditions.

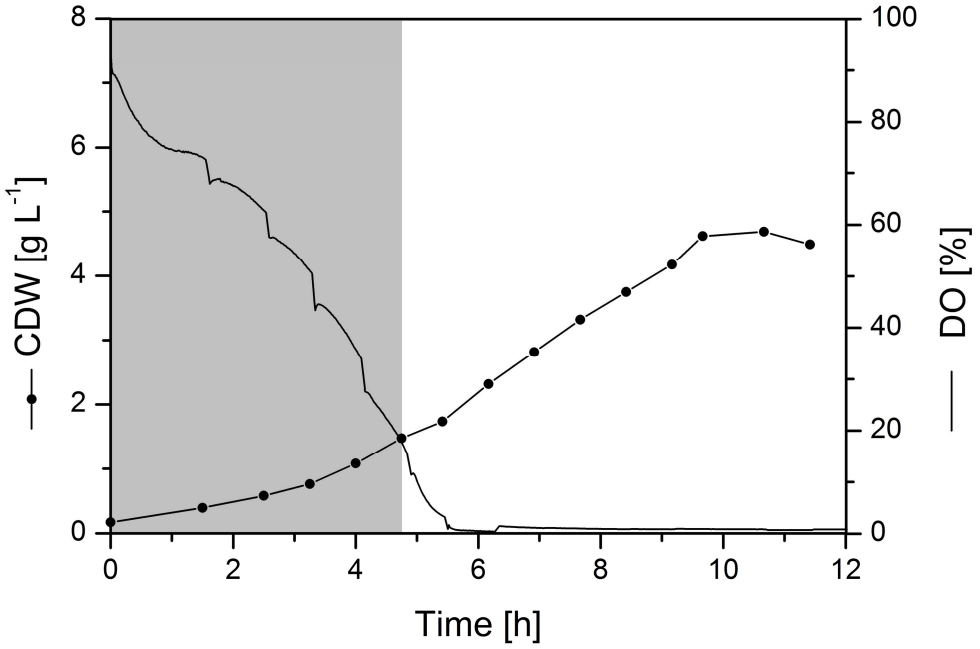

Figure 5-4: Growth and oxygen consumption of *C. glutamicum* ATCC 13032 in minimal salt medium with glucose as sole carbon source. Cultivation was performed in 250 mL baffled shake-flasks with 30 % filling at 150 rpm. The non-oxygen limited phase (gray area) was used to determine the specific growth rate μ and the specific oxygen uptake rate q_{O2} of *C. glutamicum*. For oxygen saturation, a DO level of 100 % corresponding to 0.232 (mmol O_2) L^{-1} was assumed.

Based on the established mathematical correlation, the time course of DO and cell concentration of *C. glutamicum* was predicted for another, so far untested scenario. The chosen experimental set-up comprised a 250 mL baffled shake-flask with 10 % filling and a shaking frequency of 150 rpm. The deduced k_La value of 190 h^{-1} exceeded that of the prior cultivation with 30 % filling (92 h^{-1}). Considering exponential growth and an inoculum concentration of 0.2 g CDW L^{-1}, the time-dependent increase of biomass concentration was calculated and depicted in Figure 5-5 (solid red line).

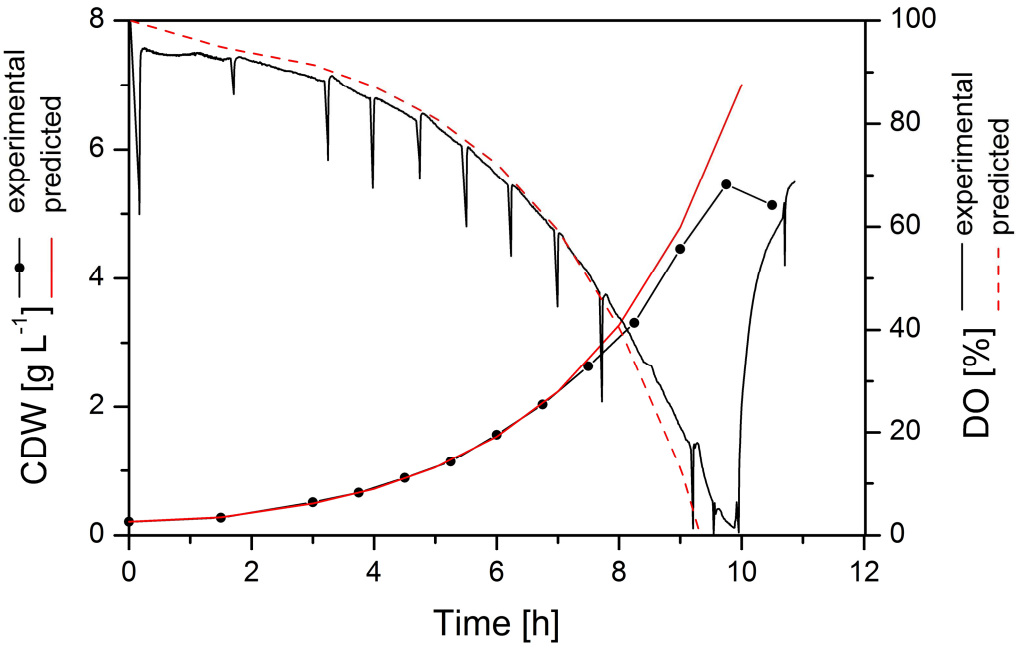

Figure 5-5: Verification of the predicted growth and oxygen consumption of *C. glutamicum* ATCC 13032 in minimal salt medium with glucose as sole carbon source. The control cultivation was performed in 250 mL baffled shake-flasks with 10 % filling at 150 rpm. Predicted values (red) and experimental data (black) have an excellent agreement. For oxygen saturation, a DO level of 100 % corresponding to 0.232 (mmol O_2) L^{-1} was assumed.

The mathematical correlation between q_{O2}, k_La, biomass and oxygen concentration (Equation 4-6) further enabled determination of the dissolved oxygen concentration in the simulated batch experiment (Figure 5-5, dashed red line). Finally, the maximal reachable cell concentration at sufficient oxygen supply was estimated. Previous cultivation (Figure 5-4) revealed a limiting oxygen concentration of 20 %. Accordingly, a maximum cell dry weight of 4.3 g L^{-1} was predicted. To see if the culture performance can be reliably predicted, *C. glutamicum* was then cultivated under these conditions. As illustrated in Figure 5-5, growth and oxygen consumption – reflected by the dissolved oxygen concentration – were indeed rather well predicted. Experimental (black) and simulated (red) values were almost identical. This also holds true for the predicted cell concentration at limiting oxygen supply (4.3 g L^{-1}). This value well matched with the experimentally achieved cell concentration of 4.6 ± 0.3 g L^{-1} at a DO level of 20 %. The results underline the value of the demonstrated approach for a priori characterization of aerobic batch cultivation processes. Furthermore, the findings revealed that the established correlation for k_La calculation can be transferred from the buffer-based abiotic system to standard shake-flask cultivations. The ability to predict the oxygen availability for specific experimental set-ups can improve the design of experiments by decreasing the risk of failures related to oxygen deprivation, typically associated with reduced cell viability and the occurrence of fermentation products such as acetate, lactate or ethanol. Beyond this, the described approach can facilitate and improve working schedules and cost-efficient medium design, as knowledge on k_La and oxygen consumption is essential for experimental design and operation (Casas López et al., 2006). In this regard, the described method can be used to optimize inoculum

preparation and to adjust the medium composition for a desired cell concentration. This seems especially valuable for cultivations with costly carbon sources and nutrient additives. Related to the broad coverage of different experimental conditions and relevant cultivation parameters the present work is highly interesting for scientists from diverse fields working with most prominent model organisms such as *C. glutamicum* (Becker and Wittmann, 2012b), *E. coli* (Thongchuang et al., 2012) or *Bacillus subtilis* (Nicolas et al., 2012).

5.2 Genetic Engineering – Engineering of Cofactor Specificity

Among the effective metabolic engineering strategies to improve lysine production in *C. glutamicum* are optimization of (i) precursor supply, (ii) enhancement of the biosynthetic pathways and (iii) attenuation of undesired side reactions. Particularly, an enhanced supply of NADPH results in increased product yields (Becker et al., 2005; Becker et al., 2011; Ohnishi et al., 2005). Consequently, attenuation of NADPH-consuming reactions as well as an increased regeneration of NADPH are expected to improve lysine production (Yokota and Lindley, 2005).

5.2.1 Proof of concept – Impact of the redox supply by glyceraldehyde-3-phosphate dehydrogenase

First, the influence of *gapDH*, encoding glyceraldehyde-3-phosphate dehydrogenase, on lysine production was analyzed. In nature, different types of GapDH exist, which differ by their cofactor specificity. *C. glutamicum* ATCC 13032, for example, possesses two kinds of phosphorylating GapDH. GapA (EC: 1.2.1.12) is a NAD-dependent enzyme, while GapB (EC: 1.2.1.13) has a dual-coenzyme specificity with a preference for NADP. Since GapB is only active in the gluconeogenetic direction, it is inapplicable for growth on glucose after deletion of *gapA* (Fillinger et al., 2000; Omumasaba et al., 2004; Takeno et al., 2010). Additionally, non-phosphorylating NADP-dependent GapDH, referred to as GapN (EC: 1.2.1.9), are found in many other microorganisms (Iddar et al., 2002). As example, *Streptococcus mutans* UA159 possesses not only the NAD-dependent GapA, but also uses the NADP-dependent enzyme GapN (Crow and Wittenberger, 1979). Since synthesis of one mol lysine requires four mol of NADPH (Michal and Schomburg, 2012), expression of GapN is considered to enhance lysine production as the enzyme might increase the availability of this cofactor actively by an additional NADPH-generating glycolytic pathway.

Here, the two different enzymes (GapA and GapN) should be expressed separately in the basic and the hyper production host of *C. glutamicum* BS1 and BS244, respectively, by an episomally replicating vector system. First, the target genes were amplified from genomic DNA and ligated into the MCS of pClik_5a_MCS. After transformation into *C. glutamicum* BS1 and

BS244, the genes were episomally expressed under control of their native promoters. In addition, the basic plasmid was transformed into both host strains to generate suitable Kan^R reference strains. Strain verification was performed by PCR, while the functionality of the enzyme was confirmed via enzymatic measurements (Figure 5-6).

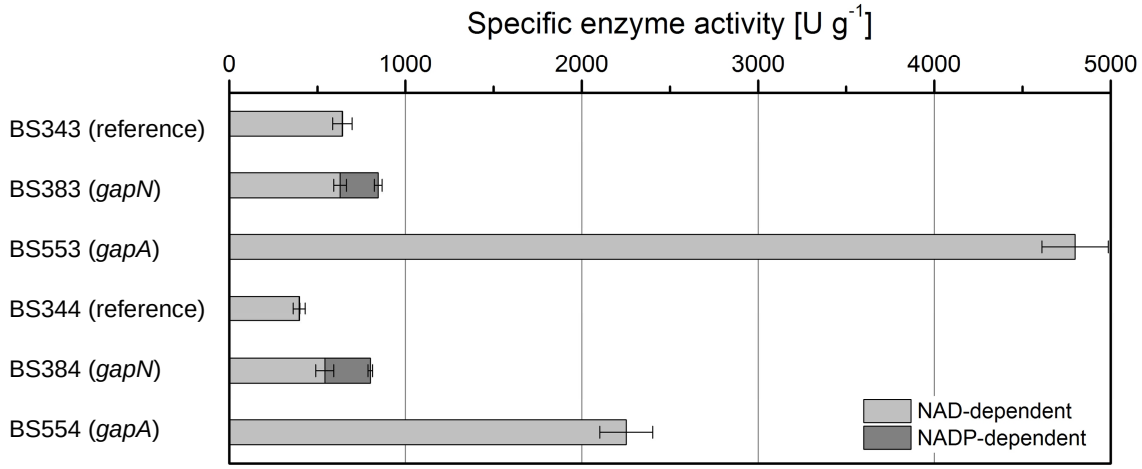

Figure 5-6: Analysis of the specific enzyme activity [U g^{-1}] of episomally expressed glyceraldehyde-3-phosphate dehydrogenases *gapA* and *gapN* depending on the cofactors NAD^+ and $NADP^+$, respectively. Cultivation of different *C. glutamicum* strains was performed in minimal salt medium with glucose as sole carbon source, supplemented with 50 µg mL^{-1} kanamycin to maintain plasmid-based expression at 30 °C. The basic plasmid served as reference. BS343, BS383 and BS553 originate from the basic lysine producer BS1, while the other strains are based on the lysine hyper producer BS244.

The enzymatic assay revealed that the vector systems including *gapDH* were successfully expressed (Figure 5-6). The enzyme activities detected in the reference strains BS343 (642 U g^{-1}) and BS344 (397 U g^{-1}) reflected the basic GapDH activity of BS1 and BS244, respectively, since both host strains only possess the native gene copy of *gapA* within their genome. Apart from that, no NADP-dependent activity was detected for both strains. The results agree with that of Takeno et al. (2010) and Xu et al. (2014b), who observed comparable activities in *C. glutamicum* for the NAD-dependent GAPDH of 440 U g^{-1} and 318 U g^{-1}, respectively. For the modified strains, BS383 and BS384 nearly the same GapA activities were determined. The estimated additional NADP-dependent activity could be assigned to the plasmid-based *gapN* expression. Even though *gapN* was expressed episomally which generally results in a strong overexpression of the target gene, the resulting enzyme activities of GapN were still rather low (34-48 %), as compared to the genome-based expression of *gapA*. The same was also observed by Takeno et al. (2010), who replaced the native gene of *gapA* by *gapN* from *S. mutans* and detected a reduced GapDH activity of only 32 % for GapN, as compared to the native GapA expression. In contrast to that, the episomal-based *gapA* expression in BS553 and BS554 revealed significantly increased enzyme activities (4798 U g^{-1} and 2252 U g^{-1}, respectively). Regarding GapDH activity linked to episomal gene expression, the cofactor-depending ratios of NAD:NADP were 19:1 and 7:1, respectively, in the genetic background of

BS1 and BS244. Thus, NAD-dependent GapA activity seemed to be considerably higher as NADP-dependent GapN activity. Crow and Wittenberger (1979) came to the same conclusion, analyzing *S. mutans*' native GapA and GapN activities. They even found that in *S. mutans* the activity of GapA was about 40 times higher, as compared to that of GapN. Obviously, the native GapN activity is rather low by nature. Hereby, it cannot be excluded that the activity of GapN might be limited by the weak strength of the promoter of *S. mutans* used in *C. glutamicum.*

The different strains were further compared, concerning growth and production (Table 5-2).

Table 5-2: Growth and production characteristics of different *C. glutamicum* strains, bearing the plasmid pClik_5a_MCS for episomal expression of *gapDH*. The basic plasmid served as reference. BS343, BS383 and BS553 originate from the basic lysine producer BS1, while the other strains are based on the lysine hyper producer BS244. The data given are yields for biomass production ($Y_{X/S}$), lysine formation ($Y_{Lys/S}$) and glycine formation ($Y_{Gly/S}$) as well as growth rates (μ), specific glucose uptake rates (q_{Glc}) and specific lysine production rates (q_{Lys}). All experiments were performed in triplicate in MTP-48-FlowerPlates in 1 mL minimal salt medium with glucose as sole carbon source, supplemented with 50 μg mL^{-1} kanamycin to maintain plasmid-based expression.

Strain	Construct	Yields		
		$Y_{X/S}$ [g mol^{-1}]	$Y_{Lys/S}$ [mmol mol^{-1}]	$Y_{Gly/S}$ [mmol mol^{-1}]
BS343	reference	91.4 ± 3.4	99.8 ± 7.5	4.9 ± 0.7
BS383	*gapN*	91.8 ± 4.3	134.6 ± 7.3	7.8 ± 0.5
BS553	*gapA*	89.7 ± 1.2	114.4 ± 1.1	2.5 ± 0.1
BS344	reference	73.0 ± 1.2	267.5 ± 7.2	7.4 ± 0.3
BS384	*gapN*	68.2 ± 1.1	301.3 ± 4.4	7.1 ± 0.3
BS554	*gapA*	44.6 ± 1.1	423.7 ± 4.7	3.9 ± 0.1
Strain	**Construct**	**Rates**		
		μ [h^{-1}]	q_{Glc} [mmol g^{-1} h^{-1}]	q_{Lys} [mmol g^{-1} h^{-1}]
BS343	reference	0.28 ± 0.2	3.10 ± 0.11	0.31 ± 0.02
BS383	*gapN*	0.31 ± 0.00	3.40 ± 0.17	0.46 ± 0.00
BS553	*gapA*	0.23 ± 0.01	2.61 ± 0.06	0.30 ± 0.01
BS344	reference	0.25 ± 0.01	3.38 ± 0.13	0.91 ± 0.06
BS384	*gapN*	0.23 ± 0.00	3.33 ± 0.05	1.00 ± 0.02
BS554	*gapA*	0.10 ± 0.01	2.25 ± 0.17	0.95 ± 0.06

The cultivation experiment revealed that expression of *gapDH* influenced lysine production positively. Both *gapA* and *gapN* expression resulted in an improved lysine formation yield.

Regarding strains based on BS1, expression of *gapN* had the strongest impact on lysine production, even though it was shown that its enzyme activity was rather low. Here, the lysine production yield of BS383 was increased by 35 %. Additionally, the specific glucose uptake rate and the specific lysine production rate were increased by about 10 % and 50 %, respectively. Takeno et al. (2010) also analyzed the impact of *gapN* expression on lysine production using *C. glutamicum* ATCC 13032 with a deficient *lysC* gene. After replacing the native *gapA* gene against *gapN* of *S. mutans*, they found that the lysine production yield was increased by

38 % from 169 mmol mol^{-1} to 234 mmol mol^{-1}. Consequently, exclusive expression of *gapN* in a *gapA* deletion strain might have the potential of further enhancing lysine production. This seems to be due to the increased availability of NADPH in the genetic background of BS1. Apart from this, expression of *gapA* in BS553 also resulted in a final lysine production yield improved by 6 %. Because this improvement was less strong and coincided with a slightly retarded growth rate, rates for glucose uptake and lysine production were decreased accordingly. In summary it can be ascertained that expression of NADPH-regenerating *gapN* seemed to have the strongest effect on lysine production on BS1 indicating that the strain might be limited by the scarcity of this cofactor. This holds true, as described for the wild type of *C. glutamicum* as well as BS1 (Becker et al., 2005; Kiefer et al., 2004; Yokota and Lindley, 2005). Thus, overexpression of *gapN* might be particularly advantageous for strains without metabolic pathways optimized for NADPH-metabolism.

In the genetic background of BS244, however, the highest improvement was provided by episomal-based expression of *gapA* (strain BS554). Here, overexpression of *gapA* increased the lysine yield considerably by 58 %, which has not been described so far. Though Neuner et al. (2013) overexpressed *gapA* by promoter exchange in order to enhance lysine production, no significant improvement was observed. Nevertheless, there is evidence that expression of *gapA* might be a bottleneck in lysine production. Particularly during growth on fructose high amounts of dihydroxyacetone and glycerol have been observed as well as an increased NADH/NAD ratio (Dominguez et al., 1998; Kiefer et al., 2004). Since NADH is known to repress GapA activity (Kiefer et al., 2004), this might explain GapA limitations. Taken together, GapA seems to be a bottleneck during lysine production in BS244, which seems to be compensated by its overexpression. As for *gapN*, expression only resulted in a slightly improved lysine yield by 13 %. In addition, GapN exhibits a rather low activity by nature, as compared to GapA, and *S. mutans* has no GRAS-status. Thus, transgene expression of *gapN* is not recommended for industrial lysine production.

Overall, lysine production in BS244 could be improved by increased availabilities of GapDH as well as of NADPH. Consequently, modulation of the cofactor binding site of the native *gapA* gene from *C. glutamicum* might be a suitable strategy in future. Overexpression of GapA might further enhance lysine production. By doing so, heterologous gene expression would also be avoided. With regard to engineering of the cofactor binding site, first attempts have been published already. Lately, the cofactor binding site of GapA was manipulated systematically by rational protein design. Based on the modulation of distinct key residues, the cofactor specificity was changed from NAD to NADP and lysine production was successfully increased in a basic production strain of *C. glutamicum* (*lysC*^{Q298G}, *ppc*^{N917G}) (Bommareddy et al., 2014). In future, additional targets might be identified using computational designs, for example by the software OptSwap (King and Feist, 2013), while a simultaneous overexpression of NAD

kinase (EC: 2.7.1.23) might further enhance the positive effect of NADP-dependent GapDHs on lysine formation, as was indicated experimentally (Lindner et al., 2010; Wang et al., 2013). Moreover, optimization of the gene expression level of *gapA* seems to be a suitable strategy especially in the genetic background of *C. glutamicum* BS244. In this case, it is interesting to note that expression of *gapA* retarded the glucose uptake rate in strains based on BS244, while this effect was less strong in BS1 even though the enzyme activity detected for this genetic background was even higher. The results indicate that the metabolic network of BS244 reacts more sensitive to alterations, as compared to BS1. Since *C. glutamicum* BS244 is a highly specialized organism for lysine production, this illustrates the complexity of a metabolite equilibrium optimized for production processes and request for a genetic "fine-tuning" using promoter libraries (section 5.3 and 5.4).

5.2.2 Analysis of cofactor binding sites

As was shown before, increased availability of NADPH results in an improved lysine production performance in *C. glutamicum*, particularly in basic production strains. In order to reduce the amount of NADPH-consuming reactions, the nucleotide binding sites of DapB (EC: 1.3.1.26) and DDH (EC: 1.4.1.16) were modified by rational designs on the level of the native gene sequence. By introduction of distinct point mutations, amino acid exchanges were generated to manipulate the cofactor specificity of the native enzyme.

Nucleotide binding folds, so called the *βαβ*-folds, of different NAD(P)(H)-dependent dehydrogenases generally contain conserved consensus sequences. They are characterized by a conserved (V/I)(A/G)(V/I)-XGX(X)GXXG motif at the C-terminal end of the first *β*-strand B1, followed by an acidic or basic residue at the C-terminus of the second *β*-strand B2 approximately 20-30 amino acids further downstream (Cirilli et al., 2003; Scapin et al., 1995). This residue interacts with the 2'- and 3'-hydroxyl group of the adenosyl ribose ring and with the negatively charged 2'-phosphate of NADPH, respectively, via hydrogen bonds (Cirilli et al., 2003; Reddy et al., 1996). Thereby, acidic residues (Asp and Glu) are most prominent in enzymes with a cofactor specificity for NAD(H), while basic residues, particularly Arg, are typically present in NADP(H)-dependent enzymes (Reddy et al., 1996; Scrutton et al., 1990).

Functional analyses were performed using bioinformatics tools to identify the nucleotide binding site required for modification. In *C. glutamicum*, the *dapB* and *ddh* genes encode for 248 and 320 amino acids, respectively. A comparison of the N-terminal amino acid sequence revealed that the Gly-rich motif was present in both DapB and DDH (Table 5-3).

Table 5-3: Comparison of the N-terminal amino acid sequence of DapB (EC: 1.3.1.26) and DDH (EC: 1.4.1.16) revealing the (V/I)(A/G)(V/I)-XGX(X)GXXG motif (bold letters). This conserved motif indicates the cofactor binding site and was used to identify suitable modification targets (underlined letters). A list of all proteinogenic amino acids with their corresponding 3-letter and 1-letter code is depicted in section 8.2.

Protein	Amino Acid Sequence
DapB	^{1}MGIK**VGV**L**G**A K**G**RV**G**QTIVA AVNESDDLEL V<u>AEIGVDDD</u>L SLLVDNGAEV^{50}
DDH	^{1}MTNIR**VAI**V**G** Y**G**NL**G**RSVEK LIAKQPDMDL VG<u>IFSRR</u>ATL DTKTPVFDVA^{50}

Approximately 20 amino acids downstream of the N-terminal motif, the second pattern was identified. The native amino acid sequences were AEIGVDDD (amino acid 32-39) and IFSRR (amino acid 33-37) for DapB and DDH, respectively. Both sequences appear as promising targets for modification by bioinformatics analysis. This is strengthened by the fact that both sequences are located at the C-terminus of the second *β*-strand B2 and the loop that connects B2 with the next *α*-strand (Scapin et al., 1995; Scapin et al., 1996). While the amino acid residues of the former sequence (AEIGVDDD) do not allow any conclusions about the cofactor specificity of DapB, the IFSRR motif includes two basic arginine residues characteristically for NADP(H)-dependent enzymes. Geertz-Hansen et al. (2014) recently published a tool, called “Cofactory”, to identify potential Rossmann folds and to predict their specificity for a certain cofactor. Applied to this case study, the algorithm predicted the Rossmann fold of DapB and DDH to expand over amino acid 1-44 and 2-44, respectively. Interestingly, the software also forecasted a NAD(H)-dependency for DapB, while DDH seemed to be specific for NADP(H).

As for DapB from *E. coli*, there is also evidence that the enzyme has a dual cofactor specificity due to an acidic and a basic residue (Glu38 and Arg39) (Reddy et al., 1996; Scapin et al., 1995). Based on a sequence alignment, the corresponding positions in *C. glutamicum* were identified as Gly35 and Val36. Therefore, the modifications within the AEIGVDDD sequence of DapB were targeted to these key amino acids. Relating to the IFSRR motif of DDH, Scapin et al. (1996) confirmed that these amino acids are involved in binding of the cofactor NADPH. In particular, Ser35 and the basic amino acids Arg36 and Arg37 interact with the negatively charged 2’-phosphate residue of $NADP^+$ by shaping a pocket with Gly10 and Tyr11 from the N-terminal motif. In doing so, the binding is stabilized including two molecules of water to form eight hydrogen bonds with the 2’-phosphate, which might be the reason for the high specificity of DDH for NADPH as Misono et al. (1986) concluded. Consequently, an alteration of the annotated IFSRR sequence might result in a change of the cofactor specificity.

5.2.3 Episomal expression of modified dihydrodipicolinate reductase (DapB)

As mentioned above, the sequence motif AEIGVDDD of DapB was modulated in order to change its cofactor specificity to NAD^+. The native sequence of the cofactor binding site as well as the engineered sequence motives are depicted in Table 5-4.

The major difference between NAD^+ and $NADP^+$ is obviously the 2'-phosphate. This residue has a negative charge that interacts with basic residues via hydrogen bonds and possesses a relatively large atomic diameter. To prevent interactions with the 2'-phosphate of $NADP^+$, the binding pocket of DapB was modified in charge and size. The focus was set on the exchange of Gly35 as it is supposed to form hydrogen bonds with the 2'- and 3'-hydroxyl group of the adenosyl ribose ring. In addition, all modifications include the amino acid exchange of Val36 to alanine to reduce the binding pockets dimension. Further modifications were introduced in adjacent amino acids within the sequence motif AEIGVDDD that are supposed to tighten the size of the binding pocket (Table 5-4).

Table 5-4: Comparison of different cofactor binding sites of *dapB*. Deviations to the native sequence (*dapB*_R) are depicted in bold letters (*dapB*_1-5).

Construct	DNA Sequence (5' → 3')	Protein sequence
*dapB*_R	GCAGAGATCGGCGTCGACGATGAT	^{32}AEIGVDDD^{39}
*dapB*_1	GCAGAG**C**TCG**A**CG**C**CG**G**CGAT**CC**T	^{32}AE**LDAG**D**P**^{39}
*dapB*_2	GCAGAG**C**TCG**A**CG**C**CG**G**CGATGAT	^{32}AE**LDAG**DD^{39}
*dapB*_3	GCAGAGATCG**A**CG**C**CGACGATGAT	^{32}AEI**DA**DDD^{39}
*dapB*_4	GCAGAG**C**TCG**AA**G**C**CG**G**CGATGAT	^{32}AE**LEAG**DD^{39}
*dapB*_5	GCAG**C**G**C**TCG**AA**G**C**CG**G**CGATGAT	^{32}A**ALEAG**DD^{39}

All constructs were introduced in the episomally replicating vector pClik_5a_MCS under control of the native *dapB* promoter and expressed in the basic lysine producer *C. glutamicum* BS1. The strains were characterized on their productivity by cultivation in glucose minimal salt medium (Figure 5-7 and Table 5-5).

As depicted in Figure 5-7, all strains showed exponential growth without oxygen limitation. Only the production yield of the side product glycine varied slightly. Regarding Table 5-4, the constructed strains could be classified in two groups: The first group included BS372-BS374 (*dapB*_1-3) bearing the modifications G35D and V36A to change the binding pocket's charge and dimension while the other consisted of BS375 (*dapB*_4) and BS376 (*dapB*_5) bearing the modification G35E instead of G35D with a higher molecular weight and a slightly lower acidity. This pattern was also reflected by the results depicted in Table 5-5. In contrast to the reference strain BS371 (*dapB*_R) the modifications *dapB*_1-3 led to an increased lysine yield while *dapB*_4-5 resulted in a reduction. The best result was achieved with BS373 (*dapB*_2) showing an improved lysine yield of about 4 %. This was also confirmed by the relatively low biomass production yield. Furthermore, the growth rate of BS373 was only slightly increased, which resulted in a strong increase of the lysine production rate as well as an increased glucose uptake rate. The strains BS372 (*dapB*_1) and BS374 (*dapB*_3) exposed very similar values as BS373. In contrast to that, BS375 (*dapB*_4) and BS376 (*dapB*_5) had considerably lower production values, which might indicate an inactivation of the modulated enzyme.

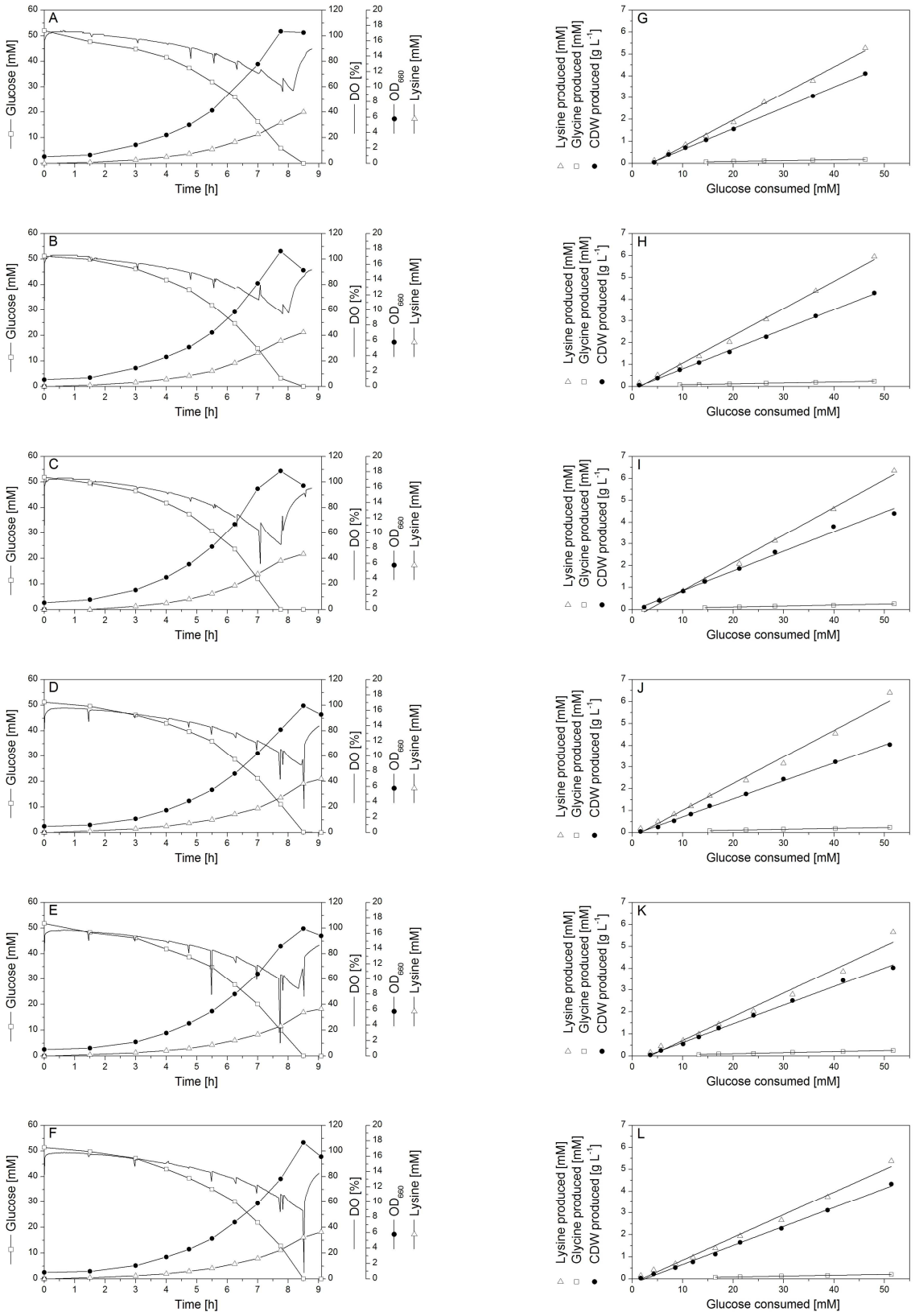

Figure 5-7: Growth and production characteristics of strains based on BS1 bearing different plasmids of pClik_5a_MCS_*dapB* with engineered cofactor binding sites. The data comprise cultivation profiles of BS371-BS376 (A-F) as well as the corresponding yields for lysine, glycine and biomass formation (G-L). All experiments were performed as single cultivation in 250 mL baffled disposable shake-flasks equipped with online sensor spots for O_2 and pH determination in minimal salt medium with glucose as sole carbon source, supplemented with 50 µg mL^{-1} kanamycin to maintain plasmid-based expression. The linear correlations between growth as well as product formation and glucose consumption, respectively, indicate metabolic steady-state during the cultivation.

Table 5-5: Growth and production characteristics on minimal salt medium with glucose as sole carbon source. All strains based on BS1 bearing the plasmid pClik_5a_MCS_*dapB* with engineered cofactor binding sites. The data given are yields for biomass production ($Y_{X/S}$), lysine formation ($Y_{Lys/S}$) and glycine formation ($Y_{Gly/S}$) as well as growth rates (μ), specific glucose uptake rates (q_{Glc}) and specific lysine production rates (q_{Lys}). All experiments were performed as single cultivation in 250 mL baffled disposable shake-flasks equipped with online sensor spots for O_2 and pH determination. The medium was additionally supplemented with 50 μg mL^{-1} kanamycin to maintain plasmid-based expression.

Strain	Construct	Yields		
		$Y_{X/S}$ [g mol^{-1}]	$Y_{Lys/S}$ [mmol mol^{-1}]	$Y_{Gly/S}$ [mmol mol^{-1}]
BS371	*dapB*_R	95.4	121.6	3.6
BS372	*dapB*_1	90.7	125.2	4.3
BS373	*dapB*_2	90.0	127.0	4.5
BS374	*dapB*_3	82.3	122.1	4.0
BS375	*dapB*_4	85.0	107.6	4.8
BS376	*dapB*_5	86.4	103.5	3.8
Strain	**Construct**	**Rates**		
		μ [h^{-1}]	q_{Glc} [mmol g^{-1} h^{-1}]	q_{Lys} [mmol g^{-1} h^{-1}]
BS371	*dapB*_R	0.45	4.68	0.57
BS372	*dapB*_1	0.45	4.91	0.62
BS373	*dapB*_2	0.46	5.06	0.64
BS374	*dapB*_3	0.44	5.30	0.65
BS375	*dapB*_4	0.44	5.12	0.55
BS376	*dapB*_5	0.43	4.93	0.51

However, it must be considered that all strains held the native *dapB* within their genome reducing the effect of the modified *dapB* gene gained by episomal expression. For a better elucidation of the role of *dapB*, another cultivation set up was used. It is known that during cultivation on fructose only 14.4 % of the carbon flux is directed through the PPP compared to 62.3 % on glucose resulting in a lack of NADPH (Becker et al., 2005; Kiefer et al., 2004). It seemed reasonable that the effect caused by a change of the cofactor specificity of DapB would become more pronounced if this sugar was used. Since high lysine production yields were observed for BS372 and BS373, both strains were then additionally cultivated in minimal salt medium with fructose as sole carbon source. BS371 served as a reference (Table 5-6).

The results revealed just marginal differences between the tested strains. In contrast to the results on glucose, the lysine production yields of BS372 and BS373 no longer exceeded that of BS371. The reference strain even seemed to be superior as it had a slightly higher lysine production yield and rate. But since the intermediates required for an enzymatic assay were not available, it was not possible to verify the cofactor specificity of DapB. Thus, it cannot be ruled out that the positive effects of the modifications G35D and V36A on the lysine production yield observed for BS372-BS374 on glucose were based on another reason besides a change in cofactor specificity. Otherwise, decreased consumption of NADPH should have influenced lysine production positively, especially under limiting conditions like growth on fructose.

Table 5-6: Growth and production characteristics in minimal salt medium with fructose as sole carbon source. All strains based on BS1 bearing the plasmid pClik_5a_MCS_*dapB* with engineered cofactor binding sites. The data given are yields for biomass production ($Y_{X/S}$), lysine formation ($Y_{Lys/S}$) and glycine formation ($Y_{Gly/S}$) as well as growth rates (μ), specific fructose uptake rates (q_{Frc}) and specific lysine production rates (q_{Lys}). All experiments were performed as single cultivation in 250 mL baffled disposable shake-flasks equipped with online sensor spots for O_2 and pH determination. The medium was additionally supplemented with 50 μg mL^{-1} kanamycin to maintain plasmid-based expression.

Strain	Construct	Yields		
		$Y_{X/S}$ [g mol^{-1}]	$Y_{Lys/S}$ [mmol mol^{-1}]	$Y_{Gly/S}$ [mmol mol^{-1}]
BS371	*dapB*_R	61.5	91.0	1.4
BS372	*dapB*_1	62.3	89.1	2.0
BS373	*dapB*_2	63.0	85.5	1.8
Strain	**Construct**	**Rates**		
		μ [h^{-1}]	q_{Frc} [mmol g^{-1} h^{-1}]	q_{Lys} [mmol g^{-1} h^{-1}]
BS371	*dapB*_R	0.34	5.50	0.50
BS372	*dapB*_1	0.34	5.47	0.49
BS373	*dapB*_2	0.36	5.73	0.49

Cirilli et al. (2003) also investigated the cofactor dependency of DapB. They analyzed the Gram-positive bacterium *Mycobacterium tuberculosis* and made an alignment of the cofactor binding site of DapB with different bacteria including *C. glutamicum*. According to Cirilli et al. (2003), the identity and similarity of the alignment between *M. tuberculosis* and *C. glutamicum* was 65 % and 76 %, respectively, presenting the highest homology detected in this study. Interestingly, the homologue sequence to the AEIGVDDD motif of *C. glutamicum* was found to be AELDAGDP (amino acid 30-37) in *M. tuberculosis*. Thus, it not only reflects the main modifications G35D and V36A of *dapB*_1-3, but also further similarities that were introduced (Table 5-7). In the same study, Cirilli et al. (2003) tried to change the cofactor specificity of *dapB* in favor of NADH. Thereby, they focused on the (V/I)(A/G)(V/I)-XGX(X)GXXG motif and introduced the modifications K9A and K11A. According to the study, these modifications led to an increased selectivity for NADH over NADPH of about 6-fold and 31-fold, respectively, as compared to the wild type.

Table 5-7: Sequence alignment of the N-terminal amino acid sequence of DapB (EC: 1.3.1.26) from *M. tuberculosis* and *C. glutamicum* revealing the (V/I)(A/G)(V/I)-XGX(X)GXXG motif (bold letters) as well as the second motif at the C-terminus of the second *β*-strand B2 (underlined letters) (Cirilli et al., 2003).

Organism	Construct	Amino Acid Sequence
M. tuberculosis	native	^{1}MR**VGV**L**G**AK**G** KV**G**ATMVRAV AAADDLTLSA ELDAGDPLSL^{40}
C. glutamicum	native	^{3}IK**VGV**L**G**AK**G** RV**G**QTIVAAV NESDDLELVA EIGVDDDLSL^{42}
BS371	*dapB*_1	^{3}IK**VGV**L**G**AK**G** RV**G**QTIVAAV NESDDLELVA ELDAGDPLSL^{42}
BS372	*dapB*_2	^{3}IK**VGV**L**G**AK**G** RV**G**QTIVAAV NESDDLELVA ELDAGDDLSL^{42}
BS373	*dapB*_3	^{3}IK**VGV**L**G**AK**G** RV**G**QTIVAAV NESDDLELVA EIDADDDLSL^{42}

Furthermore, the modification K11A resulted in an increased enzyme activity of 276 % for NADH. Cirilli et al. (2003) pointed out that even though K9 and K11 would not directly interact with NADPH, both residues would promote its binding due to their highly positively charged environment in the region adjacent to the 2'-phosphate of NADPH. Consequently, the same strategy would be an attractive attempt for further analyses in *C. glutamicum* bearing the basic residues Lys11 and Arg13 at the corresponding positions.

5.2.4 Modification of diaminopimelate dehydrogenase (DDH)

Bioinformatics analysis revealed that the IFSRR motif (amino acid 33-37) of DDH might be a promising target for modification due to its interaction with the 2'-phosphate residue of $NADP^+$. The native sequence of the cofactor binding site as well as the engineered sequence motives are depicted in Table 5-8.

Table 5-8: Comparison of different cofactor binding sites of *ddh*. Deviations to the native sequence (*ddh*_R*)* are depicted in bold letters (*ddh*_1-9).

Construct	DNA Sequence (5' → 3')	Protein sequence
*ddh*_R	ATCTTCTCGCGCCGG	^{33}IFSRR^{37}
*ddh*_1	ATCTTC**GA**GCGCCGG	^{33}IF**E**RR^{37}
*ddh*_2	ATCTTC**CA**GCGCCGG	^{33}IF**Q**RR^{37}
*ddh*_3	ATCTTCTCGCGC**TT**G	^{33}IFSR**L**^{37}
*ddh*_4	ATCTTCTCGCGC**GA**G	^{33}IFSR**E**^{37}
*ddh*_5	ATCTTCTCG**GA**C**GA**T	^{33}IFS**DD**^{37}
*ddh*_6	ATCTTC**GA**GCGC**TT**G	^{33}IF**E**R**L**^{37}
*ddh*_7	ATCTTC**GA**GCGC**GA**G	^{33}IF**E**R**E**^{37}
*ddh*_8	ATCTTC**GA**G**GA**C**GAT**	^{33}IF**EDD**^{37}
*ddh*_9	ATC**A**TC**GATGT**CC**A**G	^{33}**IIDVQ**^{37}

Being directly involved in the binding and stabilization of $NADP^+$ the main interest was focused on Ser35, Arg36 and Arg37. Since serine is a small amino acid and arginine has a basic residue, modifications were introduced to weaken the bond with the 2'-phosphate, which is characterized by a comparatively large atomic diameter and a negative charge. For this reason, both the binding pocket's dimension as well as the number of hydrogen bonds formed had to be reduced. This should be achieved by replacement of serine on the one hand (*ddh*_1-2) and by introduction of amino acids with acidic residues like glutamate and aspartate, on the other hand (*ddh*_3-5). Furthermore, combinations of both were constructed (*ddh*_6-9).

All constructs were ligated into the episomally replicating vector pClik_5a_MCS under control of the strong promoter P_{eftu} to enhance *ddh* expression. Afterwards, the plasmids were introduced into *C. glutamicum* BS27, which carried a deletion within the *ddh* gene resulting in its

inactivation. Thus, interference by genome based *ddh* expression was eliminated. Furthermore, the plasmids holding the constructs P_{eftu}*ddh*_R and P_{eftu}*ddh*_1, were introduced into the lysine hyper producer *C. glutamicum* BS244.

The mutants were analyzed by an enzymatic assay using either $NADP^+$ or NAD^+ as a cofactor (Table 5-9 and Figure 5-8).

Determination of the specific enzyme activities confirmed that native *ddh* is specific for $NADP^+$. For the basic strain *C. glutamicum* BS244 (2x*ddh*), a strong $NADP^+$-dependent activity (508 U g^{-1}) was detected matching with previous findings (Becker et al., 2011). As expected, the *ddh* deletion strain BS27 (Δ*ddh*) exposed no activity. Interestingly, the strains BS453 and BS474, each bearing the reference plasmid, showed very high activities for $NADP^+$ (64 U mg^{-1}). These activities can probably be ascribed to the episomal expression of *ddh* as well as its overexpression under control of the strong promoter P_{eftu}. Typical *ddh* activities are about 200 U g^{-1} in the wild type of *C. glutamicum* (Becker et al., 2011; Cremer et al., 1988) and 2.5 U mg^{-1} under episomal *ddh* expression (Cremer et al., 1991).

Table 5-9: Analysis of the specific enzyme activity [U g^{-1}] of diaminopimelate dehydrogenase depending on the cofactor $NADP^+$ and NAD^+ of different *C. glutamicum* strains cultivated in deep well plates on BHI, supplemented with 50 µg mL^{-1} kanamycin to maintain plasmid-based expression at 30 °C. BS453 and BS454 originate from the lysine hyper producer BS244 while the other strains are based on BS27 (Δ*ddh*). All P_{eftu}*ddh* constructs were expressed by the episomal replicating plasmid pClik_5a_MCS. Enzyme activities were determined in triplicate. Mean values (± standard deviation) of $NADP^+$/NAD^+-dependent and total enzyme activities are depicted as well as the relative NAD^+ and total enzyme activity.

Strain	Construct	Specific Enzyme Activities [U g^{-1}]			Relative Specific Enzyme Activities [%]		
		$NADP^+$-dependent	NAD^+-dependent	Total	$NADP^+$-dependent	NAD^+-dependent	Total
BS244	basic strain	508 ± 19	20 ± 1	528 ± 19	96.2	3.8	0.8
BS453	P_{eftu}*ddh*_R	64211 ± 983	2044 ± 70	66255 ± 985	96.9	3.1	100.0
BS454	P_{eftu}*ddh*_1	661 ± 33	1140 ± 84	1801 ± 90	36.7	63.3	2.7
BS27	basic strain	0	> 0.01	> 0.01	-	-	> 0.1
BS474	P_{eftu}*ddh*_R	64259 ± 1817	2096 ± 81	66356 ± 1819	96.8	3.2	100.0
BS475	P_{eftu}*ddh*_1	81 ± 6	879 ± 77	960 ± 77	8.5	91.5	1.4
BS476	P_{eftu}*ddh*_2	2378 ± 182	191 ± 6	2569 ± 183	92.6	7.4	3.9
BS477	P_{eftu}*ddh*_3	1301 ± 58	170 ± 26	1471 ± 64	88.4	11.6	2.2
BS478	P_{eftu}*ddh*_4	400 ± 34	168 ± 4	568 ± 34	70.5	29.5	0.9
BS479	P_{eftu}*ddh*_5	> 1	34 ± 1	35 ± 1	1.0	99.0	> 0.1
BS487	P_{eftu}*ddh*_6	5 ± 1	205 ± 13	210 ± 13	2.2	97.8	0.3
BS488	P_{eftu}*ddh*_7	0	5 ± 3	5 ± 3	0	100.0	> 0.1
BS489	P_{eftu}*ddh*_8	> 1	16 ± 2	17 ± 2	1.8	98.2	> 0.1
BS490	P_{eftu}*ddh*_9	8 ± 0	104 ± 3	112 ± 3	6.8	93.2	0.2

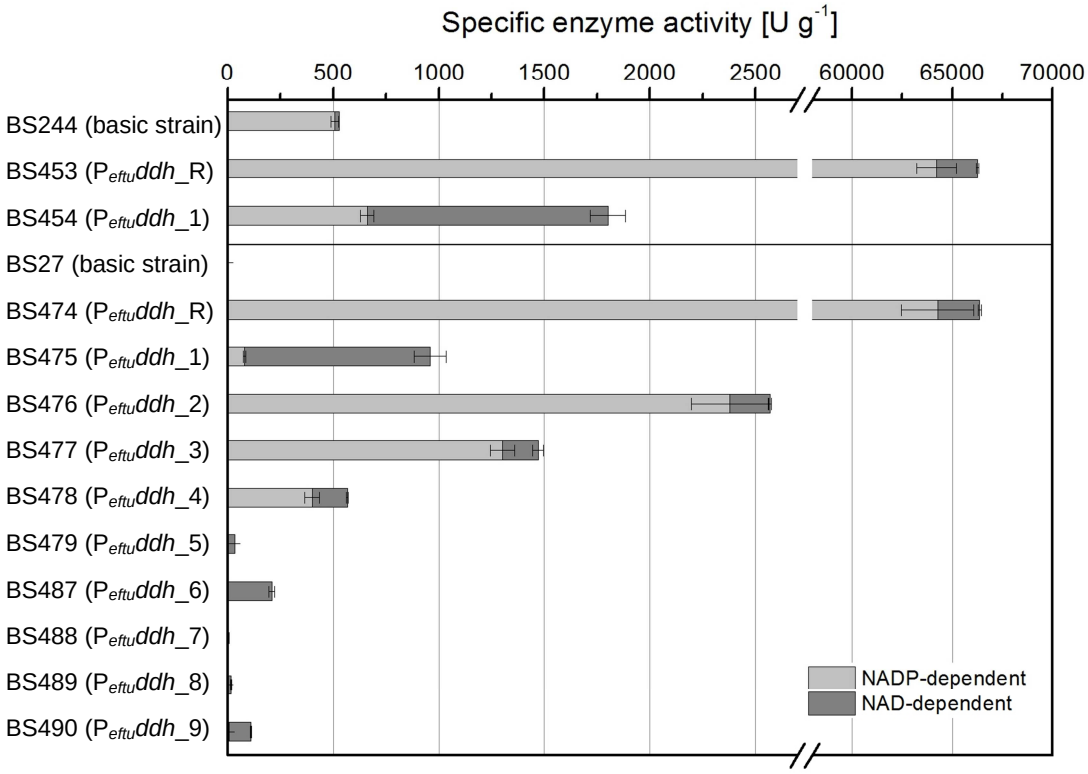

Figure 5-8: Analysis of the specific enzyme activity [U g^{-1}] of the diaminopimelate dehydrogenase depending on the cofactors $NADP^+$ and NAD^+ of different *C. glutamicum* strains cultivated in BHI which was supplemented with 50 µg mL^{-1} kanamycin to maintain plasmid-based expression at 30 °C. BS453 and BS454 originate from the lysine hyper producer BS244 while the other strains are based on BS27.

Regarding the constructs P_{eftu}*ddh*_1-9, it had to be noticed that total enzyme activities were considerably reduced, as compared to their corresponding reference strains BS453 and BS454. The highest activity was detected for BS476 (P_{eftu}*ddh*_2) of 2.4 U mg^{-1} (4 % of the total enzyme activity, as compared to BS474), while the constructs P_{eftu}*ddh*_5-9 seemed to result in inactive enzymes. Here, total specific DDH activity was below 1 % of the reference level (BS474). This might be due to the higher number of modifications within the IFSRR motif as well as their positions. While the sequence motif P_{eftu}*ddh*_2 possesses only one amino acid exchange (S35Q), P_{eftu}*ddh*_5-9 had at least two modifications at position 36+37 (P_{eftu}*ddh*_5), 35+37 (P_{eftu}*ddh*_6-8) and 34-37 (P_{eftu}*ddh*_9). The comparison of the total enzyme activities of P_{eftu}*ddh*_1 (S35E) with P_{eftu}*ddh*_4 (R37E) on the one hand and P_{eftu}*ddh*_2 (S35Q) with P_{eftu}*ddh*_3 (R37L) on the other hand, revealed that a conversion of the amino acid Arg37 resulted in a stronger reduction of the enzyme activity than an exchange of Ser35 (Table 5-9 and Figure 5-8) since both groups possess comparable modifications against an acidic and a small amino acid, respectively. Consequently, the amino acids Arg36 and Arg37 seemed to fulfill an important role in the enzyme's functionality as they are strongly conserved. This might be explained by the number of hydrogen bonds being formed with the 2'-phosphate residue of $NADP^+$. While Ser35 forms only one hydrogen bond, Arg36 and Arg37 interact by four bonds giving much more stability (Scapin et al., 1996).

In addition, the reference strains BS244, BS453 and BS454 further revealed a low activity of about 3-4 % with NAD^+ as a cofactor. These results matched perfectly with those of Misono et al. (1986) who found that DDH not only uses $NADP^+$ as a cofactor, but also NAD^+ naturally, although with a lower specificity of 3 %. The constructs P_{eftu}*ddh*_5-9 showed a high dependency for NAD^+ according to the relative NAD^+-dependent enzyme activities, however, this can be neglected due to the low total enzyme activities indicating an inactivation of DDH. Regarding BS476-478 (P_{eftu}*ddh*_2-4) the relative NAD^+-dependent enzyme activities shifted just slightly in favor of this cofactor. Interestingly, expression of P_{eftu}*ddh*_1 resulted in a strong reduction of $NADP^+$-dependent DDH activity while the NAD^+-dependent activity was conserved. As a consequence, only the strains BS454 and BS475, both bearing the construct P_{eftu}*ddh*_1, showed a reliable preference for NAD^+ over $NADP^+$ of 63 % and 92 %, respectively, as compared to the reference constructs BS453 and BS474 (3 %). Thereby, the lower specificity of BS454 for NAD^+ can probably be ascribed to the gene duplication of native *ddh* within its genome increasing its specificity for $NADP^+$. Compared to the reference strains BS453 (2045 U g^{-1}) and BS474 (2097 U g^{-1}), the specific enzyme activities using NAD^+ as a cofactor were reduced by about 50 % in BS454 (1141 U g^{-1}) and BS475 (880 U g^{-1}) indicating that not only the enzymes preference for a cofactor was changed, but also its activity. Since NAD^+-dependent DDH activity did not compensate the loss of $NADP^+$-dependent activity, the reduction of total enzyme activity for the constructs P_{eftu}*ddh*_1 was even stronger. It was found that modification of the cofactor binding site often goes hand in hand with improved specific enzyme activities, but also with reduced overall enzyme activities. Thus, it is a general challenge in rational protein design to guarantee sufficient catalytic enzyme activities (Chen et al., 1995; Katzberg et al., 2010). Here, a total enzyme activity of 2-3 % for P_{eftu}*ddh*_1 remained, when compared to the reference (P_{eftu}*ddh*_R).

Nevertheless, the cofactor specificity of P_{eftu}*ddh*_1 was changed successfully by only one amino acid exchange (S→E) reducing the specificity of the new enzyme for $NADP^+$ by about 90 %. Future attempts should focus on the enhanced binding and stabilization of NAD^+. This might be achieved by advanced variation of the IFSRR motif, in particular of Ser35. Another strategy to increase the specific enzyme activity using NADH might be the modulation of the N-terminal motif. For DDH, the residues Gly10 and Tyr11 seem to be attractive targets for modification, since they are involved in the binding of the negatively charged 2'-phosphate residue of $NADP^+$ (Scapin et al., 1996).

All strains were then characterized on the level of lysine production by cultivation on glucose minimal salt medium involving an end point determination of the lysine concentration to derive the product yield (Table 5-10).

Table 5-10: Characterization of the productivity by end point determination of the lysine concentration of different *C. glutamicum* strains. BS453 and BS454 originate from the lysine hyper producer BS244, while the other strains are based on BS27 (Δ*ddh*). The P_{eftu}*ddh* constructs were expressed by the episomal replicating plasmid pClik_5a_MCS. The data given are final yields for biomass production ($Y_{X/S}$), lysine formation ($Y_{Lys/S}$) and glycine formation ($Y_{Gly/S}$) as well as growth rates (μ), specific glucose uptake rates (q_{Glc}) and specific lysine production rates (q_{Lys}). All experiments were performed in triplicate in MTP-48-FlowerPlates in 1 mL minimal salt medium with glucose as sole carbon source, supplemented with 50 μg mL^{-1} kanamycin to maintain plasmid-based expression.

Strain	Construct	Final Yields		
		$Y_{X/S}$ [g mol^{-1}]	$Y_{Lys/S}$ [mmol mol^{-1}]	$Y_{Gly/S}$ [mmol mol^{-1}]
BS244	basic strain	59.8 ± 1.2	342.4 ± 1.5	8.2 ± 0.3
BS453	P_{eftu}*ddh*_R	51.8 ± 1.1	352.0 ± 4.4	6.6 ± 0.1
BS454	P_{eftu}*ddh*_1	68.7 ± 0.2	235.4 ± 5.3	9.0 ± 0.3
BS27	basic strain	81.0 ± 2.7	122.8 ± 0.5	14.0 ± 0.2
BS474	P_{eftu}*ddh*_R	48.5 ± 1.3	177.6 ± 0.4	3.4 ± 0.0
BS475	P_{eftu}*ddh*_1	64.7 ± 1.1	94.7 ± 1.8	6.4 ± 0.0
BS476	P_{eftu}*ddh*_2	71.8 ± 0.3	129.1 ± 0.2	10.7 ± 0.0
BS477	P_{eftu}*ddh*_3	65.2 ± 0.7	138.5 ± 4.3	6.5 ± 0.2
BS478	P_{eftu}*ddh*_4	64.4 ± 0.9	120.1 ± 0.1	6.5 ± 0.1
BS479	P_{eftu}*ddh*_5	68.3 ± 0.3	115.3 ± 3.2	7.0 ± 0.1
BS487	P_{eftu}*ddh*_6	76.7 ± 0.9	77.3 ± 0.5	10.7 ± 0.1
BS488	P_{eftu}*ddh*_7	75.6 ± 0.7	84.7 ± 0.8	11.9 ± 0.1
BS489	P_{eftu}*ddh*_8	78.4 ± 0.3	77.9 ± 0.0	9.1 ± 0.1
BS490	P_{eftu}*ddh*_9	68.1 ± 1.3	104.1 ± 2.0	7.8 ± 0.2

Strain	Construct	Rates		
		μ [h^{-1}]	q_{Glc} [mmol g^{-1} h^{-1}]	q_{Lys} [mmol g^{-1} h^{-1}]
BS244	basic strain	0.15 ± 0.01	2.49 ± 0.05	0.85 ± 0.01
BS453	P_{eftu}*ddh*_R	0.08 ± 0.00	1.63 ± 0.03	0.58 ± 0.01
BS454	P_{eftu}*ddh*_1	0.15 ± 0.01	2.12 ± 0.01	0.50 ± 0.01
BS27	basic strain	0.20 ± 0.00	2.48 ± 0.08	0.30 ± 0.01
BS474	P_{eftu}*ddh*_R	0.05 ± 0.00	1.13 ± 0.03	0.20 ± 0.01
BS475	P_{eftu}*ddh*_1	0.11 ± 0.01	1.77 ± 0.03	0.17 ± 0.01
BS476	P_{eftu}*ddh*_2	0.14 ± 0.02	1.92 ± 0.01	0.25 ± 0.00
BS477	P_{eftu}*ddh*_3	0.13 ± 0.00	1.94 ± 0.02	0.27 ± 0.01
BS478	P_{eftu}*ddh*_4	0.11 ± 0.00	1.74 ± 0.03	0.21 ± 0.00
BS479	P_{eftu}*ddh*_5	0.10 ± 0.00	1.50 ± 0.01	0.17 ± 0.01
BS487	P_{eftu}*ddh*_6	0.17 ± 0.01	2.28 ± 0.03	0.18 ± 0.00
BS488	P_{eftu}*ddh*_7	0.15 ± 0.01	1.99 ± 0.02	0.17 ± 0.00
BS489	P_{eftu}*ddh*_8	0.17 ± 0.00	2.16 ± 0.01	0.17 ± 0.00
BS490	P_{eftu}*ddh*_9	0.14 ± 0.01	2.04 ± 0.04	0.21 ± 0.01

Except for BS454, all generated strains exhibited reduced values for biomass formation and growth (Table 5-10). Obviously, *C. glutamicum* was stressed by the high *ddh* expression due to the plasmid-based expression in combination with overexpression via P_{eftu}. The same also applies for the strains exhibiting low *ddh* activities (BS479-BS490). Though, introduced modifications resulted in inactive DDH, the expression level of the inactive protein was expected to be high. Such strains possessed the lowest lysine production yield. Obviously, they had suffered from the metabolic burden by the high *ddh* expression, without a benefit through increased enzyme activity. The strain BS478 on the other hand showed a DDH activity of about 570 U g^{-1}. Here, the positive effect of the additional *ddh* expression on the lysine production compensated the extra costs associated with the high expression level. As a consequence, BS478 showed a similar lysine production yield as BS27.

As already mentioned, high levels of active DDH do influence lysine production positively. This was even more obvious in the genetic background of BS27 (Δ*ddh*) confirming previous results (Becker et al., 2011) in which a duplication of the *ddh* gene resulted in an increased lysine production yield by 25 % in the basic lysine producer *C. glutamicum* BS1. In the study presented here, the lysine production yield of the reference strain BS474 expressing the native *ddh* gene was increased by 45 %. In contrast to the results of Becker et al. (2011) the growth was retarded, here. Thus, the lysine production yield was not only promoted by a high DDH activity, but could also have resulted from a decreased growth. Regarding by-product formation, the strain BS474 further exhibited the lowest glycine production yield (Table 5-5).

In the genetic background of BS244 the effect of *ddh* overexpression was less clear. Here, the lysine production yield was only slightly increased (3 %) in BS453.

The impact of increased *ddh* expression should further be analyzed to improve the lysine production performance of *C. glutamicum* (section 5.4.1).

5.3 Generation of a synthetic Promoter Library for rational Strain Engineering

Since it is interesting to know how gene expression can be controlled by fine adjustment, another strategy to optimize lysine production in *C. glutamicum* focused on generation of a promoter library required for identification of the optimal gene expression level.

This promoter library based on the strong promoter of the superoxide dismutase P_{sod} and was constructed by random mutagenesis using *GFPmut1* (Cormack et al., 1996) as a reporter gene. Mutagenesis of P_{sod} was performed as described in section 4.6.5. To ensure a broad spectrum of different *sod* promoters, all ligation products, gained after transformation of *E. coli*, were isolated. The plasmid DNA mix was further used to transform the wild-type of *C. glutamicum* ATCC 13032 by electroporation and the plasmid-based *gfp* expression was analyzed using black light (Figure 5-9) and the micro bioreactor system BioLector®. The strain *C. glutamicum* BS388 (P_{sod}*GFPmut1*) bearing the native *sod* promoter served as reference.

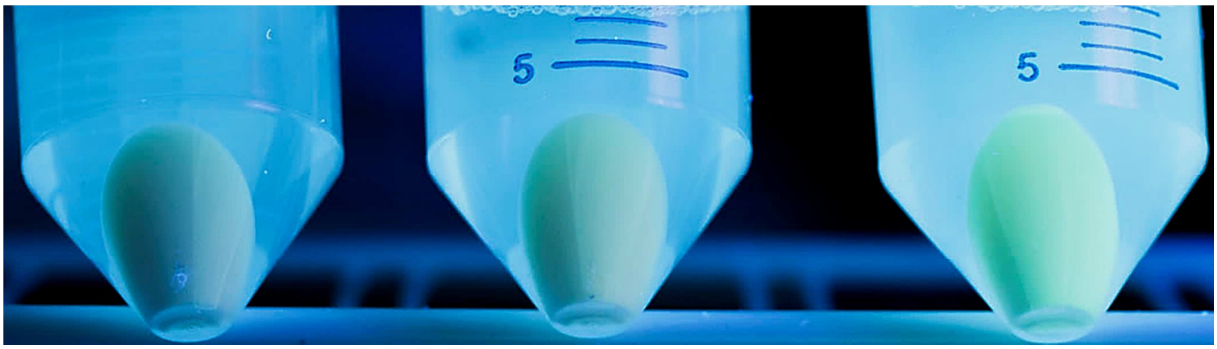

Figure 5-9: Example of *gfp* expression in *C. glutamicum* ATCC 13032 under black light. Different strains of *C. glutamicum* bearing the plasmid pClik_5a_MCS_P_{sod}*GFPmut1* were cultivated in BHI at 30 °C and harvested by centrifugation resulting in varying fluorescent signals.

Based on the results, preselected mutant plasmids were chosen for sequencing and distinct promoters were passed through another round of random mutagenesis. In the end, a total of four mutation rounds were performed, 400 colonies were analyzed for their *gfp* activity and thereof about 50 were further analyzed by sequencing. By doing so, 23 different mutated P_{sod} sequences were determined. From the same promoters, the relative promoter activities were calculated (Table 5-11) and specific constructs were selected for gene expression studies (Figure 5-10).

Regarding Table 5-11 and Figure 5-10, the increase of relative promoter activity with every new mutation round can be nicely observed. While the native P_{sod} promoter showed the same activity of about 3.6 ± 0.6 [$BS_{G:100}$:$BS_{G:5}$] (100 %) in all measurements, this activity was already exceeded by 5-fold after the first mutation round. Further rounds of mutagenesis finally resulted in the strongest promoter analyzed. The promoter $P_{9\text{-}42}$ had the highest relative promoter activity of 73.2 [$BS_{G:100}$:$BS_{G:5}$], which is equivalent to the activity of the native construct by more than the 20-fold.

Table 5-11: Analysis of the relative P_{sod} promoter activity of selected P_{sod} mutants. The promoter activity was calculated from the GFP activity plotted against the increase of biomass at a gain of 100 and 5, respectively. Data were derived from cultivation experiments on BHI supplemented with 50 µg mL^{-1} kanamycin to maintain plasmid-based expression at 30 °C using the micro bioreactor system BioLector®. Standard deviations were derived from duplicates identified by DNA sequencing.

Construct	Mutation Round	Relative Promoter Activity [$BS_{G:100}$: $BS_{G:5}$]	Construct	Mutation Round	Relative Promoter Activity [$BS_{G:100}$: $BS_{G:5}$]
P_{sod}*	0	3.63 ± 0.57	P_{5-25}	2	14.60
P_{1-37}	1	4.99	P_{5-28}	2	16.02
P_{1-11}	1	5.09 ± 0.24	P_{5-13}	2	18.28
P_{1-08}	1	11.59 ± 1.09	P_{6-43}	2	20.69 ± 1.83
P_{1-33}	1	16.27 ± 0.92	P_{6-26}	2	22.11
P_{2-21}	1	18.63	P_{5-16}	2	27.04 ± 1.39
P_{1-49}*	1	18.91 ± 0.89	P_{6-49}	2	33.10
P_{5-15}	2	6.36 ± 0.46	P_{5-02}*	2	34.33 ± 1.71
P_{5-19}	2	7.90 ± 1.01	P_{7-29}	3	53.79 ± 5.09
P_{6-47}	2	10.29	P_{7-19}*	3	58.28 ± 2.05
P_{5-20}	2	11.11 ± 0.94	P_{10-18}	4	58.41
P_{5-22}	2	12.93	P_{9-42}	4	73.19

*** P_{sod} constructs that were used as template for the next mutation round**

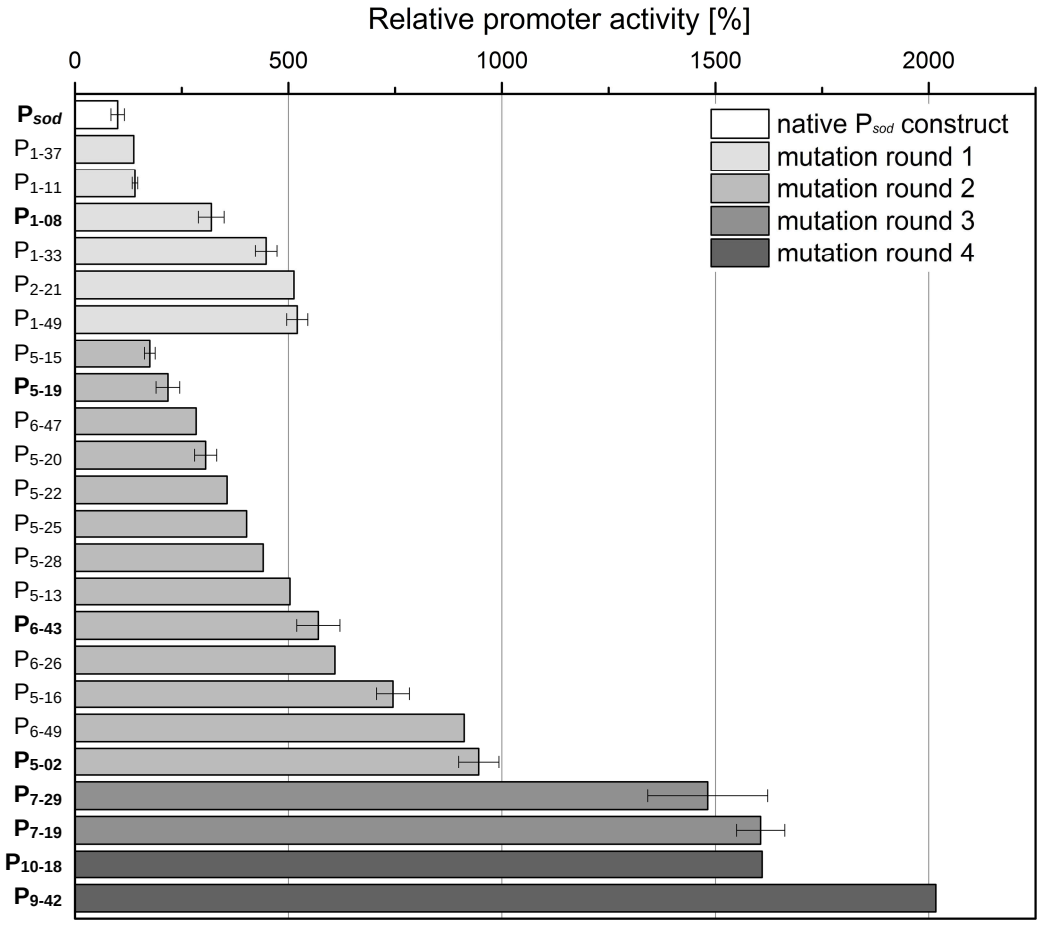

Figure 5-10: Relative promoter activities (in %) of different promoter mutants, as compared to the reference P_{sod}. Bold letters indicate mutants used for further studies while P_{sod} mutants derived from the same mutation round are depicted in the same shades of grey.

In addition, a sequence alignment was performed and the TSS of the native P_{sod} construct predicted using the software BPROM (http:// www.softberry.com/berry.phtml). Accordingly, the TSS was located at position +1 and seemed to be highly conserved, as no promoter sequence showed a modification at this position. Referred to the native promoter sequence, the regulatory -35 and -10 elements of the RNA polymerase binding site were predicted to be at position -35 to -30 (C**TGAC**G) and -15 to -7 (G**TATAT**GCT), respectively (Figure 5-11). Both sequence elements showed a good agreement with the results published by Pátek et al. (2013). They reported consensus sequences for *C. glutamicum* of T**TGNC**A and G**NTANAN**TNG for the -35 and the extended -10 element of housekeeping promoters, respectively (homologies are depicted in bold letters, core hexamers are underlined).

As shown in Figure 5-11, the -35-motif, proposed by Pátek et al. (2013), was identified in the mutated P_{sod} sequences of $P_{7\text{-}19}$, $P_{10\text{-}18}$ and $P_{9\text{-}42}$, all bearing the transitions C35T and G30A. Interestingly, these sequences also showed the highest relative promoter activity confirming the importance of this functional consensus sequence. Especially the modification C35T seemed to be highly conserved since nearly 80 % of the analyzed promoter sequences contained this transition. Moreover, further sequence motifs were identified that were only present in $P_{7\text{-}19}$, $P_{10\text{-}18}$ and $P_{9\text{-}42}$ namely CATGGCNC (-100 to -93), ACGTTG (-62 to -57) and ACA (-4 to -2). Though the latter promoters were derived from $P_{7\text{-}19}$ by random mutagenesis, these motives might be responsible for their strong promoter activities as they were conserved. The extended -10-motif (GNTANANTNG) was also identified for $P_{1\text{-}33}$, $P_{2\text{-}21}$, $P_{5\text{-}15}$, $P_{5\text{-}28}$ and $P_{5\text{-}13}$ at position -13 to -5.

Almost all promoter studies only focus on the -35 and -10 regions as they mediate the binding of the RNA polymerase, while the sequence upstream of -35 is mostly regarded as unimportant. Nevertheless, it had to be noticed that all mutated promoter sequences had an increased GC-content in common of up to 63.5 % in $P_{10\text{-}18}$, as compared to 45.3 % in the native P_{sod} sequence. Particularly, at the positions -144 to -141, -127 to -123, -111 to -106, -93 to -84, -66 to -48, -28 to -16 and +3 to +9 transitions lead to GC-rich regions. This might be attributed to the use of the JBS dNTP-Mutagenesis Kit (Jena Bioscience, Jena, Germany). During mutagenesis, the dNTP analogs 8-oxo-dGTP and dPTP were used leading to random mutations of A→C:T→G in a ratio of 1:1.5 and A→G:T→C:G→A:C→T in a ratio of 5:4:1:1, respectively. Each mutation round comprised 25 mutation cycles corresponding to a rate of mutagenesis of about 15 %. According to the manufacture's protocol, the mutagenesis rate is the sum of the individual rates of the mutagenic substances. For 8-oxo-dGTP and dPTP this is in accordance with 2.2 % and 12.8 %, respectively. Thus, random mutagenesis promotes the formation of GC-rich sequences by transitions. The repetitive modification process might have enhanced this phenomenon, additionally. Consequently, any further mutation round resulted not only in

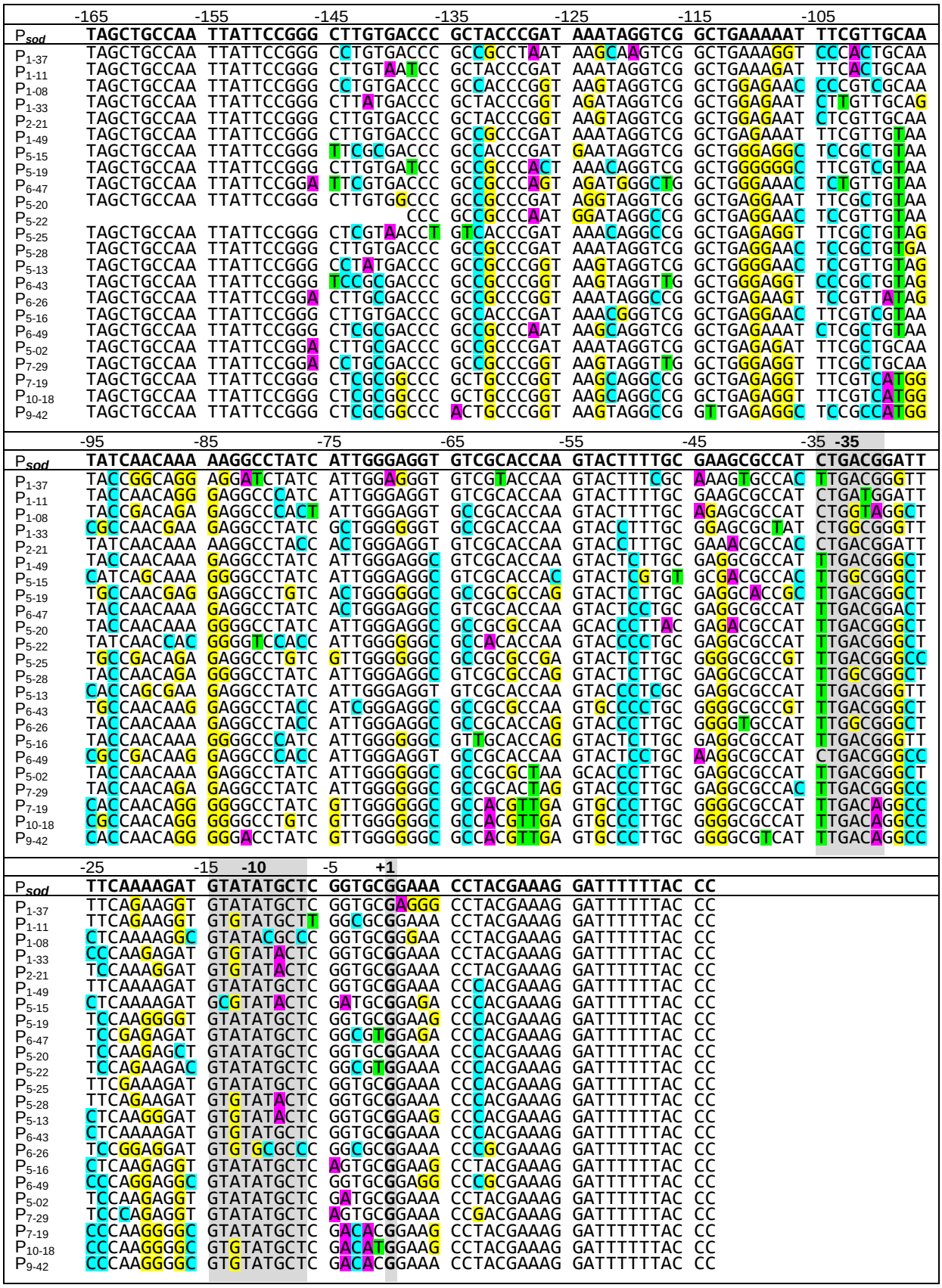

Figure 5-11: Sequence alignment of selected P_{sod} mutants derived from the random promoter library. The alignment was performed with Geneious® V. 6.1.6. Aberrations from the native P_{sod} sequence are highlighted in color, while the TSS and the regulatory -35 and -10 element are marked in grey.

stronger promoter activities, but also correlated with increased GC-contents in all subsequent promoter sequences within this study. The same was observed for the spacer region between the -35 and -10 element located at position -29 to -16. In the past, it was assumed that only its length would be important facilitating the interaction of the -35 and -10 element with the RNA polymerase holoenzyme (Dombroski et al., 1996; Young et al., 2002). Recently, studies also focused on the spacer's sequence. It was found that AT-rich sequences resulted in a higher flexibility of the helix which is required in the downstream area during transcription. As a result, the activity of the promoter would be significantly increased (Hook-Barnard and Hinton, 2007; Liu et al., 2004). In this study, the sequence alignment depicted in Figure 5-11 demonstrated that the promoter activities were increased steadily with the GC-content as described before. While the native spacer element had a GC-content of 21.4 %, the strongest promoters ($P_{7\text{-}19}$, $P_{10\text{-}18}$ and $P_{9\text{-}42}$) bearing the motif CCCCAAGGGG (-27 to -17) showed a content of 85.7 % after up to four rounds of random mutagenesis. This clearly indicates that the AT-content of the spacer region plays a rather minor role for the promoter activity, here.

Summarized, these results demonstrate that a broad spectrum of different promoter activities based on the native *sod* promoter P_{sod} was achieved creating a promoter library with only four rounds of random mutagenesis PCR. In a next step, this promoter library was used for gene expression studies aiming on strain engineering to improve lysine production (section 5.4). The calculated relative promoter activities depicted in Figure 5-10 were used to give an orientation about the promoter's strength, which can also be transferred to stable modification attempts. Furthermore, the applied mutagenesis strategy might not only be interesting for the construction of promoter libraries, but also for site-directed mutagenesis of cofactor binding sites in future (section 5.2).

5.4 Gene Expressions Studies based on the P_{sod} random Promoter Library

Selected promoters, derived from the P_{sod} library (section 5.3), were further used for gene expression studies of diaminopimelate dehydrogenase, the transketolase operon and the lysine exporter LysE. The modulations aimed at optimization of lysine production by fine adjustment of the optimal gene expression level using different P_{sod} promoters.

5.4.1 Diaminopimelate dehydrogenase as bottleneck

In *C. glutamicum*, lysine is produced by the multi-stage succinylase or the single-stage dehydrogenase pathway, respectively. The latter branch was predicted to be the most promising route for lysine production via an *in silico* elementary mode analysis (Melzer et al., 2009). In addition, Becker et al. (2011) observed that overexpression of *ddh* improved the lysine production yield by about 25 % in the feedback-deregulated lysine overproducer *C. glutamicum* BS1 (Lys-1). Accordingly, *ddh* appears a promising target for gene expression studies using the P_{sod} promoter library.

For *ddh* expression studies, strain construction was performed, using *C. glutamicum* BS1 as a host and BS222 (Lys-2) (Becker et al., 2011) as an additional reference bearing the duplicated *ddh* gene. A total of eight different P_{sod} promoters including the native P_{sod} construct were inserted adjacent to the start codon of *ddh*. Successful strain construction was verified by PCR while enzymatic assays were conducted as proof for gene expression and for quantification of the promoter activity (Figure 5-12).

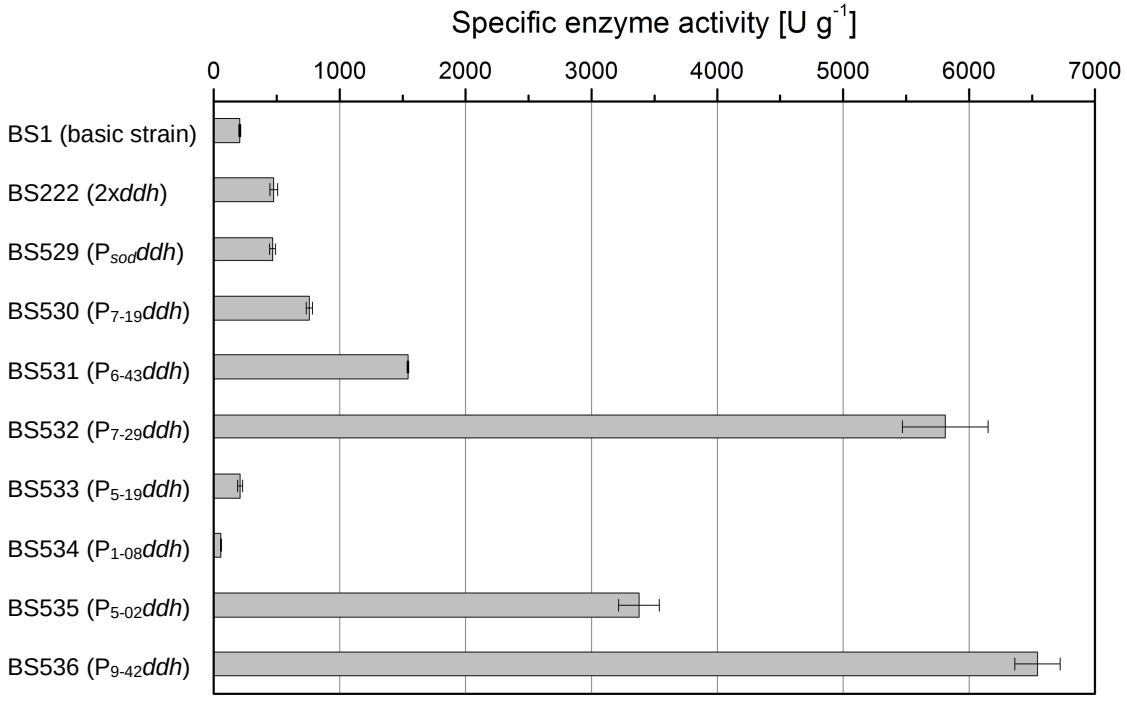

Figure 5-12: Analysis of the specific enzyme activity [U g^{-1}] of the diaminopimelate dehydrogenase of different P_{sod} mutants based on BS1. Cultivation was performed in deep well plates in BHI at 30 °C. Enzyme activities were determined in triplicate.

The resulting specific enzyme activities for DDH indicated a broad spectrum of different gene expression levels as desired (Figure 5-12). For the basic strain, *C. glutamicum* BS1 and the reference strain BS222, enzyme activities were 206 U g^{-1} and 476 U g^{-1}, respectively. These values confirm previous results (Becker et al., 2011). Interestingly, the strain *C. glutamicum* BS529 bearing the native P_{sod} promoter obtained about the same activity as BS222 with 467 U g^{-1} indicating a duplication of *ddh* expression. Only in individual cases ($P_{1\text{-}08}$ and $P_{7\text{-}19}$), the promoters induced lower enzyme activities than expected (Figure 5-10). It is known that gene expression depends on the genomic context. Thus, related secondary structures influence transcription as well as translation (Eyre-Walker and Bulmer, 1993; Kudla et al., 2009). In the view of this, the other promoter activities coincided very well with the former results (Figure 5-10). Promoters $P_{7\text{-}29}$ and $P_{5\text{-}02}$, for example, were expected to increase the enzyme activities by the 15- and 9-fold, respectively. Here, increased *ddh* activities by the 12- and 7-fold, respectively, were determined. A good agreement was also observed for $P_{9\text{-}42}$. Again, the promoter enabled the highest enzyme activity (6543 U g^{-1}). As a consequence, it exceeded the reference strain BS529 by 14-fold compared to 20-fold as determined above (Figure 5-10). The results demonstrate that the measured DDH enzyme activities, when referred to P_{sod}, have a good and reliable agreement to the determined relative promoter activities presented in section 5.3.

In a next step, cultivations were performed on minimal salt medium with glucose as sole carbon source to analyze growth and production characteristics of the novel library strains. The cultivations were conducted in the micro fermenter system BioLector® using a working volume of 1 mL. Six replicates of each strain were performed. From these, three were used to gain a cultivation profile (Table 5-12) while the others were harvested and pooled during exponential growth for RNA isolation and subsequent qRT-PCR analysis (Figure 5-13).

Surprisingly, the overexpression of *ddh* via promoter exchange had no significant effect on lysine production. Even though BS529 showed the same *ddh* expression level as BS222, only the latter strain had an increased lysine yield. Apart from some variations in the by-product formation of glycine, no significant differences in the cultivation profile were observed for the strains BS529-BS536. Former publications testified that the plasmid-based overexpression of *ddh* had no influence on the production performance of lysine (Cremer et al., 1991; Shaw-Reid et al., 1999). Shaw-Reid et al. (1999) explained this observation by calculating the desired *ddh* enzyme activity needed for lysine production assuming that the estimated enzyme activity would have the same efficiency in both directions and a protein content of 50 % of cell dry weight. They declared that already the native DDH activity would exceed the cellular demand to achieve the maximum production rate by four times in the basic lysine production strain used. Caused by episomal gene expression it would even rise to the 50-fold. Consequently, lysine production would not be limited via the *ddh* expression level.

Table 5-12: Growth and production characteristics of different P_{sod} mutants based on BS1 for gene expression studies of the diaminopimelate dehydrogenase. The data given are yields for biomass production ($Y_{X/S}$), lysine formation ($Y_{Lys/S}$) and glycine formation ($Y_{Gly/S}$) as well as growth rates (μ), specific glucose uptake rates (q_{Glc}) and specific lysine production rates (q_{Lys}). All experiments were performed in triplicate in MTP-48-FlowerPlates in 1 mL minimal salt medium with glucose as sole carbon source.

Strain	Construct	Yields		
		$Y_{X/S}$ [g mol^{-1}]	$Y_{Lys/S}$ [mmol mol^{-1}]	$Y_{Gly/S}$ [mmol mol^{-1}]
BS1	*ddh*	97.1 ± 0.1	88.4 ± 0.9	8.2 ± 0.8
BS222	2x*ddh*	82.2 ± 1.3	118.9 ± 3.1	8.9 ± 1.2
BS529	P_{sod}*ddh*	93.4 ± 3.0	83.0 ± 3.2	7.1 ± 0.6
BS530	$P_{7\text{-}19}$*ddh*	101.9 ± 1.9	78.6 ± 2.2	8.4 ± 0.5
BS531	$P_{6\text{-}43}$*ddh*	96.8 ± 4.6	83.5 ± 2.2	6.3 ± 1.4
BS532	$P_{7\text{-}29}$*ddh*	94.0 ± 3.4	82.0 ± 5.0	5.5 ± 1.2
BS533	$P_{5\text{-}19}$*ddh*	96.7 ± 3.0	80.4 ± 1.8	6.8 ± 0.2
BS534	$P_{1\text{-}08}$*ddh*	93.1 ± 3.1	87.0 ± 3.4	3.0 ± 1.2
BS535	$P_{5\text{-}02}$*ddh*	98.1 ± 1.8	78.5 ± 2.1	8.7 ± 0.8
BS536	$P_{9\text{-}42}$*ddh*	95.5 ± 2.2	83.9 ± 1.3	6.3 ± 0.6
Strain	**Construct**	**Rates**		
		μ [h^{-1}]	q_{Glc} [mmol g^{-1} h^{-1}]	q_{Lys} [mmol g^{-1} h^{-1}]
BS1	*ddh*	0.29 ± 0.00	3.02 ± 0.02	0.27 ± 0.00
BS222	2x*ddh*	0.27 ± 0.01	3.28 ± 0.03	0.39 ± 0.01
BS529	P_{sod}*ddh*	0.30 ± 0.01	3.17 ± 0.04	0.26 ± 0.01
BS530	$P_{7\text{-}19}$*ddh*	0.32 ± 0.00	3.11 ± 0.05	0.24 ± 0.01
BS531	$P_{6\text{-}43}$*ddh*	0.30 ± 0.00	3.06 ± 0.14	0.26 ± 0.01
BS532	$P_{7\text{-}29}$*ddh*	0.29 ± 0.01	3.05 ± 0.01	0.25 ± 0.02
BS533	$P_{5\text{-}19}$*ddh*	0.30 ± 0.01	3.08 ± 0.15	0.25 ± 0.01
BS534	$P_{1\text{-}08}$*ddh*	0.31 ± 0.01	3.32 ± 0.09	0.29 ± 0.00
BS535	$P_{5\text{-}02}$*ddh*	0.31 ± 0.00	3.11 ± 0.06	0.24 ± 0.01
BS536	$P_{9\text{-}42}$*ddh*	0.29 ± 0.00	3.03 ± 0.10	0.25 ± 0.00

Taking the same assumptions, the basic strain BS1 could reach a maximum lysine production rate of 6.2 mmol g^{-1} h^{-1} according to its enzyme activity of 206.5 mU mg^{-1}. This value exceeds the lysine production rate calculated for the cultivation process by 23 times. Though, this value is a theoretical production rate based on values derived from an *in vitro* experiment, the *in vivo* DDH activity might be different depending on the availability of reaction intermediates. However, the highest maximum production rates of nearly 200 mmol g^{-1} h^{-1} were observed for strains *C. glutamicum* BS532 and BS536, both exceeding the calculated lysine production rates by nearly the 700- and 800-fold, respectively. The lowest maximum rate was calculated for BS534 with 1.7 mmol g^{-1} h^{-1} which is still six times higher as required. Thus, it seems likely that the native DDH activity is already sufficient for lysine production. Minor deviations of the final production rates might be caused by variations of the growth behavior as well as measurement inaccuracies. Interestingly, BS222 revealed a remarkable increased lysine production

performance based on the overproduction of *ddh* via gene duplication even though calculation of the maximum production rate (14.3 mmol g^{-1} h^{-1}) exceeded the observed value by the 37-fold. Regarding the gene locus of *ddh*, the autoregulatory transcriptional regulator *lysR* (*cg2899*) was identified about 400 bp downstream of *ddh*. In contrast to overexpression of *ddh* by gene duplication, overexpression via promoter exchange might influence the gene expression level of *lysR* additionally. Though the family of LysR-type transcriptional regulators (LTTRs) is known to function as positive regulator in prokaryotes (Schell, 1993), this does not exclude that induction of its target gene might influence lysine production negatively. Expression of *lysR* was analyzed in parallel to *ddh* to provide evidence if the promoter exchange, resulting in an overexpression of *ddh*, does also influence gene expression of *lysR*. In this case, only the duplication of *ddh* in BS222 should have no effect on the expression of *lysR* and would be identical to those of BS1 while in the strains BS529-BS536 the expression levels would vary. Gene expression studies were performed via qRT-PCR. For this reason, RNA was isolated from exponential grown cells and analyzed with distinct primer pairs for *ddh* (Figure 5-13) and *lysR* (Figure 5-14).

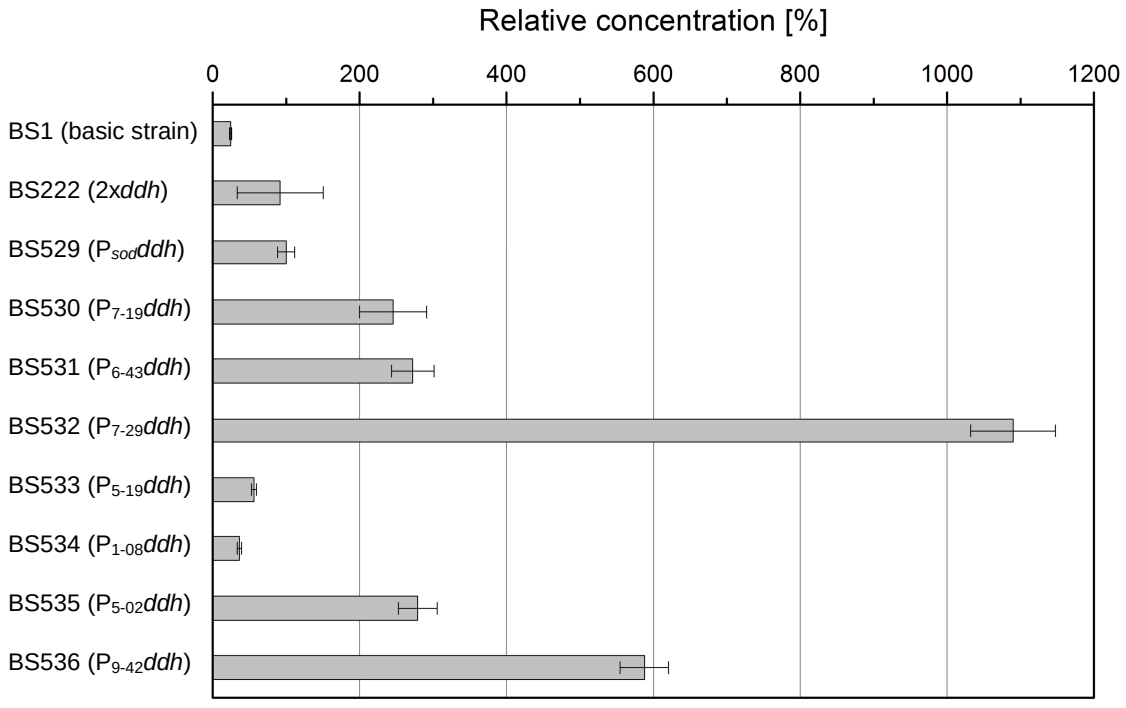

Figure 5-13: Quantification of the *ddh*-expression in different P_{sod} mutants based on BS1 by qRT-PCR. RNA samples were derived from the cultivation experiment depicted in Table 5-12. Three replicates were harvested and pooled during exponential growth. The data represent mean values with standard deviations from six technical replicates referred to the native P_{sod} promoter (BS529).

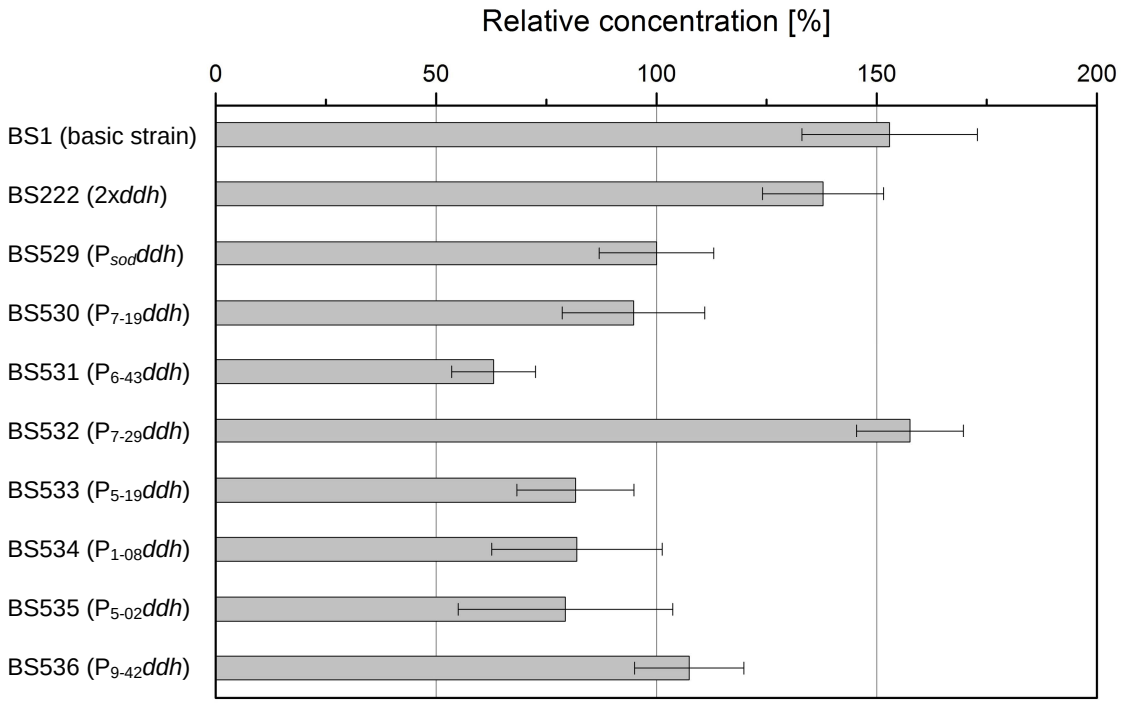

Figure 5-14: Quantification of the *lysR*-expression in different P_{sod} mutants based on BS1 by qRT-PCR. RNA samples were derived from the cultivation experiment depicted in Table 5-12. Three replicates were harvested and pooled during exponential growth. The data represent mean values with standard deviations from six technical replicates referred to the native P_{sod} promoter (BS529).

The experiment revealed that *ddh* expression was indeed significantly increased. The relative concentrations of *ddh* transcripts gained by qRT-PCR matched very well with the enzyme activity analyzed via enzymatic analysis. Again, BS222 and BS529 showed similar transcription levels while the highest was observed for BS532. Here, BS532 exceeded BS529 by the 11-fold instead of the 14-fold as observed by the enzymatic assay. The good agreement indicated a high precision of both quantification methods.

Regarding Figure 5-14, the quantification of the *lysR* expression level revealed only minor variations around a relative concentration of 100 % referred to the native P_{sod} construct for all strains. This indicates that expression of *lysR* was not influenced by the overexpression of *ddh*.

In parallel to expression analysis of *lysR*, the strains BS222 (2x*ddh*) and BS529 (P_{sod}*ddh*) were further analyzed in detail, since both strains showed the same *ddh* expression level while varying significantly in lysine production. For that reason, deletion strains of *C. glutamicum* BS222 and BS529 were constructed bearing a 430 bp deletion within the *lysR* gene. Afterwards, both deletion strains as well as the corresponding host strains were cultivated in MTP-48-FlowerPlates on minimal salt medium with glucose as sole carbon source. The lysine production was characterized via end point determination of the concentration. The basic lysine producer *C. glutamicum* BS1 served as additional reference (Table 5-13).

Table 5-13: Characterization of the productivity via end point determination of the lysine concentration of *lysR*-deletion strains based on *C. glutamicum* BS1. The data given are yields for biomass production ($Y_{X/S}$), lysine formation ($Y_{Lys/S}$) and glycine formation ($Y_{Gly/S}$) as well as growth rates (μ), specific glucose uptake rates (q_{Glc}) and specific lysine production rates (q_{Lys}). All experiments were performed in triplicate in MTP-48-FlowerPlates in 1 mL minimal salt medium with glucose as sole carbon source.

Strain	Construct	Final Yields		
		$Y_{X/S}$ [g mol^{-1}]	$Y_{Lys/S}$ [mmol mol^{-1}]	$Y_{Gly/S}$ [mmol mol^{-1}]
BS1	*ddh*	106.6 ± 0.8	117.0 ± 4.4	6.4 ± 0.1
BS222	2x*ddh*	81.8 ± 0.9	140.6 ± 7.1	8.4 ± 0.2
BS566	2x*ddhΔlysR*	104.0 ± 1.0	87.0 ± 1.3	7.4 ± 0.2
BS529	P_{sod}*ddh*	106.6 ± 0.5	105.5 ± 3.2	6.5 ± 0.3
BS567	P_{sod}*ddhΔlysR*	105.1 ± 0.6	107.9 ± 5.0	6.4 ± 0.2
Strain	**Construct**	**Rates**		
		μ [h^{-1}]	**q_{Glc} [mmol g^{-1} h^{-1}]**	**q_{Lys} [mmol g^{-1} h^{-1}]**
BS1	*ddh*	0.26 ± 0.01	2.48 ± 0.02	0.28 ± 0.01
BS222	2x*ddh*	0.28 ± 0.00	3.45 ± 0.04	0.50 ± 0.02
BS566	2x*ddhΔlysR*	0.27 ± 0.01	2.57 ± 0.03	0.22 ± 0.00
BS529	P_{sod}*ddh*	0.26 ± 0.00	2.41 ± 0.01	0.25 ± 0.01
BS567	P_{sod}*ddhΔlysR*	0.27 ± 0.00	2.61 ± 0.01	0.29 ± 0.01

Again only BS222 showed an increased lysine production yield by 20 %. Interestingly, inactivation of *lysR* in the genetic background of BS222 influences lysine production negatively while for the strains based on BS529 no effect was observed. Thus, the lysine production yield of BS566 (2x*ddh*_Δ*lysR*) dropped by 25 % compared to BS1.

Subsequent sequence analyses of BS222 and BS529 as well as their corresponding *lysR* deletion strains exposed no inadvertent modifications in the sequences of *ddh* or *lysR* that would explain the improved lysine production performance of BS222. Since a duplication of *ddh* in BS222 showed a significant influence on the production profile, the same would have been expected for a promoter-based overproduction of *ddh*. But for reasons not yet understood, this was not observed.

5.4.2 Analysis of the transketolase operon

The rationally designed strain *C. glutamicum* BS244 (Lys-12) by Becker et al. (2011) is well-known for its high lysine production yield and titer as well as for its productivity. In contrast to traditionally derived production strains, it just comprises 12 distinct modifications. The final modification was the overexpression of the *tkt*-operon through integration of the native promoter of *sod*. Consequently, this operon appeared to be a highly suitable target for gene expression studies using variations of P_{sod} promoters derived from a promoter library (section 5.3).

For the determination of an optimal expression level, the native promoter of the *tkt* gene was replaced by the modulated P_{sod} promoters $P_{5\text{-}19}$, $P_{1\text{-}08}$, $P_{6\text{-}43}$, $P_{7\text{-}29}$, $P_{9\text{-}42}$ and $P_{10\text{-}18}$ in the genetic

background of *C. glutamicum* BS242 (Lys-11) (Becker et al., 2011). *C. glutamicum* BS244, bearing the native P_{sod} promoter for overexpression of *tkt*, served as reference. Strain verification was performed by PCR, while enzymatic assays were applied to quantify gene expression and promoter activity (Figure 5-15).

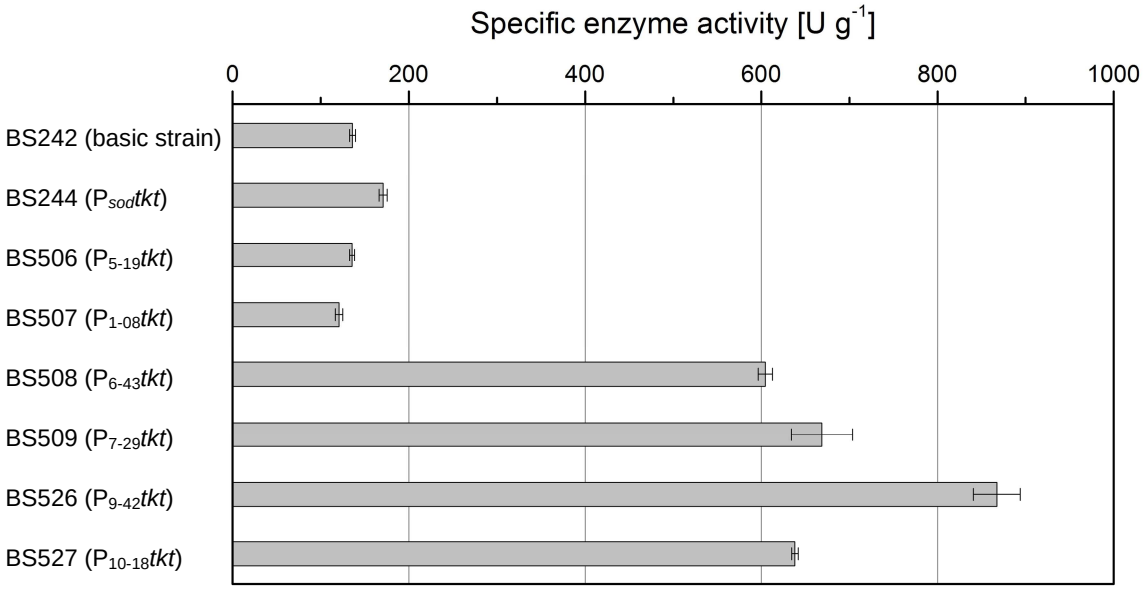

Figure 5-15: Analysis of the specific enzyme activity [U g^{-1}] of the transketolase of different P_{sod} mutants based on BS242. Cultivation was performed in deep well plates in minimal salt medium with glucose as sole carbon source at 30 °C. Enzyme activities were determined in triplicate.

Measurement of the specific enzyme activities indicated that the *tkt* expression level and, thus, the *tkt*-operon was indeed modified successfully. Regarding Figure 5-15, the activities determined for the references BS242 (136 ± 3 U g^{-1}) and BS244 (171 ± 5 U g^{-1}) fitted perfectly with those published by Becker et al. (2011) presenting 140 ± 10 U g^{-1} and 180 ± 10 U g^{-1}, respectively. Interestingly, the specific enzyme activities were either under 200 U g^{-1} or above 600 U g^{-1} even though the chosen P_{sod} promoters were expected to induce a broad range of enzyme activities (Figure 5-10). Though enzyme activities were in total lower as expected (section 5.3), there was still an obvious rise of TKT activity of up to 867 ± 27 U g^{-1} (P_{9-42}). Compared to the native P_{sod} construct, the *tkt* expression was increased by about four times using P_{6-43}, P_{7-29} and P_{10-18} and even five times with P_{9-42}.

To analyze the effect of different *tkt* expression levels on the lysine production performance, cultivations were performed in a micro fermenter system using a working volume of 1.5 mL minimal salt medium with glucose as sole carbon source. Six replicates of each strain were performed. Thereof, three were used for growth and production characteristics (Table 4-14) while the others were harvested and pooled during exponential growth for RNA isolation and subsequent qRT-PCR analysis (Figure 5-16).

Table 5-14: Growth and production characteristics of different P_{sod} mutants based on BS242 for gene expression studies of the transketolase operon. The data given are yields for biomass production ($Y_{X/S}$), lysine formation ($Y_{Lys/S}$) and glycine formation ($Y_{Gly/S}$) as well as growth rates (μ), specific glucose uptake rates (q_{Glc}) and specific lysine production rates (q_{Lys}). All experiments were performed in triplicate in MTP-48-FlowerPlates in 1.5 mL minimal salt medium with glucose as sole carbon source.

Strain	Construct	Yields		
		$Y_{X/S}$ [g mol^{-1}]	$Y_{Lys/S}$ [mmol mol^{-1}]	$Y_{Gly/S}$ [mmol mol^{-1}]
BS242	*tkt*	54.1 ± 0.9	301.6 ± 21.4	2.8 ± 0.5
BS244	P_{sod}*tkt*	50.2 ± 1.6	358.2 ± 8.4	3.5 ± 0.4
BS506	$P_{5\text{-}19}$*tkt*	57.4 ± 0.8	330.5 ± 17.3	3.4 ± 0.2
BS507	$P_{1\text{-}08}$*tkt*	56.9 ± 0.8	356.0 ± 25.5	3.6 ± 0.1
BS508	$P_{6\text{-}43}$*tkt*	51.9 ± 0.8	359.7 ± 9.2	5.2 ± 0.3
BS509	$P_{7\text{-}29}$*tkt*	56.6 ± 1.2	319.7 ± 12.2	5.7 ± 0.2
BS526	$P_{9\text{-}42}$*tkt*	56.7 ± 2.2	315.9 ± 3.7	5.4 ± 0.2
BS527	$P_{10\text{-}18}$*tkt*	59.4 ± 0.5	298.4 ± 2.6	6.2 ± 0.2
Strain	**Construct**	**Rates**		
		μ [h^{-1}]	**q_{Glc} [mmol g^{-1} h^{-1}]**	**q_{Lys} [mmol g^{-1} h^{-1}]**
BS242	*tkt*	0.15 ± 0.00	3.28 ± 0.21	0.99 ± 0.06
BS244	P_{sod}*tkt*	0.16 ± 0.01	3.55 ± 0.20	1.27 ± 0.10
BS506	$P_{5\text{-}19}$*tkt*	0.15 ± 0.01	3.08 ± 0.15	1.02 ± 0.02
BS507	$P_{1\text{-}08}$*tkt*	0.16 ± 0.00	3.30 ± 0.11	1.17 ± 0.05
BS508	$P_{6\text{-}43}$*tkt*	0.14 ± 0.00	3.16 ± 0.01	1.14 ± 0.03
BS509	$P_{7\text{-}29}$*tkt*	0.17 ± 0.00	3.54 ± 0.10	1.13 ± 0.02
BS526	$P_{9\text{-}42}$*tkt*	0.16 ± 0.01	3.16 ± 0.25	1.00 ± 0.09
BS527	$P_{10\text{-}18}$*tkt*	0.15 ± 0.00	2.98 ± 0.10	0.89 ± 0.04

The cultivation experiments revealed significantly improved lysine production yields for BS244, BS507 and BS508, as compared to BS242. Again the results correlated with those of Becker et al. (2011) neglecting differences in the growth rate and the lysine concentration that might be caused due to the different cultivation systems. The reported that an overexpression of *tkt* enhanced lysine production by about 18 % in BS244 using the native P_{sod} promoter. In this study, the lysine production yield of BS244 was increased by 19 % referred to BS242. Nearly the same was observed for BS507 and BS508. Since in some cases variations of the inoculum's vitality and cell concentration might cause aberrations from the actual cultivation profile, a replication of the cultivation experiment with subsequent determination of the final lysine concentrations was performed. The determined values are depicted in the appendix (Table 7-2) and revealed that only BS244 and BS507 showed a reliable improved lysine production performance.

Subsequently, RNA of exponentially grown cells was isolated and qRT-PCR with a distinct primer pair was performed to analyze the transcription level of *tkt* (Figure 5-16).

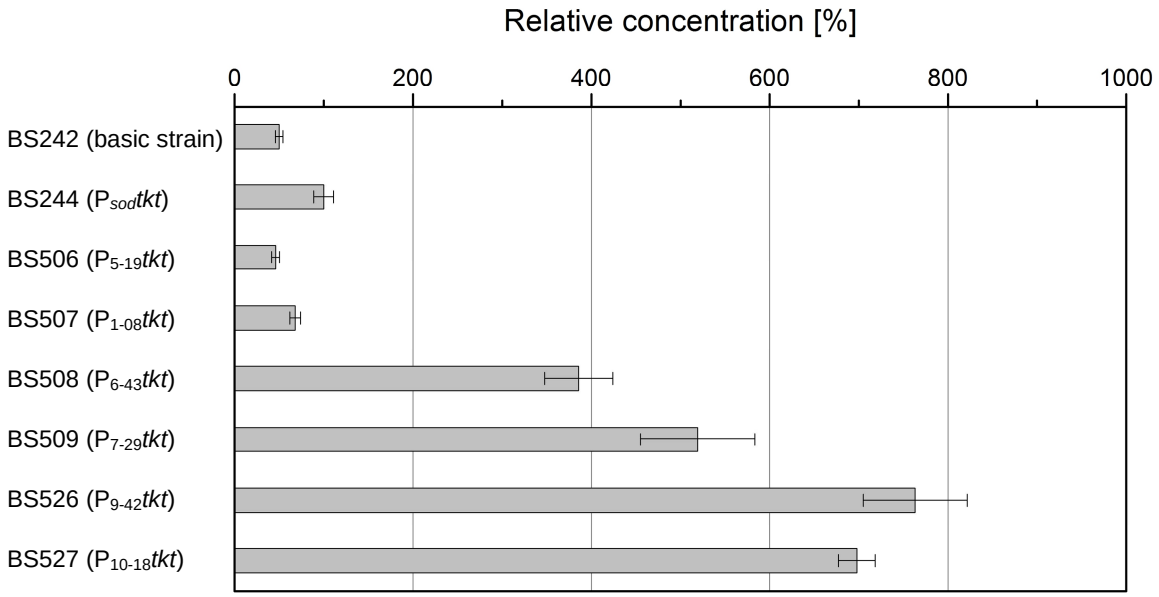

Figure 5-16: Quantification of the *tkt*-expression in different P_{sod} mutants based on BS242 by qRT-PCR. RNA samples were derived from the cultivation experiment depicted in Table 5-14. Three replicates were harvested and pooled during exponential growth. The data represent mean values with standard deviations from six technical replicates referred to the native P_{sod} promoter (BS244).

Quantification of the relative *tkt* expression level by qRT-PCR verified the results gained via the enzymatic assay. Again, the strongest *tkt* activity was observed for P_{9-42} followed by P_{6-43}, P_{7-29} and P_{10-18}. Comparing the cultivation profile with Figure 5-15 and Figure 5-16, the data revealed that significantly increased TKT activities caused increased biomass and glycine production yields as well as growth rates, but did not further improve lysine production. In contrast to that, the highest lysine production yields were found for TKT activities that varied around the activity of the native P_{sod} construct. This indicates that for further optimization attempts, a more restricted selection of promoter activities needs to be chosen that does not exceed P_{6-43} but rather varies around the activity of the native *sod* promoter and P_{1-08}.

Nevertheless, it is interesting to note that the final lysine production yield of BS244 and BS507 was enhanced by about 20 % compared to BS242 even though very similar TKT activities and expression levels were observed (125-200 % in BS244 and 89-137 % in BS507). This observation underlines the importance of promoter libraries for transcriptional “fine-tuning” to modulate metabolic fluxes and, thus, to improve lysine production. Other authors also emphasized that it is important to regulate gene expression accurately (Ravasi et al., 2012; Rytter et al., 2014). Jensen et al. (1993) for example were able to regulate gene expression in a small range and in both directions by a promoter exchange against inducible promoters using IPTG. They suggested that gene expression should be controlled around its native level. As depicted in Figure 5-10, the promoter library constructed in this study also provides a broad range of different expression intensities as well as the opportunity to modulate gene expression in small doses. A further plus of this study is that the generated production hosts are genetically stable and the production processes are independently from further additives (e.g. inducer).

5.4.3 Variation of the lysine export rate by LysE

It was reported that lysine export was realized via the translocator LysE which is particularly important in the case of high intracellular lysine concentrations to ensure the cellular functionality. It was also found that overexpression of *lysE* in *C. glutamicum* ATCC13032 increased the lysine excretion rate significantly (Vrljic et al., 1996). By elementary mode analyses, it was further predicted that overexpression of *lysE* would enhance lysine production (Melzer et al., 2009). Consequently, expression of *lysE* and its influence on lysine production should be analyzed in more detail. For this reason, the strain BS244 (Lys-12) (Becker et al., 2011) was regarded as a suitable host for gene expression studies of *lysE* using the P_{sod} promoter library described in section 5.3.

Strain construction was performed by fusion PCR, electroporation and homologue recombination. A total of three strains were designed with stable genomic modifications bearing the promoters $P_{7\text{-}29}$, $P_{7\text{-}19}$ and $P_{9\text{-}42}$. Besides the host strain BS244, the strain BS290 served as reference controlling *lysE* expression by the native P_{sod} promoter. As for LysR, analysis of the protein's functionality via enzymatic assay was inapplicable for LysE. Consequently, verification of gene modulation and its impact on transcription were verified via PCR and qRT-PCR, respectively. Therefore, all strains were cultivated in a micro fermentation system and analyzed for their growth and production characteristics in minimal salt medium using glucose as sole carbon source (Table 5-15). RNA was isolated from cells harvested during exponential growth and expression studies of *lysE* were performed via qRT-PCR (Figure 5-17).

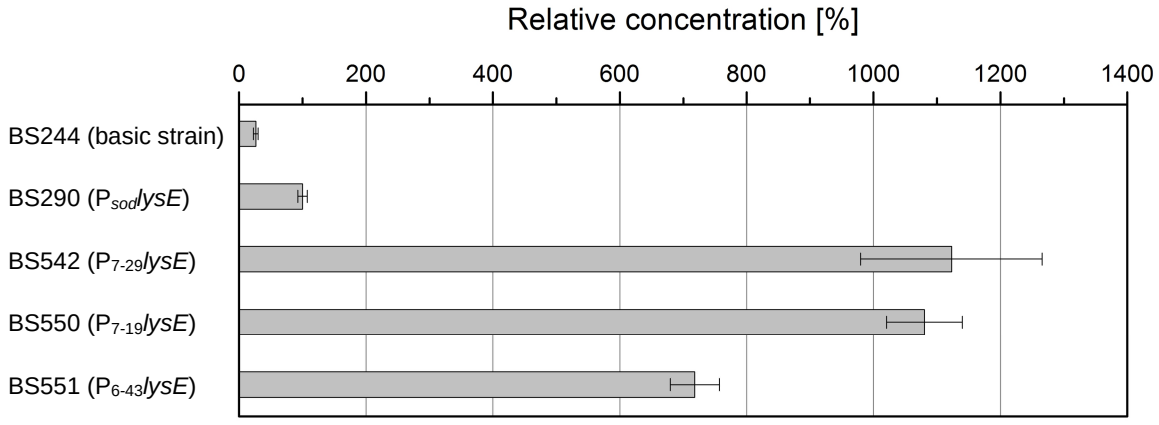

Figure 5-17: Quantification of the *lysE*-expression in different P_{sod} mutants based on BS244 by qRT-PCR. RNA samples were derived from the cultivation experiment depicted in Table 5-15. Three replicates were harvested and pooled during exponential growth. The data represent mean values with standard deviations from six technical replicates referred to the native P_{sod} promoter (BS290).

According to the results gained by qRT-PCR, *lysE* expression was successfully altered. It was found that already the native P_{sod} promoter increased the native *lysE* expression level by four times while the promoters $P_{7\text{-}29}$, $P_{7\text{-}19}$ and $P_{9\text{-}42}$ exceeded those level considerably. Compared to the native P_{sod} promoter, the strongest expression was quantified for $P_{7\text{-}29}$ correlating to an overexpression by up to the 11-fold. Interestingly, nearly the same expression level was observed for $P_{7\text{-}19}$ while it provoked a rather low gene expression of *ddh* (section 5.4.1). Again, this demonstrates that the genomic context is significantly involved in gene regulation (Eyre-Walker and Bulmer, 1993; Kudla et al., 2009).

The functionality of the export protein was analyzed by its impact on the cultivation profile. It is obvious that an excessive overexpression of a target gene would influence lysine production and bacterial growth negatively. In this case, a shift of metabolic fluxes might result in an imbalance of metabolites or cause new bottle necks. In addition, production of the target protein is not only metabolically cost-intensive, but high amounts of the same protein might also disturb the cellular functionality as observed before (section 5.2.4). Besides, it is evident that especially overexpression of an exporter like *lysE* needs to be regulated with caution to avoid destruction of the cell wall. This was also confirmed by the results of Bellmann et al. (2001), who found that by nature *lysE* expression is strongly controlled through the positive regulator LysG and an additional inducer (lysine or arginine). They further described that the system seemed to be able to react highly flexible indicated by an overexpression of *lysE* by up to the 20-fold using LysG.

Table 5-15: Growth and production characteristics of different P_{sod} mutants based on BS244 for gene expression studies of the lysine exporter. The data given are yields for biomass production ($Y_{X/S}$) and lysine formation ($Y_{Lys/S}$) as well as growth rates (μ), specific glucose uptake rates (q_{Glc}) and specific lysine production rates (q_{Lys}). All experiments were performed in triplicate in MTP-48-FlowerPlates in 1 mL minimal salt medium with glucose as sole carbon source. The data of BS244 were derived from Table 5-14.

Strain	Construct	Yields	
		$Y_{X/S}$ [g mol^{-1}]	$Y_{Lys/S}$ [mmol mol^{-1}]
BS244	*lysE*	50.2 ± 1.6	358.2 ± 8.4
BS290	P_{sod}*lysE*	59.4 ± 2.7	318.3 ± 5.5
BS542	$P_{7\text{-}29}$*lysE*	43.7 ± 3.0	391.9 ± 5.9
BS550	$P_{7\text{-}19}$*lysE*	36.4 ± 1.2	369.0 ± 13.8
BS551	$P_{6\text{-}43}$*lysE*	54.4 ± 0.8	330.9 ± 2.5

Strain	Construct	Rates		
		μ [h^{-1}]	q_{Glc} [mmol g^{-1} h^{-1}]	q_{Lys} [mmol g^{-1} h^{-1}]
BS244	*lysE*	0.16 ± 0.01	3.55 ± 0.20	1.27 ± 0.10
BS290	P_{sod}*lysE*	0.23 ± 0.01	3.81 ± 0.38	1.21 ± 0.12
BS542	$P_{7\text{-}29}$*lysE*	0.08 ± 0.01	1.78 ± 0.29	0.70 ± 0.11
BS550	$P_{7\text{-}19}$*lysE*	0.11 ± 0.01	3.10 ± 0.24	1.11 ± 0.04
BS551	$P_{6\text{-}43}$*lysE*	0.15 ± 0.01	2.77 ± 0.18	0.92 ± 0.06

Regarding the results gained by cultivation (Table 5-15), it can be seen that the highest lysine production yields were determined for *C. glutamicum* BS542 and BS550. Thus, lysine production was improved by 9 % and 3 %, respectively, as compared to the reference strain BS244. This can probably be ascribed to their increased *lysE* expression levels. Quantification via qRT-PCR indicated that both strains revealed similar high expression rates. As observed before, improved lysine production yields partly correlate with slightly retarded glucose uptake rates. According to the cultivation profile, this also holds for BS542 and BS550 as compared to BS244. In contrast to that, increased biomass production yields were determined for BS290 and BS551 while their lysine production performances were reduced. Especially the 4-fold overexpression of *lysE* induced by P_{sod} in BS290 had a positive impact on the cell viability as indicated by the increased values for growth, biomass formation and glucose uptake. Nevertheless, the best results were achieved using BS244. The host strain revealed not only a good production performance, but also good values related to bacterial growth resulting in the highest specific lysine production rate.

As mentioned before, overexpression of *lysE* needs to be regulated carefully to maintain the cellular functionality. This can not only be characterized by the cultivation profile, but also by analysis of the by-product formation (Table 5-16).

Table 5-16: Characteristic of by-product formation of different P_{sod} mutants based on BS244 for gene expression studies of the lysine exporter. The data given are yields for glycine ($Y_{Gly/S}$), glutamate ($Y_{Glu/S}$), arginine ($Y_{Arg/S}$) and alanine ($Y_{Ala/S}$) formation. All experiments were performed in triplicate in MTP-48-FlowerPlates in 1 mL minimal salt medium with glucose as sole carbon source. The data of BS244 were derived from Table 5-14.

Strain	Construct	Yields			
		$Y_{Gly/S}$ [mmol mol^{-1}]	$Y_{Glu/S}$ [mmol mol^{-1}]	$Y_{Arg/S}$ [mmol mol^{-1}]	$Y_{Ala/S}$ [mmol mol^{-1}]
BS244	*lysE*	4.5 ± 0.6	0.0 ± 0.0	0.0 ± 0.0	0.0 ± 0.0
BS290	P_{sod}*lysE*	6.2 ± 0.6	0.0 ± 0.0	0.0 ± 0.0	0.0 ± 0.0
BS542	$P_{7\text{-}29}$*lysE*	3.6 ± 0.3	0.0 ± 0.0	48.9 ± 2.2	20.9 ± 0.8
BS550	$P_{7\text{-}19}$*lysE*	1.5 ± 0.0	0.0 ± 0.0	41.6 ± 1.9	0.5 ± 0.5
BS551	$P_{6\text{-}43}$*lysE*	3.9 ± 0.4	5.1 ± 0.2	29.1 ± 1.0	8.0 ± 1.0

Regarding Table 5-16, the production yields of glycine varied only slightly in all strains. Interestingly, the yields for arginine and alanine production were increased for BS542, BS550 and BS551 correlating with slightly decreased glycine production yields. BS551 even secreted small amounts of glutamate, a pre-curser in arginine production. According to qRT-PCR analysis, those strains revealed the highest *lysE* expression levels analyzed indicating high enzyme activities. It was found that LysE not only transports lysine, but also arginine (Bellmann et al., 2001). Consequently, the presence of extracellular arginine can probably be ascribed to the increased export activity of LysE resulting in a correlation of boosted lysine as well as arginine export.

Taken together, it was shown that the transcription level of *lysE* was successfully modulated. All strains constructed indicated a functional *lysE* expression as was revealed by the differences in their cultivation profiles. Furthermore, two strains (BS542 and BS550) were identified with improved lysine production yields by about 9 % and 3 %, respectively. Quantification via qRT-PCR confirmed that both strains had very similar *lysE* transcription levels. Though this seemed to be just a marginal improvement, even small changes of the final titer have a big impact on the profitability of a production process regarding the high production capacity of industrial fermentation processes. Considering the loss of carbon that coincided with the by-product formation of arginine (C_6-molecule) and alanine (C_3-molecule) a redirection of the fluxes towards lysine production might have the potential to further improve the lysine production profile by up to 17 %.

6 Conclusion and Outlook

In the present work, novel tools were generated to improve lysine production in *C. glutamicum*, on the level of bioprocess and genetic engineering.

In the first part of this work, a method was developed that allows robust prediction of the dissolved oxygen concentration during aerobic growth. This method based on a mathematical correlation and predicted the volumetric gas-liquid mass transfer coefficient (k_La) in disposable shake-flasks from filling volume, vessel size and agitation speed. Exemplified for cultivation of *C. glutamicum*, it was demonstrated that the application enables a reliable design of culture conditions and allows the prediction of the maximum possible cell concentration achievable without oxygen limitation. The new approach is of particular value for cultivations with costly carbon sources and nutrient additives to minimize costs. It can further be used to avoid anaerobic growth which is related to by-product formation like acetate.

The second part of this work focused on rational genetic engineering of *C. glutamicum*. To begin with, the influence of two isozymes of glyceraldehyde-3-phosphate dehydrogenase (GapA and GapN) on lysine production was analyzed. In the background of the lysine hyper producer of *C. glutamicum*, it was found that episomal-based overexpression of *gapA* resulted in a considerably increased lysine yield by 58 %. The different cofactor specificity of GapA and GapN further revealed that both the basic and the lysine hyper producer of *C. glutamicum* were limited by the availability of NADPH. As a consequence, strategies were developed to overcome this limitation. One strategy was the modulation of the nucleotide binding fold of NADP(H)-dependent enzymes, in order to change their cofactor specificity to NAD(H) on DNA level. Based on bioinformatics analysis, site-directed modifications were successfully introduced within the nucleotide binding sites of diaminopimelate dehydrogenase (DDH) and dihydrodipicolinate reductase (DapB). Cultivation experiments revealed an improved final lysine yield of 9 % by episomal expression of DapB. In the case of DDH, enzymatic assays showed that the cofactor specificity was modified by only one amino acid exchange resulting in an almost complete deregulation of DDH for the cofactor NADP(H), while its native NAD(H)-dependency was conserved. However, lysine production was not increased which might be due to the reduced overall enzyme activity of 2-3 %. This, however, is a general challenge in protein design often described (Chen et al., 1995; Katzberg et al., 2010). The results illustrated that engineering of cofactor specificity is an effective instrument to modify the cofactor dependency and availability in a metabolic network. The implementation of further modifications within the nucleotide binding fold might enhance the cofactor specificity as well as the enzyme activity, in future.

Besides, a promoter library based on the strong promoter of *sod*, encoding superoxide dis-

mutase, was constructed by random mutagenesis using *gfp* as a reporter gene. The generated library showed an extraordinary broad range of different relative promoter activities. For metabolic engineering of *C. glutamicum*, selected promoters were used to modulate the gene expression of DDH, the transketolase operon and the lysine exporter LysE as was successfully demonstrated by enzymatic assays and qRT-PCRs. Modulation of *ddh* expression by promoter exchange, however, had no effect on lysine production, even though for reasons not yet understood, a duplication of *ddh* in the same host strain resulted in an increased lysine production yield. Calculation of the theoretical maximum lysine production rate indicated that lysine production might not be limited by *ddh* expression, since its native activity exceeded the cellular demand at least *in vitro*. In contrast to that, overexpression of the *tkt*-operon and *lysE* improved the lysine yield significantly by 19 % and 9 %, respectively. Only in a few cases, much higher lysine yields were partly linked to slightly decreased glucose uptake rates which might be overcome by further rounds of engineering. In summary, it was successfully demonstrated that the promoter library has a high potential to improve lysine production by modulation of distinct gene expression levels. The success of this engineering strategy was proven at different gene loci. Particularly, the *tkt*-operon and *lysE* seem to be attractive targets for transcriptional "fine-tuning" in future. By doing so, one should focus on a more restricted selection of promoter activities to achieve accurate gene regulation. Besides, *gapA* might be an interesting target for metabolic engineering of cofactor specificity as well as of gene expression levels. There is also evidence that lysine production might be further enhanced by a simultaneous overexpression of *gapA* and NAD kinase (Lindner et al., 2010; Wang et al., 2013).

Henceforth, validated targets (Becker et al., 2011; Wittmann and Becker, 2007; Xu et al., 2014b) can be re-investigated for fine-tuned expression to identify optimal gene expression levels using the promoter library. In addition, the identification of new bottle necks is indispensable to ensure a progressive strain optimization. Implementation of a plasmid library including all genes that are involved in substrate consumption and lysine production might be a chance to overcome this issue. Introduction of target genes into an episomal replicating vector system, e.g. pClik_5a_MCS, would not only offer easy vector and strain construction, but also high flexibility and adaptability to current host strains. By integration of the P_{sod} promoter library, a more specific genome-based fine-tuning might be achieved.

Beyond, strategies presented in this work can be integrated with other production processes using *C. glutamicum* that are limited by an insufficient cofactor supply like the biosynthesis of L-methionine (Park et al., 2007) and the production of lysine from lactic acid derived from grass silage juice (Neuner et al., 2013). In future, sustainable production processes will gain increasingly in importance to avoid a competition with food industry and human nutrition (Buschke et al., 2013) as well as for economic aspects (Banat et al., 1998). The approaches presented here might contribute this development.

7 Appendix

7.1 Primers

All primers used for strain construction and verification were purchased from Life Technologies (Glasgow, Paisley, United Kingdom) and are listed in Table 7-1.

Table 7-1: Sequence and annealing temperature T_a of the site-specific primers used in the present work for plasmid construction and strain validation

Primer	DNA Sequence (5' → 3')	T_a [°C]	Construction
212 _BamHI_rv	GATCGGATCCAATTTAACTTGTTCGGCC	57	*dapB* end primer with restriction site BamHI
213_XhoI_ fw	GATCCTCGAGAACTACCTGCGGAACGGG	63	*dapB* end primer with restriction site XhoI
214_*dapB*_1_rv	CAAAGGATCGCCGGCGTCGAGCTCTGCAAC	65	AELDAGDP
236_*dapB*_1_fw	GCAGAGCTCGACGCCGGCGATCCTTTGAGCCTT	68	AELDAGDP
216_*dapB*_2_rv	CAAATCATCGCCGGCGTCGAGCTCTGCAAC	64	AELDAGDD
217_*dapB*_2_fw	GTTGCAGAGCTCGACGCCGGCGATGATTTG	64	AELDAGDD
218_*dapB*_3_rv	CAAATCATCGTCGGCGTCGATCTCTGCAAC	61	AEIDADDD
219_*dapB*_3_fw	GTTGCAGAGATCGACGCCGACGATGATTTG	61	AEIDADDD
220_*dapB*_4_rv	CAAATCATCGCCGGCTTCGAGCTCTGCAAC	63	AELEAGDD
221_*dapB*_4_fw	GTTGCAGAGCTCGAAGCCGGCGATGATTTG	63	AELEAGDD
222_*dapB*_5_rv	CAAATCATCGCCGGCTTCGAGCGCTGCAAC	64	AALEAGDD
223_*dapB*_5_fw	GTTGCAGCGCTCGAAGCCGGCGATGATTTG	64	AALEAGDD
224 _SmaI_rv	GATCCCCGGGGGTCCAGCGAAGACACCC	67	*ddh* end primer with restriction site SmaI
385_MluI_ fw	GCATACGCGTCATCCCAGGTATCGATC	60	*ddh* end primer with restriction site MluI
378_fusion_fw	TGGAGGATTACAAGAACTGGCCGTTACCCTGCGA	64	Fusion primer P_{eftu}*ddh*
379_fusion_rv	TCGCAGGGTAACGGCCAGTTCTTGTAATCCTCCA	64	Fusion primer P_{eftu}*ddh*
380_fusion_fw	TCCAGGAGGACATACAATGACCAACATCCGCG	63	Fusion primer P_{eftu}*ddh*
381_fusion_rv	CGCGGATGTTGGTCATTGTATGTCCTCCTGGA	63	Fusion primer P_{eftu}*ddh*
226_*ddh*_1_rv	GGTGGCCCGGCGCTCGAAGATTCC	63	IFERR
227_*ddh*_1_fw	GGAATCTTCGAGCGCCGGGCCACC	63	IFERR
228_*ddh*_2_rv	GGTGGCCCGGCGCTGGAAGATTCC	63	IFQRR
229_ *ddh*_2_fw	GGAATCTTCCAGCGCCGGGCCACC	63	IFQRR
230_ *ddh*_3_rv	GGTGGCCAAGCGCGAGAAGATTCC	61	IFSRL
231_ *ddh*_3_fw	GGAATCTTCTCGCGCTTGGCCACC	61	IFSRL
232_ *ddh*_4_rv	GGTGGCCTCGCGCGAGAAGATTCC	61	IFSRE
233_ *ddh*_4_fw	GGAATCTTCTCGCGCGAGGCCACC	61	IFSRE
234_ *ddh*_5_rv	GGTGGCATCGTCCGAGAAGATTCC	58	IFSDD
235_ *ddh*_5_fw	GGAATCTTCTCGGACGATGCCACC	58	IFSDD
270_*ddh*_6_rv	GGTGGCCAAGCGCTCGAAGATTCC	60	IFERL
271_*ddh*_6_fw	GGAATCTTCGAGCGCTTGGCCACC	60	IFERL

Primer	DNA Sequence (5' → 3')	T_a [°C]	Construction
272_*ddh*_7_rv	GGTGGCCTCGCGCTCGAAGATTCC	61	IFERE
273_*ddh*_7_fw	GGAATCTTCGAGCGCGAGGCCACC	61	IFERE
274_*ddh*_8_rv	GGTGGCATCGTCCTCGAAGATTCC	58	IFEDD
275_*ddh*_8_fw	GGAATCTTCGAGGACGATGCCACC	58	IFEDD
291_ *ddh*_9_rv	GGTGGCCTGGACATCGATGATTCC	58	IIDVQ
292_ *ddh*_9_fw	GGAATCATCGATGTCCAGGCCACC	58	IIDVQ
254_*GFPmut1*_rv	GATCTCTAGATTATTTGTAGAGCTC	60	*GFPmut1* end primer with restriction site ApaI
257_ApaI_fw	CGTCGGGCCCTAGCTGCCAATTATTCCGG	64	P_{sod} end primer with restriction site ApaI
258_fusion_fw	CGAAAGGATTTTTTACCCATGGTCCAAACTAGTTC	59	Fusion primer P_{sod}*GFPmut1*
259_fusion_rv	GAACTAGTTTGGACCATGGGTAAAAAATCCTTTCG	59	Fusion primer P_{sod}*GFPmut1*
418_BamHI_fw	TTCAGGATCCGCCACGGGATTAGCTTCAC	61	P_{sod} end primer with restriction site BamHI
423_XbaI_rv	CGTCTCTAGACGCATTCGGGTTCAACCAG	61	*lysE* end primer with restriction site XbaI
419_fusion_rv	TTGGCAGCTACGTGACCTATGGAAGTACT	59	Fusion primer P_{sod}*lysE*
420_fusion_fw	ATAGGTCACGTAGCTGCCAATTATTCCGG	59	Fusion primer P_{sod}*lysE*
421_fusion_rv	TGATCACCATGGGTAAAAAATCCTTTCG	54	Fusion primer P_{sod}*lysE*
422_fusion_fw	GATTTTTTACCCATGGTGATCATGGAAATCTTCATT ACAGG	61	Fusion primer P_{sod}*lysE*
428_XhoI_fw	AAGGCTCGAGATGTGTCTTGAAGGTTTTCA	57	P_{sod} end primer with restriction site XhoI
433_XbaI_rv	AGGTTCTAGAGGACTGCCTTTTGAACGCCA	60	*ddh* end primer with restriction site XbaI
429_fusion_rv	TTGGCAGCTAGTTCTTGTAATCCTCCAAA	56	Fusion primer P_{sod}*ddh*
430_fusion_fw	TTACAAGAACTAGCTGCCAATTATTCCGG	56	Fusion primer P_{sod}*ddh*
431_fusion_rv	TGTTGGTCATGGGTAAAAAATCCTTTCG	54	Fusion primer P_{sod}*ddh*
432_fusion_fw	TTTTTTACCCATGACCAACATCCGCGTAG	57	Fusion primer P_{sod}*ddh*
442_BamHI_fw	AAGGCTCGAGATGTGTCTTGAAGGTTTTCA	59	P_{sod} end primer with restriction site BamHI
447_XbaI_rv	AGGTTCTAGAGGACTGCCTTTTGAACGCCA	59	*tkt* end primer with restriction site XbaI
443_fusion_rv	TTGGCAGCTAGTTCTTGTAATCCTCCAAA	61	Fusion primer P_{sod}*tkt*
444_fusion_fw	TTACAAGAACTAGCTGCCAATTATTCCGG	55	Fusion primer P_{sod}*tkt*
445_fusion_rv	TGTTGGTCATGGGTAAAAAATCCTTTCG	55	Fusion primer P_{sod}*tkt*
446_fusion_fw	TTTTTTACCCATGACCAACATCCGCGTAG	59	Fusion primer P_{sod}*tkt*
489_Δ*lysR*_fw	CGTGCTCGAGATCTGGATTTCCGCCAGGTT	63	Deletion of *lysR*
490_Δ*lysR*_rv	GTGGAATTCCGCGGCAGTTAACTCCACCGA	63	Deletion of *lysR*

Primer	DNA Sequence (5' → 3')	T_a [°C]	Construction
491_Δ*lysR*_fw	TAACTGCCGCGGAATTCCACCTTTCAGTTG	60	Deletion of *lysR*
492_Δ*lysR*_rv	TCAATCTAGAGCCAGGCTGAAACAGTCGGG	61	Deletion of *lysR*
239_*gapN*_fw	GATCCTCGAGCTATTATTTGCTGTTTGACA	56	*gapN* end primer with restriction site XhoI
240_*gapN*_rv	GATCGGATCCCAATCAACCACTGTGTTAAA	57	*gapN* end primer with restriction site BamHI
476_*gapA*_fw	AGATGGATCCGCCGAAGATCTGAAGATTCC	60	*gapA* end primer with restriction site BamHI
477_*gapA*_rv	ATTGTCTAGAATTGTGTGGCGCTGGCACCG	61	*gapA* end primer with restriction site XbaI

7.2 Analyses of *tkt* Mutants

The strains were analyzed by end point determination of the lysine concentration.

Table 7-2: Growth and production characteristics of different P_{sod} mutants based on BS242 for gene expression studies of the transketolase operon. The data given are yields for lysine formation ($Y_{Lys/S}$) gained by end point determination of the final lysine and substrate concentration. Cultivation was performed in triplicate in deep well plates using 1.5 mL minimal salt medium with glucose as sole carbon source at 30 °C.

Strain	Construct	Final Lysine Concentration [mM]			Final Yields
		1.	2.	3.	$Y_{Lys/S}$ [mmol mol^{-1}]
BS242	*tkt*	18.8	18.6	17.9	331.9 ± 9.2
BS244	P_{sod}*tkt*	20.7	21.3	21.4	380.8 ± 6.7
BS506	$P_{5\text{-}19}$*tkt*	20.0	18.5	18.5	342.4 ± 16.0
BS507	$P_{1\text{-}08}$*tkt*	22.4	21.9	21.8	397.2 ± 6.3
BS508	$P_{6\text{-}43}$*tkt*	20.4	20.3	20.2	365.4 ± 2.0
BS509	$P_{7\text{-}29}$*tkt*	21.3	21.2	20.6	379.2 ± 6.7
BS526	$P_{9\text{-}42}$*tkt*	19.9	18.9	19.2	348.1 ± 9.3
BS527	$P_{10\text{-}18}$*tkt*	20.5	19.6	19.7	358.9 ± 9.3

8 Abbreviations and Symbols

8.1 Abbreviations

aa	amino acid
ABU	*α*-amino butyric acid
acnA	gene, encoding aconitrate hydratase
asd	gene, encoding aspartate-semialdehyde dehydrogenase
aspC	gene, encoding aspartate aminotransferase
ATCC	American Type Culture Collection
ATG	adenine-thymidine-guanine, start codon
ATP	adenosine triphosphate
ADP	adenosine diphosphate
BHI	brain heart infusion
BHIS	brain heart infusion with sorbitol
bp	base pair(s)
BLAST	Basic Local Alignment Search Tool
BSA	bovine serum albumin
cDNA	complementary DNA
CM	complex medium
CO_2	carbon dioxide
CP	crossing point
dapA	gene, encoding dihydrodipicolinate synthetase
dapB	gene, encoding dihydrodipicolinate reductase
DapB	dihydrodipicolinate reductase
dapC	gene, encoding succinyldiaminopimelate aminotransferase
dapD	gene, encoding tetrahydrodipicolinate succinylase
dapE	gene, encoding succinyl-L-diaminopimelate desuccinylase
dapF	gene, encoding diaminopimelate epimerase
DHB	dihydroxybenzoic acid
ddh	gene, encoding diaminopimelate dehydrogenase
DDH	diaminopimelate dehydrogenase
DMSO	dimethyl sulfoxide
DNA	deoxyribonucleic acid
FADH	flavin adenine dinucleotide, reduced
fbaA	gene, encoding fructose bisphosphate aldolase
fbp	gene, encoding fructose 1,6-bisphosphatase

fumC	gene, encoding fumarase
gapA	gene, encoding NAD-dependent glyceraldehyde-3-phosphate dehydrogenase
GapA	NAD-dependent glyceraldehyde-3-phosphate dehydrogenase
gapDH	gene, encoding glyceraldehyde-3-phosphate dehydrogenase
GapDH	glyceraldehyde-3-phosphate dehydrogenase
gapN	gene, encoding NADP-dependent glyceraldehyde-3-phosphate dehydrogenase
GapN	NADP-dependent glyceraldehyde-3-phosphate dehydrogenase
GDH	glycerophosphate dehydrogenase
gltA	gene, encoding citrate synthase
gnd	gene, encoding 6-phosphogluconate dehydrogenase
gpmA	gene, encoding phosphoglycerate mutase
GRAS	generally recognized as safe
Gre2p	genes de respuesta a estres (protein, encoded by a stress-response gene)
GTG	guanine-thymine-guanine, start codon
GTP	guanosine triphosphate
GTP	guanosine diphosphate
hom	gene, encoding homoserine dehydrogenase
Hom	homoserine dehydrogenase
HPLC	high-performance liquid chromatography
icd	gene, encoding isocitrate dehydrogenase
ICD	isocitrate dehydrogenase
int	integrative
Kan	kanamycine
KEGG	Kyoto Encyclopedia of Genes and Genomes
kgd	gene, encoding *α*-ketoglutarate dehydrogenase
LB	lysogeny broth
kb	kilo base pairs
LTTR	LysR-type transcriptional regulators
lysA	gene, encoding diaminopimelate decarboxylase
lysC	gene, encoding aspartokinase
LysC	aspartokinase
lysE	gene, encoding lysine exporter
LysE	lysine exporter
lysR	gene, encoding autoregulatory transcriptional regulator
LysR	autoregulatory transcriptional regulator
malE	gene, encoding malic enzyme
MCS	multiple cloning site

mdh	gene, encoding malate dehydrogenase
ME	malic enzyme
min	minute
NAD(P)	nicotinamide adenine dinucleotide (phosphate), oxidized
NAD(P)H	nicotinamide adenine dinucleotide (phosphate), reduced
O_2	oxygen
odc	gene, encoding oxaloacetate decarboxylase
OD	optical density
OPA	*ortho*-phthaldialdehyde
opcA	gene, encoding a putative subunit of glucose 6-phosphate dehydrogenase
ORI	origin of replication
ORF	open reading frame
P	promoter
PCR	polymerase chain reaction
pdh	gene, encoding pyruvate dehydrogenase
PEP	phosphoenolpyruvate
pepc	gene, encoding phosphoenolpyruvate carboxylase
pepck	gene, encoding PEP-carboxykinase
PEPCK	PEP-carboxykinase
pfk	gene, encoding phosphofructokinase
pgi	gene, encoding glucose-6-phosphate isomerase
pgl	gene, encoding 6-phosphogluconolactonase
pgk	gene, encoding phosphoglycerate kinase
PPP	pentose phosphate pathway
PTS	phosphotransferase system
PWO	DNA polymerase from *Pyroccocus woesei*
pyc	gene, encoding pyruvate carboxylase
pyk	gene, encoding pyruvate kinase
qRT-PCR	quantitative-real-time PCR
R5P	ribose 5-phosphate
RNA	ribonucleic acid
rpe	gene, encoding ribulose-phosphate 3-epimerase
RPE	ribulose-phosphate 3-epimerase
rpi	gene, encoding ribose-5-phosphate isomerase
RPI	ribose-5-phosphate isomerase
rpm	rounds per minute
sacB	gene, encoding levansucrase in *Bacillus subtilis*

sdh	gene, encoding succinate dehydrogenase
SDM	second derivative maximum
SOB	super optimal broth
SOC	super optimal broth with catabolite repression
SPL	synthetic promoter libraries
sucCD	gene, encoding succinyl-CoA-synthetase
TAE	buffer consisting of Tris, EDTA and acetic acid
tal	gene, encoding transaldolase
TCA	tricarboxylic acid
Tet	tetracycline
tkt	gene, encoding transketolase
TKT	transketolase
tkt-operon	genes, encoding transketolase operon
TPI	triosephosphate isomerase
tpiA	gene, encoding triosephosphate isomerase
TPP	thiaminpyrophosphate
zwf	gene, encoding glucose 6-phosphate dehydrogenase

8.2 Proteinogenic Amino Acids

A	Ala	alanine	M	Met	methionine
C	Cys	cysteine	N	Asn	asparagine
D	Asp	aspartic acid	P	Pro	proline
E	Glu	glutamic acid	Q	Gln	glutamine
F	Phe	phenylalanine	R	Arg	arginine
G	Gly	glycine	S	Ser	serine
H	His	histidine	T	Thr	threonine
I	Ile	isoleucine	V	Val	valine
K	Lys	lysine	W	Trp	tryptophan
L	Leu	leucine	Y	Tyr	tyrosine

8.3 Symbols

μ	specific growth rate	[h^{-1}]
a	specific area	[m^2 m^{-3}]
A	area	[m^2]
BS	backscatter	[-]
c	concentration	[mol m^{-3}] or [mmol L^{-1}] or [%]
CDW	cell dry weight	[g L^{-1}]
D	molecular diffusivity	[m^2 s^{-1}]
DO	dissolved oxygen	[%]
g	acceleration	[m s^{-2}]
H	Henry's law constant	[bar m^3 kg^{-1}]
J	mass flux	[mol m^{-2} s^{-1}]
k	mass transfer coefficient	[m s^{-1}]
K	overall mass transfer coefficient	[m s^{-1}]
k_La	volumetric gas-liquid mass transfer coefficient	[h^{-1}]
n	shaking frequency	[rpm]
OTR	oxygen transfer rate	[mol_{O2} m^{-3} s^{-1}]
OUR	oxygen uptake rate	[mol_{O2} m^{-3} s^{-1}]
pK	dissociation constant	[-]
q'	volumetric mass transfer rate	[mol m^{-3} s^{-1}]
q	specific uptake/production rate	[mmol g^{-1} h^{-1}]
T	temperature	[°C]
t	time	[min] or [h]
U	unit	[μmol min^{-1}]
V	volume	[m^3] or [mL]
X	biomass concentration	[g L^{-1}]
Y	production yield	[mmol mol^{-1}] or [g mol^{-1}]
Z	film thickness	[m]

8.4 Empirical Parameters

a, b, c, x_0, y_0 Gaussian fitting

a, b, c, d, x_0, y_0 Parabolic fitting

8.5 Indices

*	refers to equilibrium concentration
660	refers to 600 nm
A	refers to compound A
a	refers to acid
a	refers to annealing
Ala	refers to alanine
Arg	refers to arginine
e	refers to elongation
eftu	refers to gene, encoding elongation factor thermo unstable
Frc	refers to fructose
G	refers to gas
G:5	refers to gain of 5
G:100	refers to gain of 100
Glc	refers to glucose
Glu	refers to glutamate
Gly	refers to glycine
i	refers to interface
L	refers to liquid
Lys	refers to lysine
max	refers to maximum
O_2	refers to oxygen
R	refers to resistance
S	refers to substrate
sod	refers to gene, encoding superoxide dismutase
X	refers to biomass

9 References

Abe S. (1967) “Taxonomical studies on glutamic acid-producing bacteria.” J. Gen. Appl. Microbiol. 13:279–301.

Akita K. (1981) “Diffusivities of gases in aqueous electrolyte solutions.” Ind. Eng. Chem. Fundam. 20:89–94.

Alper H, Fischer C, Nevoigt E, Stephanopoulos G. (2005) “Tuning genetic control through promoter engineering.” Proc. Natl. Acad. Sci. U. S. A. 102:12678–12683.

Anastassiadis S. (2007) “L-Lysine Fermentation.” Recent Pat. Biotechnol.11–24.

Archer JA, Solow-Cordero DE, Sinskey AJ. (1991) “A C-terminal deletion in *Corynebacterium glutamicum* homoserine dehydrogenase abolishes allosteric inhibition by L-threonine.” Gene 107:53–59.

Azuma T, Nakanishi T. (1988) “Factors Affecting L-Arginine Production in the continuous culture of an L-arginine producer of *Corynebacterium acetoacidophilum*.” J. Ferment. Technol. 66:285–290.

Azuma T, Nakanishi T, Sugimoto M. (1988) “Isolation and characterization of a stable L-arginine producer from continuous culture broth of *Corynebacterium acetoacidophilum*.” J. Ferment. Technol. 66:279–284.

Bailey JE, Ollis DF. (1986) “Biochemical Engineering Fundamentals.” 2nd ed. McGraw-Hill Education.

Banat IM, Nigam P, Singh D, Marchant R, McHale AP. (1998) “Review: Ethanol production at elevated temperatures and alcohol concentrations: Part I - Yeasts in general.” World J. Microbiol. Biotechnol. 14:809–821.

Band L, Henner DJ. (1984) “*Bacillus subtilis* requires a ‘stringent’ Shine-Dalgarno region for gene expression.” DNA 3:17–21.

Barabote RD, Saier MH. (2005) “Comparative Genomic Analyses of the bacterial phosphotransferase system.” Microbiol. Mol. Biol. Rev. 69:608–634.

Becker J, Klopprogge C, Schröder H, Wittmann C. (2009) “Metabolic engineering of the tricarboxylic acid cycle for improved lysine production by *Corynebacterium glutamicum*.” Appl. Environ. Microbiol. 75:7866–7869.

Becker J, Klopprogge C, Zelder O, Heinzle E, Wittmann C. (2005) “Amplified expression of fructose 1,6-bisphosphatase in *Corynebacterium glutamicum* increases *in vivo* flux through the pentose phosphate pathway and lysine production on different carbon sources.” Appl. Environ. Microbiol. 71:8587–8596.

Becker J, Wittmann C. (2012a) “Bio-based production of chemicals, materials and fuels - *Corynebacterium glutamicum* as versatile cell factory.” Curr. Opin. Biotechnol. 23:631–640.

Becker J, Wittmann C. (2012b) “Systems and synthetic metabolic engineering for amino acid production - the heartbeat of industrial strain development.” Curr. Opin. Biotechnol. 23:718–726.

Becker J, Zelder O, Häfner S, Schröder H, Wittmann C. (2011) “From zero to hero - Design-based systems metabolic engineering of *Corynebacterium glutamicum* for L-lysine production.” Metab. Eng. 13:159–168.

Bellmann A, Vrljić M, Pátek M, Sahm H, Krämer R, Eggeling L. (2001) “Expression control and specificity of the basic amino acid exporter LysE of *Corynebacterium glutamicum*.” Microbiology 147:1765–1774.

Binder S, Schendzielorz G, Stäbler N, Krumbach K, Hoffmann K, Bott M, Eggeling L. (2012) “A high-throughput approach to identify genomic variants of bacterial metabolite producers at the single-cell level.” Genome Biol. 13:R40.

Bolten C. (2010) “Bio-based production of L-methionine in *Corynebacterium glutamicum*.” In: Wittmann, C, (ed.). Ibvt-Schriftenreihe Vol. 48. Göttingen: Cuvillier-Verlag.

Bolten CJ, Kiefer P, Letisse F, Portais J-C, Wittmann C. (2007) “Sampling for metabolome analysis of microorganisms.” Anal. Chem. 79:3843–3849.

Bommareddy RR, Chen Z, Rappert S, Zeng AP. (2014) “A *de novo* NADPH generation pathway for improving lysine production of *Corynebacterium glutamicum* by rational design of the coenzyme specificity of glyceraldehyde 3-phosphate dehydrogenase.” Metab. Eng. 25:30–37.

Bottoms CA, Smith PE, Tanner JJ. (2002) “A structurally conserved water molecule in Rossmann dinucleotide-binding domains.” Protein Sci. 11:2125–2137.

Büchs J. (2001) “Introduction to advantages and problems of shaken cultures.” Biochem. Eng. J. 7:91–98.

Buddrus J, Schmidt B. (2011) “Grundlagen der organischen Chemie.” 4th ed. Berlin/New York: Walter de Gruyter.

Buschke N, Becker J, Schäfer R, Kiefer P, Biedendieck R, Wittmann C. (2013) “Systems metabolic engineering of xylose-utilizing *Corynebacterium glutamicum* for production of 1,5-diaminopentane.” Biotechnol. J. 8:557–570.

Buschke N, Schröder H, Wittmann C. (2011) “Metabolic engineering of *Corynebacterium glutamicum* for production of 1,5-diaminopentane from hemicellulose.” Biotechnol. J. 6:306–317.

Byrne J. (2014) “Global BioChem to put the brakes on lysine production.” http://www.feednavigator.com/Suppliers/Global-BioChem-to-put-the-brakes-on-lysine-production.

Casas López JL, Rodríguez Porcel EM, Oller Alberola I, Ballesteros Martin MM, Sánchez Pérez JA, Fernández Sevilla JM, Chisti Y. (2006) “Simultaneous determination of oxygen consumption rate and volumetric oxygen transfer coefficient in pneumatically agitated bioreactors.” Ind. Eng. Chem. Res. 45:1167–1171.

Chemler JA, Fowler ZL, McHugh KP, Koffas MAG. (2010) “Improving NADPH availability for natural product biosynthesis in *Escherichia coli* by metabolic engineering.” Metab. Eng. 12:96–104.

Chen LL, Wang J Le, Hu Y, Qian BJ, Yao XM, Wang JF, Zhang JH. (2013) “Computational design of glutamate dehydrogenase in *Bacillus subtilis* natto.” J. Mol. Model. 19:1919–1927.

Chen R, Greer A, Dean AM. (1995) “A highly active decarboxylating dehydrogenase with rationally inverted coenzyme specificity.” Proc. Natl. Acad. Sci. U. S. A. 92:11666–11670.

Chen R, Yang H. (2000) “A highly specific monomeric isocitrate dehydrogenase from *Corynebacterium glutamicum*.” Arch. Biochem. Biophys. 383:238–245.

Chen Z, Bommareddy RR, Frank D, Rappert S, Zeng A. (2014) “Deregulation of feedback inhibition of phosphoenolpyruvate carboxylase for improved lysine production in *Corynebacterium glutamicum*.” Appl. Environ. Microbiol. 80:1388–93.

Chmiel H, Walitza E. (2011) “Transportvorgänge in Biosuspensionen.” In: Chmiel, H, (ed.). Bioprozesstechnik. 3rd ed. Spektrum Akademischer Verlag, pp. 175–236.

Cirilli M, Zheng R, Scapin G, Blanchard JS. (2003) “The three-dimensional structures of the *Mycobacterium tuberculosis* dihydrodipicolinate reductase-NADH-2,6-PDC and -NADPH-2,6-PDC complexes. Structural and mutagenic analysis of relaxed nucleotide specificity.” Biochemistry 42:10644–10650.

Collins MD, Cummins CS. (1986) “Genus *Corynebacterium* Lehmann and Neumann 1896.” In: Sneath, PHA, Mair, NS, Sharpe, ME, Holt, JG, (eds.). Bergey’s Man. Syst. Bacteriol. 2nd ed. Baltimore: Williams & Wilkins, Vol. 2, pp. 1266–1276.

Cormack BP, Valdivia RH, Falkow S. (1996) “FACS-optimized mutants of the green fluorescent protein (GFP).” Gene 173:33–8.

Cremer J, Eggeling L, Sahm H. (1991) “Control of the lysine biosynthesis sequence in *Corynebacterium glutamicum* as analyzed by overexpression of the individual corresponding genes.” Appl. Environ. Microbiol. 57:1746–1752.

Cremer J, Treptow C, Eggeling L, Sahm H. (1988) “Regulation of enzymes of lysine biosynthesis in *Corynebacterium glutamicum*.” J. Gen. Microbiol. 134:3221–3229.

Crow L, Wittenberger CL. (1979) “Separation and properties of NAD+- and NADP+-dependent glyceraldehyde-3-phosphate dehydrogenases from *Streptococcus mutans*.” J. Biol. Chem. 254:1134–1142.

Danckwerts P V. (1951) “Significance of liquid-film coefficients in gas absorption.” Ind. Eng. Chem. 43:1460–1467.

Dombroski AJ, Johnson BD, Lonetto M, Gross CA. (1996) “The sigma subunit of *Escherichia coli* RNA polymerase senses promoter spacing.” Proc. Natl. Acad. Sci. U. S. A. 93:8858–8862.

Dominguez H, Rollin C, Guyonvarch A, Guerquin-Kern JL, Cocaign-Bousquet M, Lindley ND. (1998) “Carbon-flux distribution in the central metabolic pathways of *Corynebacterium glutamicum* during growth on fructose.” Eur. J. Biochem. 254:96–102.

Dontsova O, Kopylov A, Brimacombe R. (1991) “The location of mRNA in the ribosomal 30S initiation complex; site-directed cross-linking of mRNA analogues carrying several photo-reactive labels simultaneously on either side of the AUG start codon.” EMBO J. 10:2613–2620.

Dunn IJ, Heinzle E, Ingham J, Pfenosil JE. (2003) “Biological reaction engineering: Dynamic modelling fundamentals with simulation examples.” 2nd ed. Wiley-VCH Verlag GmbH & Co. KGaA.

Dutta R. (2008) “Fundamentals of biochemical engineering.” Berlin, Heidelberg: Springer Berlin Heidelberg New York.

Dym O, Eisenberg D. (2001) “Sequence-structure analysis of FAD-containing proteins.” Protein Sci. 10:1712–1728.

Eggeling L, Sahm H. (1999) “L-Glutamate and L-lysine: traditional products with impetuous developments.” Appl. Microbiol. Biotechnol. 52:146–153.

Eibl R, Kaiser S, Lombriser R, Eibl D. (2010) “Disposable bioreactors: the current state-of-the-art and recommended applications in biotechnology.” Appl. Microbiol. Biotechnol. 86:41–49.

Eikmanns B. (2005) “Central metabolism tricarboxylic acid cycle and anaplerotic reactions.” In: Eggeling, L, Bott, M, (eds.). Handbook of *Corynebacterium glutamicum*. 1. ed. CRV Press, pp. 241–276.

Eyre-Walker A, Bulmer M. (1993) “Reduced synonymous substitution rate at the start of enterobacterial genes.” Nucleic Acids Res. 21:4599–4603.

Fillinger S, Boschi-Muller S, Azza S, Dervyn E, Branlant G, Aymerich S. (2000) “Two glyceraldehyde-3-phosphate dehydrogenases with opposite physiological roles in a nonphotosynthetic bacterium.” J. Biol. Chem. 275:14031–14037.

Funke M, Diederichs S, Kensy F, Müller C, Büchs J. (2009) “The baffled microtiter plate: increased oxygen transfer and improved online monitoring in small scale fermentations.” Biotechnol. Bioeng. 103:1118–1128.

Garcia-Ochoa F, Gomez E, Santos VE, Merchuk JC. (2010) “Oxygen uptake rate in microbial processes: An overview.” Biochem. Eng. J. 49:289–307.

Ge X, Rao G. (2012) “Real-time monitoring of shake flask fermentation and off gas using triple disposable noninvasive optical sensors.” Biotechnol. Prog. 28:872–877.

Geertz-Hansen HM, Blom N, Feist AM, Brunak S, Petersen TN. (2014) “Cofactory: Sequence-based prediction of cofactor specificity of Rossmann folds.” Proteins:1–10.

Goodfellow M, Collins MD, Minnikin DE. (1976) “Thin-layer chromatographic analysis of mycolic acid and other long-chain components in whole-organism methanolysates of coryneform and related taxa.” J. Gen. Microbiol. 96:351–358.

Haberhauer G, Schröder H, Pompejus M, Zelder O, Kröger B. (2004) “*Corynebacterium glutamicum* genes encoding proteins involved in membrane synthesis and membrane transport.” US Patent 6696561.

Haefner S, Heinzle E, Kiefer P, Klopprogge C, Kroeger B, Schroeder H, Wittmann C, Zelder O. (2007) “Methods for the preparation of lysine by fermentation of *Corynebacterium glutamicum*.” Patent WO/2005/059139 A2.

Hagen J. (2004) “Chemiereaktoren: Auslegung und Simulation.” 1st ed. Wiley-VCH Verlag GmbH & Co. KGaA.

Hammer K, Mijakovic I, Jensen PR. (2006) “Synthetic promoter libraries - tuning of gene expression.” Trends Biotechnol. 24:53–55.

Hartner FS, Ruth C, Langenegger D, Johnson SN, Hyka P, Lin-Cereghino GP, Lin-Cereghino J, Kovar K, Cregg JM, Glieder A. (2008) “Promoter library designed for fine-tuned gene expression in *Pichia pastoris*.” Nucleic Acids Res. 36:1–15.

Hermann R, Walther N, Maier U, Büchs J. (2001) “Optical method for the determination of the oxygen-transfer capacity of small bioreactors based on sulfite oxidation.” Biotechnol. Bioeng. 74:355–363.

Hermann T. (2003) “Industrial production of amino acids by coryneform bacteria.” J. Biotechnol. 104:155–172.

Higbie R. (1935) “The rate of absorption of a pure gas into a still liquid during short periods of exposure.” Trans. Am. Inst. Chem. Eng. 31:365–389.

Hoelsch K, Sührer I, Heusel M, Weuster-Botz D. (2013) “Engineering of formate dehydrogenase: synergistic effect of mutations affecting cofactor specificity and chemical stability.” Appl. Microbiol. Biotechnol. 97:2473–2481.

Hook-Barnard IG, Hinton DM. (2007) “Transcription initiation by mix and match elements: Flexibility for polymerase binding to bacterial promoters.” Gene Regul. Syst. Biol. 1:275–293.

Huber R, Ritter D, Hering T, Hillmer A-K, Kensy F, Müller C, Wang L, Büchs J. (2009) “Robo-Lector - a novel platform for automated high-throughput cultivations in microtiter plates with high information content.” Microb. Cell Fact. 8:1–15.

Iddar A, Valverde F, Serrano A, Soukri A. (2002) “Expression, purification, and characterization of recombinant dehydrogenase from *Clostridium acetobutylicum*.” Protein Expr. Purif. 25:519–526.

Ihnen ED, Demain AL. (1969) “Glucose-6-phosphate dehydrogenase and its deficiency in mutants of *Corynebacterium glutamicum*.” J. Bacteriol. 98:1151–1158.

Ikeda K. (2002) “New Seasonings.” Chem. Senses 27:847–849.

Ikeda M, Nakagawa S. (2003) “The *Corynebacterium glutamicum* genome: features and impacts on biotechnological processes.” Appl. Microbiol. Biotechnol. 62:99–109.

Ikeda M. (2003) “Amino acid production processes.” Adv. Biochem. Eng. Biotechnol. 79:1–35.

Ikeda M. (2012) “Sugar transport systems in *Corynebacterium glutamicum*: features and applications to strain development.” Appl. Microbiol. Biotechnol. 96:1191–1200.

Ikeda M, Takeno S. (2013) “Amino acid production by *Corynebacterium glutamicum*.” In: Yukawa, H, Masayuki, I, (eds.). *Corynebacterium glutamicum* - Biol. Biotechnol. Vol. 23. Springer Heidelberg New York Dordrecht London, pp. 107–148.

Jacob WF, Santer M, Dahlberg AE. (1987) “A single base change in the Shine-Dalgarno region of 16S rRNA of *Escherichia coli* affects translation of many proteins.” Proc. Natl. Acad. Sci. U. S. A. 84:4757–61.

Jacques N, Dreyfus M. (1990) “Translation initiation in *Escherichia coli*: old and new questions.” Mol. Microbiol. 4:1063–1067.

Jäger W, Schäfer A, Kalinowski J, Pühler A. (1995) “Isolation of insertion elements from gram-positive *Brevibacterium, Corynebacterium* and *Rhodococcus* strains using the *Bacillus subtilis sacB* gene as a positive selection marker.” FEMS Microbiol. Lett. 126:1–6.

Jäger W, Schäfer A, Puhler A, Labes G, Spring S. (1992) “Expression of the *Bacillus subtilis sacB* gene leads to sucrose sensitivity in the gram-positive bacterium *Corynebacterium glutamicum* but not in *Streptomyces lividans*.” J. Bacteriol. 174:5462–5465.

Jensen PR, Hammer K. (1998a) “Artificial promoters for metabolic optimization.” Biotechnol. Bioeng. 58:191–195.

Jensen PR, Hammer K. (1998b) “The sequence of spacers between the consensus sequences modulates the strength of prokaryotic promoters.” Appl. Environ. Microbiol. 64:82–87.

Jensen PR, Westerhoff h V, Michelsen O. (1993) “The use of *lac*-type promoters in control analysis.” Eur. J. Biochem. 211:181–91.

John GT, Klimant I, Wittmann C, Heinzle E. (2003) “Integrated optical sensing of dissolved oxygen in microtiter plates: a novel tool for microbial cultivation.” Biotechnol. Bioeng. 81:829–836.

Kalinowski J, Cremer J, Bachmann B, Eggeling L, Sahm H, Pühler A. (1991) “Genetic and biochemical analysis of the aspartokinase from *Corynebacterium glutamicum*.” Mol. Microbiol. 5:1197–1204.

Kalinowski J. (2005) “The Genomes of Amino Acid-Producing Corynebacteria.” In: Eggeling, L, Bott, M, (eds.). Handbook of *Corynebacterium glutamicum*. 1. ed. CRV Press, pp. 37–56.

Kalinowski J, Bathe B, Bartels D, Bischoff N, Bott M, Burkovski A, Dusch N, Eggeling L, Eikmanns BJ, Gaigalat L, Goesmann A, Hartmann M, Huthmacher K, Krämer R, Linke B, McHardy AC, Meyer F, Möckel B, Pfefferle W, Pühler A, Rey D a, Rückert C, Rupp O, Sahm H, Wendisch VF, Wiegräbe I, Tauch A. (2003) “The complete *Corynebacterium glutamicum* ATCC 13032 genome sequence and its impact on the production of L-aspartate-derived amino acids and vitamins.” J. Biotechnol. 104:5–25.

Katzberg M, Skorupa-Parachin N, Gorwa-Grauslund M-F, Bertau M. (2010) “Engineering cofactor preference of ketone reducing biocatalysts: A mutagenesis study on a γ-diketone reductase from the yeast *Saccharomyces cerevisiae* serving as an example.” Int. J. Mol. Sci. 11:1735–1758.

Kawaguchi H, Verte AA, Okino S, Inui M, Yukawa H, Yukawa H, Mol J. (2006) “Engineering of a xylose metabolic pathway in *Corynebacterium glutamicum*.” Appl. Environ. Microbiol. 72:3418–3428.

Kelle R, Hermann T, Bathe B. (2005) “L-Lysine Production.” In: Eggeling, L, Bott, M, (eds.). Handbook of *Corynebacterium glutamicum*. 1. ed. CRV Press, pp. 465–488.

Kiefer P, Heinzle E, Zelder O, Wittmann C, Icrobiol APPLENM. (2004) “Comparative metabolic flux analysis of lysine-producing *Corynebacterium glutamicum* Cultured on Glucose or Fructose.” Appl. Environ. Microbiol. 70:229–239.

Kimura E. (2005) “L-Glutamate Production.” In: Eggeling, L, Bott, M, (eds.). Handbook of *Corynebacterium glutamicum*. 1. ed. CRV Press, pp. 439–464.

Kind S, Neubauer S, Becker J, Yamamoto M, Völkert M, Abendroth G Von, Zelder O, Wittmann C. (2014) “From zero to hero - Production of bio-based nylon from renewable resources using engineered *Corynebacterium glutamicum*.” Metab. Eng. 25:113–123.

King ZA, Feist AM. (2013) “Optimizing cofactor specificity of oxidoreductase enzymes for the generation of microbial production strains - OptSwap.” Ind. Biotechnol. 9:236–246.

Kinoshita S. (2005) “A short history of the birth of the amino acid industry in Japan.” In: Eggeling, L, Bott, M, (eds.). Handbook of *Corynebacterium glutamicum*. 1. ed. CRV Press, pp. 3–5.

Kinoshita S, Shigezo U, Shimono M. (1957) “Studies on the amino acid fermentation. Part I: Production of L-glutamic acid by various microorganisms.” J. Gen. Appl. Microbiol. 3:193–205.

Kinoshita S. (1959) “The production of amino acids by fermentation processes.” Adv. Appl. Microbiol. 1:201–214.

Kinoshita S. (1987) “Amino acid and nucleotide fermentations: From their genesis to the current state.” Dev. Ind. Microbiol. 28:1–12.

Kinoshita S, Nakayama K, Kitada S. (1961) “Method of producing L-lysine by fermentation.” US Patent 2979439.

Kirchner O, Tauch A. (2003) “Tools for genetic engineering in the amino acid-producing bacterium *Corynebacterium glutamicum*.” J. Biotechnol. 104:287–299.

Koebmann BJ, Westerhoff h V, Snoep JL, Nilsson D, Jensen PR. (2002) “The glycolytic flux in *Escherichia coli* is controlled by the demand for ATP.” J. Bacteriol. 184:3909–3916.

Krömer JO, Fritz M, Heinzle E, Wittmann C. (2005) “In vivo quantification of intracellular amino acids and intermediates of the methionine pathway in *Corynebacterium glutamicum*.” Anal. Biochem. 340:171–173.

Kudla G, Murray AW, Tollervey D, Plotkin JB. (2009) “Coding-sequence determinants of gene expression in *Escherichia coli*.” Science 324:255–258.

Lee H-S. (2005) “Sulfur metabolism and its regulation.” In: Eggeling, L, Bott, M, (eds.). Handbook of *Corynebacterium glutamicum*. 1. ed. CRV Press, pp. 351–376.

Leuchtenberger W. (1996) “Amino acids - Technical production and use.” In: Rehm, H-J, Reed, G, (eds.). Biotechnol. Prod. Prim. Metab. 2 Vol.6 ed. Wiley-VCH Verlag GmbH, Vol. 6, pp. 465–502.

Leuchtenberger W, Huthmacher K, Drauz K. (2005) “Biotechnological production of amino acids and derivatives: current status and prospects.” Appl. Microbiol. Biotechnol. 69:1–8.

Lewis WK, Whitman WG. (1924) “Principles of gas absorption.” Ind. Eng. Chem. 16:1215–1220.

Liebl W. (2005) “Corynebacterium taxonomy.” In: Eggeling, L, Bott, M, (eds.). Handbook of *Corynebacterium glutamicum*. 1st ed. CRV Press, pp. 9–34.

Liebl W, Ehrmann M, Ludwig W, Schleifer KH. (1991) “Transfer of *Brevibacterium divaricatum* DSM 20297^T, ‘*Brevibacterium flavum*’ DSM 20411, ‘*Brevibacterium lactofermentum*’ DSM 20412 and DSM 1412, and *Corynebacterium lilium* DSM 20137^T to *Corynebacterium glutamicum*.” Int. J. Syst. Bacteriol. 41:255–260.

Lindner SN, Niederholtmeyer H, Schmitz K, Schoberth SM, Wendisch VF. (2010) “Polyphosphate/ATP-dependent NAD kinase of *Corynebacterium glutamicum*: biochemical properties and impact of *ppnK* overexpression on lysine production.” Appl. Microbiol. Biotechnol. 87:583–593.

Liu M, Tolstorukov M, Zhurkin V, Garges S, Adhya S. (2004) “A mutant spacer sequence between -35 and -10 elements makes the P_{lac} promoter hyperactive and cAMP receptor protein-independent.” Proc. Natl. Acad. Sci. U. S. A. 101:6911–6916.

Liu Q, Ouyang S-P, Kim J, Chen G-Q. (2007) “The impact of PHB accumulation on L-glutamate production by recombinant *Corynebacterium glutamicum*.” J. Biotechnol. 132:273–279.

Lunzer M, Miller SP, Felsheim R, Dean AM. (2005) “The biochemical architecture of an ancient adaptive landscape.” Science 310:499–501.

Lutz R, Bujard H. (1997) “Independent and tight regulation of transcriptional units in *Escherichia coli* via the LacR/O, the TetR/O and AraC/I1-I2 regulatory elements.” Nucleic Acids Res. 25:1203–1210.

Marx A, Eikmanns BJ, Sahm H, De Graaf AA, Eggeling L. (1999) “Response of the central metabolism in *Corynebacterium glutamicum* to the use of an NADH-dependent glutamate dehydrogenase.” Metab. Eng. 1:35–48.

Marx A, Hewitt CJ, Grewal R, Scheer S, Vandré K, Pfefferle W, Kossmann B, Ottersbach P, Beimfohr C, Snaidr J, Augé C, Reuss M. (2003a) “Anwendungen der Zytometrie in der Biotechnologie.” Chemie Ing. Tech. 75:608–614.

Marx A, Hans S, Möckel B, Bathe B, De Graaf AA. (2003b) “Metabolic phenotype of phosphoglucose isomerase mutants of *Corynebacterium glutamicum*.” J. Biotechnol. 104:185–197.

Matsumoto K, Kitagawa K, Jo S-J, Song Y, Taguchi S. (2011) “Production of poly(3-hydroxybutyrate-co-3-hydroxyvalerate) in recombinant *Corynebacterium glutamicum* using propionate as a precursor.” J. Biotechnol. 152:144–6.

Melzer G, Esfandabadi ME, Franco-Lara E, Wittmann C. (2009) “Flux Design: In silico design of cell factories based on correlation of pathway fluxes to desired properties.” BMC Syst. Biol. 3:1–16.

Michal G, Schomburg D eds. (2012) “Biochemical Pathways: An atlas of biochemistry and molecular biology.” 2. ed. John Wiley & Sons.

Mijakovic I, Petranovic D, Jensen PR. (2005) “Tunable promoters in systems biology.” Curr. Opin. Biotechnol. 16:329–335.

Misono H, Ogasawara M, Nagasaki S. (1986) “Characterization of *meso*-diaminopimelate dehydrogenase from *Corynebacterium glutamicum* and its distribution in bacteria.” Agric. Biol. Chem. 50:2729–2734.

Miyajima R, Shiio I. (1970) “Regulation of aspartate family amino acid biosynthesis in *Brevibacterium flavum*. III. Properties of homoserine dehydrogenase.” J. Biochem. 68:311–319.

Miyajima R, Shiio I. (1971) “Regulation of aspartate family amino acid biosynthesis in *Brevibacterium flavum*. Part IV. Repression of the enzymes in threonine biosynthesis.” Agric. Biol. Chem. 35:424–430.

Moll I, Grill S, Gualerzi CO, Bläsi U. (2002) “Leaderless mRNAs in bacteria: surprises in ribosomal recruitment and translational control.” Mol. Microbiol. 43:239–246.

Moon M-W, Park S-Y, Choi S-K, Lee J-K. (2007) “The phosphotransferase system of *Corynebacterium glutamicum*: features of sugar transport and carbon regulation.” J. Mol. Microbiol. Biotechnol. 12:43–50.

Morinaga Y, Takagi H, Ishida M, Miwa K, Sato T, Nakamori S, Sano K. (1987) “Threonine production by co-existence of cloned genes coding homoserine dehydrogenase and homoserine kinase in *Brevibacterium lactofermentum*.” Agric. Biol. Chem. 51:93–100.

Moritz B, Striegel K, De Graaf AA, Sahm H. (2000) “Kinetic properties of the glucose-6-phosphate and 6-phosphogluconate dehydrogenases from *Corynebacterium glutamicum* and their application for predicting pentose phosphate pathway flux *in vivo*.” Eur. J. Biochem. 267:3442–3452.

Murakami KS, Darst S a. (2003) “Bacterial RNA polymerases: the whole story.” Curr. Opin. Struct. Biol. 13:31–39.

Nakamura T, Nakayama T, Koyama Y, Shimazaki K, Miwa H, Tsuruta M, Tamura Y, Tosaka O. (2000) “Process for production of lysine by fermentation.” US Patent 6025169.

Nakayama K, Araki K, Kase H. (1978) “Microbial production of essential amino acid with *Corynebacterium glutamicum* mutants.” Adv. Exp. Med. Biol. 105:649–661.

Nernst W. (1904) “Theorie der Reaktionsgeschwindigkeit in heterogenen Systemen.” Zeitschrift für Phys. Chemie, Stoechiom. und Verwandtschaftslehre 47:52–55.

Neuner A, Heinzle E. (2011) “Mixed glucose and lactate uptake by *Corynebacterium glutamicum* through metabolic engineering.” Biotechnol. J. 6:318–329.

Neuner A, Wagner I, Sieker T, Ulber R, Schneider K, Peifer S, Heinzle E. (2013) “Production of L-lysine on different silage juices using genetically engineered *Corynebacterium glutamicum*.” J. Biotechnol. 163:217–224.

Nicolas P, Mäder U, Dervyn E, Rochat T, Leduc A, Pigeonneau N, Bidnenko E, Marchadier E, Hoebeke M, Aymerich S, Becher D, Bisicchia P, Botella E, Delumeau O, Doherty G, Denham EL, Fogg MJ, Fromion V, Goelzer A, Hansen A, Härtig E, Harwood CR, Homuth G, Jarmer H, Jules M, Klipp E, Le Chat L, Lecointe F, Lewis P, Liebermeister W, March A, Mars R a T, Nannapaneni P, Noone D, Pohl S, Rinn B, Rügheimer F, Sappa PK, Samson F, Schaffer M, Schwikowski B, Steil L, Stülke J, Wiegert T, Devine KM, Wilkinson AJ, van Dijl JM, Hecker M, Völker U, Bessières P, Noirot P. (2012) “Condition-dependent transcriptome reveals high-level regulatory architecture in *Bacillus subtilis*.” Science 335:1103–1106.

Nielsen J, Villadsen J, Lidén G. (2003) “Bioreaction engineering principles.” 2. ed. Kluwer Academic / Plenum Publishers.

Oh JW, Kim SJ, Cho YJ, Park NH, Lee JH. (1993) “Fermentation”. US Patent 526829 A.

Ohnishi J, Katahira R, Mitsuhashi S, Kakita S, Ikeda M. (2005) “A novel *gnd* mutation leading to increased L-lysine production in *Corynebacterium glutamicum*.” FEMS Microbiol. Lett. 242:265–274.

Ohnishi S, Mitsuhashi M, Hayashi J. (2002) “A novel methodology employing *Corynebacterium glutamicum* genome information to generate a new L-lysine-producing mutant.” Appl. Microbiol. Biotechnol. 58:217–223.

Okino S, Noburyu R, Suda M, Jojima T, Inui M, Yukawa H. (2008) “An efficient succinic acid production process in a metabolically engineered *Corynebacterium glutamicum* strain.” Appl. Microbiol. Biotechnol. 81:459–464.

Omumasaba CA, Okai N, Inui M, Yukawa H. (2004) “*Corynebacterium glutamicum* glyceraldehyde-3-phosphate dehydrogenase isoforms with opposite, ATP-dependent regulation.” J. Mol. Microbiol. Biotechnol. 8:91–103.

Paget MSB, Helmann JD. (2003) “Protein family review - The σ^{70} family of sigma factors.” Genome Biol. 4:1–6.

Park S-D, Lee J-Y, Sim S-Y, Kim Y, Lee H-S. (2007) “Characteristics of methionine production by an engineered *Corynebacterium glutamicum* strain.” Metab. Eng. 9:327–336.

Pátek M. (2005) “Regulation of gene expression.” In: Eggeling, L, Bott, M, (eds.). Handbook of *Corynebacterium glutamicum*. 1st ed. CRV Press, pp. 81–98.

Pátek M, Holátko J, Busche T, Kalinowski J, Nešvera J. (2013) “*Corynebacterium glutamicum* promoters: a practical approach.” Microb. Biotechnol. 6:103–117.

Pátek M, Nešvera J. (2011) “Sigma factors and promoters in *Corynebacterium glutamicum*.” J. Biotechnol. 154:101–113.

Pátek M, Nešvera J. (2013) “Promoters and plasmid vectors of *Corynebacterium glutamicum*.” In: Yukawa, H, Inui, M, (eds.). *Corynebacterium glutamicum* - Biol. Biotechnol. Berlin, Heidelberg: Springer Berlin Heidelberg. Microbiology Monographs, Vol. 23, pp. 51–88.

Petern NR, Pearson ML. (1975) “Functional inactivation of bacteriophage λ morphogenetic gene mRNA.” Nature 253:647–650.

Petersen S, Mack C, De Graaf AA, Riedel C, Eikmanns BJ, Sahm H. (2001) “Metabolic consequences of altered phosphoenolpyruvate carboxykinase activity in *Corynebacterium glutamicum* reveal anaplerotic regulation mechanisms *in vivo*.” Metab. Eng. 3:344–3461.

Peters-Wendisch PG, Schiel B, Wendisch VF, Katsoulidis E, Möckel B, Sahm H, Eikmanns BJ. (2001) “Pyruvate carboxylase is a major bottleneck for glutamate and lysine production by *Corynebacterium glutamicum*.” J. Mol. Microbiol. Biotechnol. 3:295–300.

Pfefferle W, Möckel B, Bathe B, Marx A. (2003) “Biotechnological Manufacture of Lysine.” Adv. Biochem. Eng. Biotechnol. 79:59–112.

Pisabarro A, Malumbres M, Mateos LM, Oguiza JA, Martin JF. (1993) “A Cluster of Three Genes (*dapA, orf2*, and *dapB*) of *Brevibacterium lactofermentum* Encodes Dihydrodipicolinate Synthase, Dihydrodipicolinate Reductase, and a Third Polypeptide of Unknown Function.” J. Bacteriol. 175:2743–2749.

Qin X, Qian J, Yao G, Zhuang Y, Zhang S, Chu J. (2011) “*GAP* promoter library for fine-tuning of gene expression in *Pichia pastoris*.” Appl. Environ. Microbiol. 77:3600–3608.

Ravasi P, Peiru S, Gramajo H, Menzella HG. (2012) “Design and testing of a synthetic biology framework for genetic engineering of *Corynebacterium glutamicum*.” Microb. Cell Fact. 11:147.

Reddy SG, Scapin G, Blanchard JS. (1996) “Interaction of pyridine nucleotide substrates with *Escherichia coli* dihydrodipicolinate reductase: Thermodynamic and structural analysis of binary complexes.” Biochemistry 35:13294–13302.

Reinscheid DJ, Eikmanns BJ, Sahm H. (1991) “Analysis of a *Corynebacterium glutamicum hom* gene coding for a feedback-resistant homoserine dehydrogenase.” J. Bacteriol. 173:3228–3230.

Riedel C, Rittmann D, Dangel P, Möckel B, Petersen S, Sahm H, Eikmanns BJ. (2001) “Characterization of the phosphoenolpyruvate carboxykinase gene from *Corynebacterium glutamicum* and significance of the enzyme for growth and amino acid production.” J. Mol. Microbiol. Biotechnol. 3:573–583.

Ries C, John G, John C, Eibl R, Eibl D. (2010) “A shaken disposable bioreactor system for controlled insect cell cultivations at milliliter-scale.” Eng. Life Sci. 10:75–79.

Rischbieter E, Schumpe A. (1996) “Gas Solubilities in Aqueous Solutions of Organic Substances.” J. Chem. Eng. 41:809–812.

Rittmann D, Lindner SN, Wendisch VF. (2008) “Engineering of a glycerol utilization pathway for amino acid production by *Corynebacterium glutamicum*.” Appl. Environ. Microbiol. 74:6216–6222.

Robison K, McGuire a M, Church GM. (1998) “A comprehensive library of DNA-binding site matrices for 55 proteins applied to the complete *Escherichia coli* K-12 genome.” J. Mol. Biol. 284:241–254.

Rossmann MG, Moras D, Olsen KW. (1974) “Chemical and biological evolution of a nucleotide-binding protein.” Nature 250:194–199.

Rytter JV, Helmark S, Chen J, Lezyk MJ, Solem C, Jensen PR. (2014) “Synthetic promoter libraries for *Corynebacterium glutamicum*.” Appl. Microbiol. Biotechnol. 98:2617–2623.

Sahm H, Eggeling L, Eikmanns B, Krämer R. (1995) “Metabolic design in amino acid producing bacterium *Corynebacterium glutamicum*.” FEMS Microbiol. Rev. 16:243–252.

Sahm H, Eggeling L, De Graaf AA. (2000) “Pathway analysis and metabolic engineering in *Corynebacterium glutamicum*.” Biol. Chem. 381:899–910.

Sassi AH, Fauvart L, Deschamps AM, Lebeault JM. (1998) “Fed-batch production of L-lysine by *Corynebacterium glutamicum*.” Biochem. Eng. J. 1:85–90.

Sauer U, Eikmanns BJ. (2005) “The PEP-pyruvate-oxaloacetate node as the switch point for carbon flux distribution in bacteria.” FEMS Microbiol. Rev. 29:765–794.

Scapin G, Blanchard JS, Sacchettini JC. (1995) “Three-Dimensional Structure of *Escherichia coli* Dihydrodipicolinate Reductase.” Biochemistry 34:3502–3512.

Scapin G, Reddy SG, Blanchard JS, Biol JM. (1996) “Three-Dimensional Structure of *meso*-Diaminopimelic Acid Dehydrogenase from *Corynebacterium glutamicum*.” Biochemistry 2960:13540–13551.

Schaffer S, Weil B, Nguyen VD, Dongmann G, Günther K, Nickolaus M, Hermann T, Bott M. (2001) “A high-resolution reference map for cytoplasmic and membrane-associated proteins of *Corynebacterium glutamicum*.” Electrophoresis 22:4404–4422.

Schell MA. (1993) “Molecular biology of the LysR family of transcriptional regulators.” Annu. Rev. Microbiol. 47:597–626.

Schneider J, Wendisch VF. (2010) “Putrescine production by engineered *Corynebacterium glutamicum*.” Appl. Microbiol. Biotechnol. 88:859–868.

Schneider K, Schütz V, John GT, Heinzle E. (2010) “Optical device for parallel online measurement of dissolved oxygen and pH in shake flask cultures.” Bioprocess Biosyst. Eng. 33:541–547.

Schrumpf B, Eggeling L, Sahm H. (1992) “Isolation and prominent characteristics of an L-lysine hyperproducing strain of *Corynebacterium glutamicum*.” Appl. Microbiol. Biotechnol. 37:566–571.

Schumpe A, Deckwer WD. (1979) “Communications to the editor - Estimation of O_2 and CO_2 solubiliteis in fermentation media.” Biotechnol. Bioeng. 21:1075–1078.

Scrutton NS, Berry A, Perham RN. (1990) “Redesign of the coenzyme specificity of a dehydrogenase by protein engineering.” Nature 343:38–43.

Seletzky JM, Noak U, Fricke F, Welk E, Eberhard W, Knocke C, Büchs J. (2007) “Scale-up from shake flasks to fermenters in batch and continuous mode with *Corynebacterium glutamicum* on lactic acid based on oxygen transfer and pH.” Biotechnol. Bioeng. 98:800–811.

Shaw-Reid CA, McCormick MM, Sinskey AJ, Stephanopoulos G. (1999) “Flux through the tetrahydrodipicolinate succinylase pathway is dispensable for L-lysine production in *Corynebacterium glutamicum*.” Appl. Microbiol. Biotechnol. 51:325–333.

Shine J, Dalgarno L. (1974) “The 3’-terminal sequence of *Escherichia coli* 16S ribosomal RNA: complementarity to nonsense triplets and ribosome binding sites.” Proc. Natl. Acad. Sci. U. S. A. 71:1342–1346.

Shine J, Dalgarno L. (1975) “Determinant of cistron specificity in bacterial ribosomes.” Nature 254:34–38.

Simoni RD, Levinthal M, Kundig FD, Kundig W, Anderson B, Hartman PE, Roseman S. (1967) “Genetic evidence for the role of a bacterial phosphotransferase system in sugar transport.” Biochemistry 58:1963–1970.

Solem C, Jensen PR. (2002) “Modulation of gene expression made easy.” Appl. Environ. Microbiol. 68:2397–2403.

Stackebrandt E, Rainey FA, Ward-rainey NL. (1997) “Proposal for a new hierarchical classification system, Actinobacteria classis nov.” Int. J. Syst. Bacteriol. 47:479–491.

Stephanopoulos GN. (1998) “Review of cellular metabolism metabolic engineering.” In: Stephanopoulos, GN, Aristidou, AA, Nielsen, J, (eds.). Metab. Eng. Princ. Methodol. Academic Pr Inc, pp. 21–79.

Storhas. (2003) “Bioverfahrensentwicklung.” 1st ed. Wiley-VCH Verlag GmbH & Co. KGaA.

Takeno S, Murata R, Kobayashi R, Mitsuhashi S, Ikeda M. (2010) “Engineering of *Corynebacterium glutamicum* with an NADPH-generating glycolytic pathway for L-lysine production.” Appl. Environ. Microbiol. 76:7154–7160.

Taricska JR, Chen JP, Hung Y-T, Wang LK, Zou S-W. (2009) “Surface and spray aeration.” In: Wang, LK, Pereira, NC, Hung, Y-T, Shammas, NK, (eds.). Biol. Treat. Process. Vol. 8. Springer Science & Business Media, pp. 151–206.

Tauch A, Pühler A, Kalinowski J, Thierbach G. (2003) “Plasmids in *Corynebacterium glutamicum* and their molecular classification by comparative genomics.” J. Biotechnol. 104:27–40.

Thongchuang M, Pongsawasdi P, Chisti Y, Packdibamrung K. (2012) “Design of a recombinant *Escherichia coli* for producing L-phenylalanine from glycerol.” World J. Microbiol. Biotechnol. 28:2937–2943.

Tornøe J, Kusk P, Johansen TE, Jensen PR. (2002) “Generation of a synthetic mammalian promoter library by modification of sequences spacing transcription factor binding sites.” Gene 297:21–32.

Tunac JB. (1989) “High-Aeration Capacity Shake-Flask System.” J. Ferment. Bioeng. 68:157–159.

Udagawa T, Shimizu Y, Ueda T. (2004) “Evidence for the translation initiation of leaderless mRNAs by the intact 70 S ribosome without its dissociation into subunits in eubacteria.” J. Biol. Chem. 279:8539–8546.

Udaka S. (1960) “Screening method for microorganisms accumulating metabolites and its use in the isolation of *Micrococcus glutamicus*.” J. Bacteriol. 79:754–755.

Vallino JJ, Stephanopoulos G. (1993) “Metabolic flux distributions in *Corynebacterium glutamicum* during growth and lysine overproduction.” Biotechnol. Bioeng. 41:633–646.

Veglio F, Beolchini F, Ubaldini S. (1998) “Empirical models for oxygen mass transfer: A comparison between shake flask and lab-scale fermentor and application to manganiferous ore bioleaching.” Process Biochem. 33:367–376.

Velasco AM, Leguina JI, Lazcano A. (2002) “Molecular evolution of the lysine biosynthetic pathways.” J. Mol. Evol. 55:445–459.

Vogt M, Haas S, Klaffl S, Polen T, Eggeling L, Van Ooyen J, Bott M. (2014) “Pushing product formation to its limit: Metabolic engineering of *Corynebacterium glutamicum* for L-leucine overproduction.” Metab. Eng. 22:40–52.

Vrljic M, Kronemeyer W, Sahm H, Eggeling L. (1995) “Unbalance of L-lysine flux in *Corynebacterium glutamicum* and its use for the isolation of excretion-defective mutants.” J. Bacteriol. 177:4021–4027.

Vrljic M, Sahm H, Eggeling L. (1996) “A new type of transporter with a new type of cellular function: L-lysine export from *Corynebacterium glutamicum*.” Mol. Microbiol. 22:815–826.

Wang Y, San KY, Bennett GN. (2013) “Cofactor engineering for advancing chemical biotechnology.” Curr. Opin. Biotechnol. 24:994–999.

Wehrmann A, Phillipp B, Sahm H, Eggeling L. (1998) “Different modes of diaminopimelate synthesis and their role in cell wall integrity: a study with *Corynebacterium glutamicum*.” J. Bacteriol. 180:3159–3165.

Wendisch VF. (2003) “Genome-wide expression analysis in *Corynebacterium glutamicum* using DNA microarrays.” J. Biotechnol. 104:273–285.

Wierenga RK, De Maeyer MCH, Hol WGJW. (1985) “Interaction of Pyrophosphate Moieties with *α*-Helixes in Dinucleotide Binding Proteins.” Biochemistry:672–680.

Wierenga RK, Terpstra P, Ho WGJ. (1986) “Prediction of the Occurrence of the ADP-binding pap-fold in Proteins, Using an Amino Acid Sequence Fingerprint.” J. Mol. Evol. 187:101–107.

Wittmann C, Becker J. (2007) “The L-lysine story: From metabolic pathways to industrial production.” In: Wendisch, VF, (ed.). Amin. Acid Biosynth. - Pathways, Regul. Metab. Eng. Vol. 5. Springer Berlin Heidelberg, Vol. 5, pp. 39–70.

Wittmann C, De Graaf AA. (2005) “Metabolic flux analysis in *Corynebacterium glutamicum*.” In: Eggeling, L, Bott, M, (eds.). Handbook of *Corynebacterium glutamicum*. 1. ed. CRV Press, pp. 277–304.

Wittmann C, Heinzle E. (2001) “Application of MALDI-TOF MS to lysine-producing *Corynebacterium glutamicum*: A novel approach for metabolic flux analysis.” Eur. J. Biochem. 268:2441–2455.

Wittmann C, Heinzle E. (2002) “Genealogy profiling through strain improvement by using metabolic network analysis: metabolic flux genealogy of several generations of lysine-producing corynebacteria.” Appl. Environ. Microbiol. 68:5843–5859.

Wittmann C, Kiefer P, Zelder O. (2004) “Metabolic fluxes in *Corynebacterium glutamicum* during lysine production with sucrose as carbon source.” Appl. Environ. Microbiol. 70:7277–7287.

Wittmann C, Kim HM, John G, Heinzle E. (2003) “Characterization and application of an optical sensor for quantification of dissolved O_2 in shake-flasks.” Biotechnol. Lett. 25:377–380.

Wu TJ, Wu LH, Knight JA. (1986) “Stability of NADPH: Effect of various factors on the kinetics of degradation.” Clin. Chem. 32:314–319.

Xie T, Tsong TY. (1990) “Study of mechanisms of electric field-induced DNA transfection. II. Transfection by low-amplitude, low-frequency alternating electric fields.” Biophys. J. 58:897–903.

Xu JZ, Zhang JL, Guo YF, Jia QD, Zhang WG. (2014a) “Heterologous expression of *Escherichia coli* fructose-1,6-bisphosphatase in *Corynebacterium glutamicum* and evaluating the effect on cell growth and L-lysine production.” Prep. Biochem. Biotechnol. 44:493–509.

Xu J, Han M, Zhang J, Guo Y, Zhang W. (2014b) “Metabolic engineering *Corynebacterium glutamicum* for the L-lysine production by increasing the flux into L-lysine biosynthetic pathway.” Amino Acids:[Epub ahead of print].

Yokota A, Lindley N. (2005) “Central Metabolism: Sugar Uptake and Conversion.” In: Eggeling, L, Bott, M, (eds.). Handbook of *Corynebacterium glutamicum*. 1. ed. CRV Press, pp. 215–240.

Yoshida A, Tomita T, Kurihara T, Fushinobu S, Kuzuyama T, Nishiyama M. (2007) “Structural Insight into concerted inhibition of $\alpha_2\beta_2$-type aspartate kinase from *Corynebacterium glutamicum*.” J. Mol. Evol. 368:521–536.

Young BA, Gruber TM, Gross CA, Francisco S. (2002) “View of transcription initiation.” Cell 109:417–420.

Zhou J, Petracca R. (2000) “Influence of single base change in Shine-Dalgarno sequence on the stability of *B. subtilis* plasmid PSM604.” J. Tongji Med. Univ. 20:183–185.

Zieminski SA, Hume III RM, Durham R. (1976) “Rates of oxygen transfer from air bubbles to aqueous NaCl solutions at various temperatures.” Mar. Chem. 4:333–346.

Zimmermann HF, Anderlei T, Büchs J, Binder M. (2006) “Oxygen limitation is a pitfall during screening for industrial strains.” Appl. Microbiol. Biotechnol. 72:1157–1160.